Functional analysis of the CP12 gene family in Arabidopsis

Amani Omar S Abuzaid

A thesis submitted for the degree of
Doctor of Philosophy

School of Biological Sciences
University of Essex
October 2016

To my parents, my husband and my children

Acknowledgements

All praise and thanks be to Allah for giving me the power, patience and guidance to complete this thesis.

I would like to express my sincere gratitude to my supervisor, Professor Christine Raines, for her continued support and encouragement during my PhD studies. I am also grateful to my PhD advisor, Professor Tracy Lawson, for her support and valuable feedback during supervisory meetings, and to Dr Patricia Lopez-Calcagno for her kindness, assistance and great advice.

I would also like to thank all the members of the plant biology group, for their technical expertise and help in the lab.

Thanks to King Abdul Aziz University for the scholarship, funding for my PhD, and to the University of Essex for giving me the opportunity to conduct my research.

To my parents, thank you for the love, encouragement and unwavering belief in me. Thank you also to my husband Mohammed, who has stood beside me all this time and provided me with strength and support throughout my academic journey. To my younger brother Mohammed, thank you so much for all your help and support.

Finally, a very special thank you to my children, Samir and Fatima, who have given me endless motivation, inspiration and happiness.

Abstract

The chloroplast protein CP12 is present in almost all photosynthetic organisms. This protein has been shown to regulate the activity of two enzymes of the Calvin-Benson cycle, namely glyceraldehyde 3-phosphate dehydrogenase (GAPDH) and phosphoribulokinase (PRK). The regulation of these enzymes is achieved by the reversible formation of this multiprotein complex in response to a change in light intensity. In Arabidopsis, there are three CP12 genes, CP12-1, CP12-2 and CP12-3. Expression analysis of these genes suggested that they may have a wider role in non-photosynthetic plastids through the plants' life cycle and that their function may not be restricted to the Calvin-Benson cycle.

The main aim of this study was to determine the functional significance of having three CP12 isoforms and to explore the importance of each individual isoform *in vivo.* This was done by using *Arabidopsis thaliana* T-DNA mutant and RNAi transgenic lines with a reduced level of CP12. Our results revealed that single mutant lines did not develop a severe growth phenotype. However, a reduction in the transcript of more than one CP12 gene, in a number of multiple lines, led to a significant reduction in photosynthetic capacity at early stages of development and a severe growth phenotype, including reduced fresh and dry weight, number of leaves and seed yield, as well as affected lateral roots formation. Complementation analysis of CP12-1 in the triple mutant revealed that two out of the three lines rescued the phenotype by showing normal growth and development, confirming the importance of CP12. Our results suggest that the CP12 protein family is essential for normal growth and development and that these proteins are likely to have additional functions apart from the regulation of Calvin-Benson cycle enzymes.

Abbreviations

ATP	Adenosine triphosphate
bp	Base pair
BPGA	1,3-biphosphoglycerate
C-terminal	Carboxy terminal
CaMV 35S	Cauliflower mosaic 35S promoter
CBS	Cystathionine-β synthesis
CD	Circular dicroism
CDCP	CBS domain containing proteins
cDNA	Complementary DNA
CF	chlorophyll fluorescence
CO_2	Carbon dioxide
DNA	deoxyribonucleic acid
dNTPs	Deoxynucleotide Triphosphates
DTT	Dithiothreitol
E.coli	*Escherichia coli*
EDTA	Ethylenediaminetetraacetic Acid Tetasodium Salt.
Fq'/Fm'	PSII operating efficiency
H2O2	hydrogen peroxide
HEPES	4-(2-Hydroxyethyl) piperazine-1-ethanesulfonic acid
Hg	Hygromycin
HPLC	High performance liquid chromatography
IDPs	Intrinsically disordered proteins
IUPs	Intrinsically unstructured proteins
kDa	kilo Dalton
Kn	Kanamycin
LB	Luria Bertini
MS	Murashige and Skoog basal media
NAA	1- Naphthaleneacetic acid
N-terminal	Aminoterminal
NAD	Nicotinamide adenine dinucleotide
NADP	Nicotinamide adenine dinucleotide phosphate
NMR	Nuclear Magnetic Resonance
OPPP	oxidative pentose phosphate pathway
PCR	Polymerase chain reaction
PPFD	photosynthetically active photon flux density
PSII	photosystem II
qPCR	Quantitative reverse transcriptase polymerase chain reaction
RNA	ribonucleic acid
RNAi	RNAi interference
RT	Room temperature
RT-PCR	Reverse transcriptase polymerase chain reaction
SDS	Sodium dodecyl sulphate
TAIR	The Arabidopsis Information Resource
TBE	Tris-Borate-EDTA
T-DNA	Transferred DNA
Tris	Tris-(hydroxymethyl)aminomethane
Tween 20	Polyoxyethylene sorbitan monolaureate

UTR	Untranslated region
µg	microgram
µL	micro litre
WT	Wild type

CONTENTS

List of figures

CHAPTER 1

Introduction

Autotrophic organisms use sunlight as an energy source to synthesise organic molecules from carbon dioxide and water through one of the most important metabolic processes, called photosynthesis. The photosynthetic process can be broadly divided into two stages. First, reactions at the photochemical stage are light driven; they also lead to a reduction of the ferredoxin-thioredoxin system and synthesis of the highly energised metabolites NADPH and ATP. This stage begins with the absorption of light, leading to the oxidation of water, followed by the linear flow of electrons and hydrogen through membrane-bound multiprotein complexes in the photosynthetic chain. At the end of this chain, the electrons and H+ ions generated during this process are then used to reduce NADP to NADPH and to synthesise ATP via ATP synthase.

The second stage is the Calvin-Benson cycle, which involves the reductive conversion of CO_2 into carbohydrates. This stage is energy consuming; therefore, it utilises the ATP and NADPH generated by the electron transport chain to reduce CO_2 into organic molecules. This cycle is shut off in the dark to avoid conflicts with other biosynthetic pathways. The Calvin-Benson cycle maintains a critical balance between the environmental input and biosynthetic output, and the enzymes of this cycle are regulated by various factors, such as changes in pH, Mg^{2+} concentrations, the redox state (mediated via the ferredoxin/thioredoxin system) (Scheibe, 1991, Geiger and Servaites, 1994), the levels of metabolites (ATP, NADPH) and phosphoglyceric acid (PGA). These factors do not only modulate the activities of enzymes during the day but they also completely suppress their activity at night. Calvin-Benson cycle enzymes are present in the stroma of chloroplasts at high concentrations, and researchers have suggested that a number of them contribute to the formation of several supramolecular protein complexes (Suss et al., 1993, Gontero et al., 2001).

These protein complexes and the protein-protein interactions are crucial for many biological functions (Jones and Thornton, 1996). They are also believed to play a role in the channelling of reaction intermediates of the Calvin-Benson cycle from one site to another, which in turn prevent the diffusion of these intermediates in the bulk phase (Gontero et al., 1988).

A good example in higher plants is the multienzyme complex GAPDH/CP12/PRK, which plays a role in modulating carbon fixation in response to changes in the availability of light. Glyceraldehyde-3-phosphate dehydrogenase (GAPDH) and phosphoribulokinase (PRK) are activated in light by the reduced state of the protein thioredoxin (TRX). In the dark, the oxidised state of these enzymes interacts with the redox-sensitive protein CP12 to form GAPDH/CP12/PRK.

CP12 is a small protein which was originally described in the leaves of spinach, peas and tobacco to be able to bind with GAPDH (Pohlmeyer et al., 1996). After that, it has been shown to form a supermoleculer complex with GAPDH and PRK (Wedel et al., 1997, Wedel and Soll, 1998). CP12 is the chloroplast protein of 12kDa; this term originated from its behaviour, since it migrates as a 12kDa using electrophoresis under reducing conditions. However, CP12 has approximately 80 amino acids and a theoretical molecular mass of about 8.2-8.5kDa, depending on the species. In higher plants and algae, CP12 is encoded in the nucleus and then transported into the chloroplast where it can play its role.

The best studied function for CP12 so far is its involvement in the regulation of the Calvin-Benson cycle for CO_2 assimilation. This thesis attempts to study the importance of the CP12 gene family and to explore the possibility of additional roles for each member of this protein family in *Arabidopsis thaliana*.

1.1 Regulation of the Calvin-Benson cycle

The Calvin-Benson cycle, or photosynthesis in general, fuels all life on Earth with energy with the very rare exceptional case of chemolithoautotrophic organisms (Pfannschmidt and Yang, 2012). Without this process, neither complex ecosystem nor higher life forms including men would be found (Blankenship, 2013, Buchanan et al., 2015, Michelet et al., 2013).

It is the major pathway for CO_2 fixation; it is also the basis for the generation of carbohydrates in all photosynthetic organisms and for the production of almost all organic carbon in the biosphere, assimilating about 100 billion tonnes of carbon a year (Raines, 2011). ATP and NADPH, which are produced by photosynthesis, are used by the Calvin-Benson cycle to fix atmospheric CO_2 into carbon skeletons, which in turn fuels further plant metabolism through growth or development (Stitt et al., 2010, Raines, 2011).

Following to the initial discovery of the Calvin-Benson cycle by Bassham et al. (1950), the enzymes involved in this cycle were purified and characterised from many different sources including C3 and C4 plants, algae and cyanobacteria (Bassham et al., 1950).

During this cycle, 11 different enzymes are required to catalyse 13 reactions. The processes forming the cycle can be divided into three main phases: carboxylation, reduction and regeneration. The cycle is initiated when the enzyme ribulose-1,5-bisphosphate carboxylase oxygenase (Rubisco) catalyses the carboxylation of CO_2 to the acceptor molecule ribulose-1,5-bisphosphate (RuBP). The result of this reaction is the formation of the first stable compound in the cycle, 3-phosphoglycerate (3-PGA), which is utilised to form triose phosphate (also known as glyceraldehyde

phosphate, or G-3-P), and dihydroxyacetone phosphate (DHAP) through two reactions which consume ATP and NADPH. The regeneration phase of the cycle includes several reactions that convert triose phosphate into the CO_2 acceptor molecule RuBP (Figure 1.1).

All the carbon compounds which are produced in this cycle are essential for the growth and development of plants (Raines and Paul, 2006, Smith and Stitt, 2007). To regenerate RuBP, five-sixths of the triose phosphate remains within the cycle, while one-sixth of the carbon exits the cycle and is used in the biosynthesis of a range of compounds. Triose and hexose phosphate are utilised to synthesise sucrose and starch. The Calvin-Benson cycle also supplies intermediates to other pathways in the chloroplast, such as erythrose-4-P (E-4-P), which goes to the shikimate pathway for the biosynthesis of amino acids and lignin; G-3-P, which goes to the isoprenoid pathway; and Rib-5-P, which is for nucleotide and thiamine metabolism and cell wall biosynthesis (Raines, 2011).

In the 1960s and 1970s a number of Calvin-Benson cycle enzymes activities were found to be regulated by light (Buchanan, 1980, Buchanan, 1991, Schürmann and Jacquot, 2000, Lemaire et al., 2007, Schürmann and Buchanan, 2008, Buchanan et al., 2012, Michelet et al., 2013). They were found to have low activities in the dark, however, in the light they are found to be activated. These enzymes were PRK, GAPDH, fructose-1,6-bisphosphatase (FBPase) and sedoheptulose-1,7-bisphosphatase (SBPase). However, Rubisco is activated by the carbamylation of specific lysine residues mediated by Rubisco activase. Additional control of the activities of several enzymes is further mediated by specific metabolites which can act as inhibitors or stimulators on the neighbouring enzymes (Buchanan, 1980,

Woodrow and Berry, 1988, Buchanan, 1991, Portis Jr, 1992, Geiger and Servaites, 1994, Michelet et al., 2013).

Alternatively, regulating the activities of Calvin-Benson cycle enzymes can be achieved through multienzyme complexes. The formation of a multiprotein complex between two thioredoxin-regulated enzymes, PRK and GAPDH, is mediated by the small chloroplast protein CP12 (Wedel et al., 1997, Graciet et al., 2003a, Wedel and Soll, 1998). Within the complex, the activities of these enzymes are low. However, dissociation of the complex results in an increase in PRK and GAPDH activity. The importance of the CP12 protein in mediating the formation of this complex has been established by *in vitro* experiments using recombinant expressed proteins or partially purified components. The results of these experiments demonstrate that complex formation is dependent on the presence of oxidised CP12, which is mediated by the redox state of thioredoxin *f* (Scheibe et al., 2002, Howard et al., 2008, Marri et al., 2009, Marri et al., 2005b).

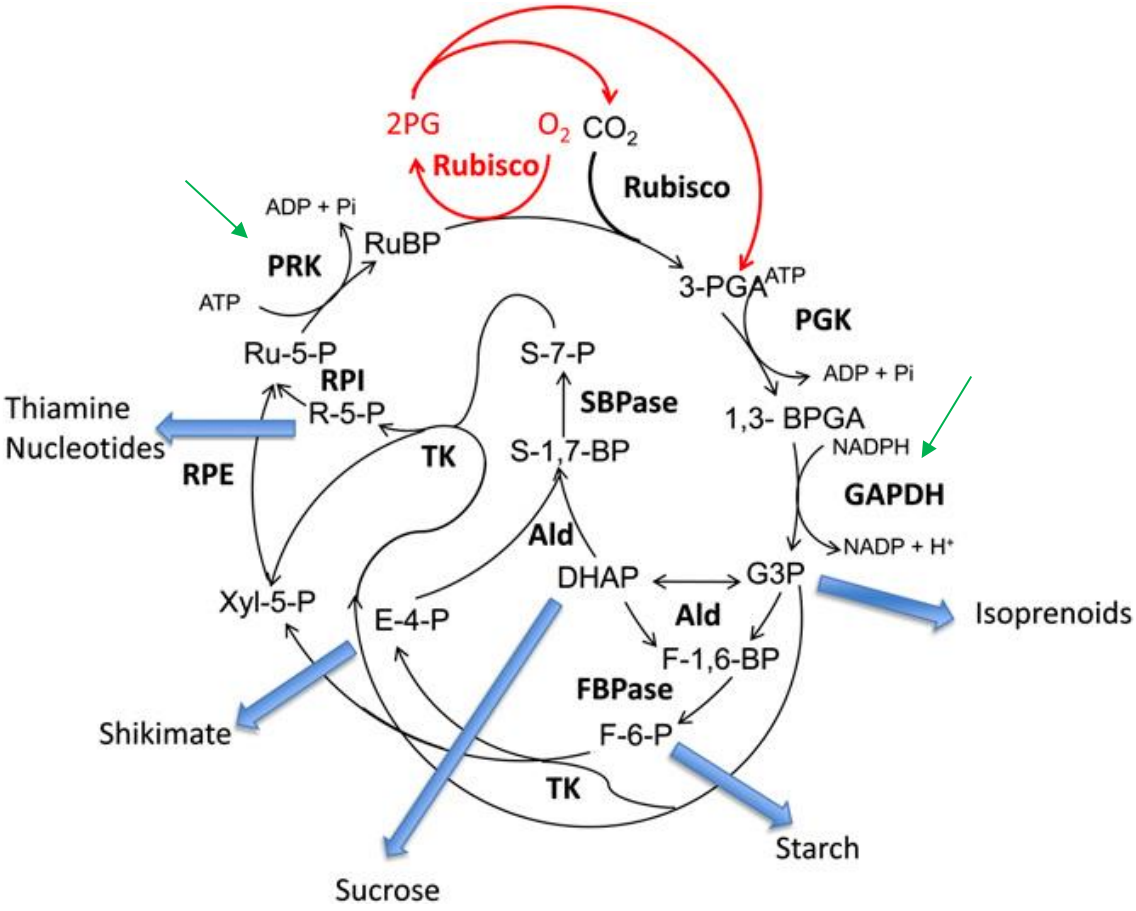

Figure 1.1 Representing the Calvin-Benson cycle. During the carboxylation reaction, CO_2 is fixed by the enzyme Rubisco into the acceptor molecule RuBP, which forms 3-phosphoglyceric acid (3-PGA).Two reactions are catalysed by 3-PGA kinase (PGK) and glyceraldehyde-3-phosphate dehydrogenase (GAPDH), which form glyceraldehyde-3-phosphate (G-3-P) in the reductive phase. The G-3-P enters the regenerative phase catalysed by aldolase (ALD) and either FBPase or SBPase, which produce fructose-6-Phosphate (F-6-P) and sedoheptulose-7-phosphate (S-7-P). F-6-P and S-7-P are utilized in reactions catalysed by transketolase (TK), R-5-P isomerase (RPI), and ribulose-5-P (Ru-5-P) epimerase (RPE), producing R-5-P. The final step which involves converting R-5-P to RuBP is catalysed by phosphoribulokinase (PRK). The oxygenation reaction of rubisco fixes O_2 into ribulose-1, 5-bisphosphate (RuBP), forming 3-Phosphoglyceric acid (PGA) and 2-phosphoglycolate (2PG), and the process of photorespiration (shown in red) releases CO_2 and PGA. Blue arrows indicate the five export points from the pathway. The green arrows indicate to the PRK and GAPDH enzymes (Raines, 2011).

1.2 The GAPDH/CP12/PRK multienzyme complex

Regulation of the Calvin-Benson cycle is essential to ensure that the activity is coordinated with the ATP and NADPH which are provided from the light reactions. In the stroma, the enzymes of Calvin-Benson cycle are present in very high concentrations; therefore, it has been suggested that a number of them might interact to form multienzyme complexes. These complexes may play a role in the regulation of the activities of Calvin-Benson cycle enzymes, and they may be involved in the mobilisation of a product/substrate from one enzyme to the next in a process called metabolic channelling. Several examples of these complexes in the Calvin-Benson cycle have been reported; Sainis and Harries (1986) reported a complex including PRK and Rubisco, and Gontero et al. (1988) identified a complex containing Rubisco, GAPDH, PRK, phosphoribose isomerase and 3-phosphoglycerate kinase (Sainis and Harris, 1986, Gontero et al., 1988, Miziorko, 2000). Additionally, one of the best-known and most studied multiprotein complexes is GAPDH/CP12/PRK, which involves Calvin-Benson cycle enzymes (Müller, 1972, Wara-Aswapati et al., 1980, CLASPER et al., 1991, Suss et al., 1993, Lebreton and Gontero, 1999, Mouche et al., 2002, Winkel, 2004, Marri et al., 2005a, Marri et al., 2005b). Although both PRK and GAPDH seem to have little control over the photosynthetic carbon fixation, they catalyse two of three energy-consuming reactions of the Calvin-Benson cycle. Therefore, the regulation of these enzymes is needed. The activities of these enzymes are regulated by the formation and disassociation of GAPDH/CP12/PRK in response to a change in light availability (Howard et al., 2008). Evidence from experiments suggests that the complex plays a regulatory role over the activity of both Calvin-Benson cycle enzymes. In the dark and under oxidising conditions, the complex is formed and the enzymes are deactivated; under reducing conditions, the

complex is disassociated, which in turn releases the active GAPDH and PRK (Wedel et al., 1997, Trost et al., 2006, Howard et al., 2008, Wedel and Soll, 1998, Tamoi et al., 2005, Marri et al., 2009).

1.2.1 GAPDH

Glyceraldehyde-3-phosphate dehydrogenase (GAPDH) enzymes are ubiquitous. It is important for glycolysis and carbon reduction in photosynthetic organisms. GAPDH catalyses the reversible reduction of 1,3-bisphosphoglycerate (BPGA) to glyceraldyhyde-3-phosphate using β-nicotinamide adenine dinucleotide (NADPH), which is generated by photosystem I in light (Buchanan, 1980).

GAPDH was the first enzyme in the Calvin-Benson cycle which was identified to be activated by light: in the leaves and the in the extracts of chloroplast which are subject to a short period of illumination, the NADP(H)-dependent activity of GAPDH was found to be higher than samples which were maintained in dark, but the NAD(H)-GAPDH remained low and stable (Ziegler and Ziegler, 1965).

Four types of genes are known to encode for GAPDHs in land plants: GAPC, GAPCp, GAPA and GAPB. GAPC and GAPCp are involved in glycolysis; the former is a cytosolic enzyme which presents in all eukaryotic cells. However, the latter has only been documented in plants. In Arabidopsis, at least two genes encode GAPCp: GAPCp1 and GAPCp2 (Petersen et al., 2003). The deficiency of this enzyme results in modifications in the carbon flux and mitochondrial dysfunction, effecting the seed production as well as the plant development (Rius et al., 2008). Chloroplast GAPDH contains two subunits, GAPA (36KDa) and GAPB (39KDa), which are oligomers of either GAPA or GAPA and GAPB. In cyanobacteria and green algae, only the GapA

subunit is present, so a homotetramer of A_4 isoform exists. However, several isoforms in higher plants have been documented, which include both GAPA and GAPB genes; these isoforms may include enzymes that contain only GapA subunits or both GapA or GapB subunits (Sparla et al., 2002).

Additionally, the subunits A and B of chloroplast GAPDH are homologous and highly conserved with the exception of the C-terminal extension of GapB (CTE). The CTE of subunit B includes 30 additional amino acids and is essential in the regulation and aggregation state of NADP-GAPDH (Ferri et al., 1990, ZAPPONI et al., 1993). This extension is also crucial for the enzyme's redox regulation which is mediated via thioredoxins (TRXs). Removal of the CTE, including the two regularity Cys residues, leaves the GapB subunit as insensitive to regulation as the GapA (Sparla et al., 2002).

1.2.2 PRK

Phosphoribulokinase is an enzyme which is restricted to photosynthetic organisms. It catalyses the synthesis of ribulose-1,5- biphosphate, from ribulose 5-phosphate using ATP. The PRK light-dependent activation was first documented in the unicellular green algae Chlorella (Pedersen et al., 1966, Bassham, 1971) and following by that it was confirmed by isolated chloroplasts from spinach (Sparla et al., 2002).

Although the mechanism of this reaction appears to be the same for all PRKs, the differences between PRKs in eukaryotic and prokaryotic organisms are significant. The eukaryotic PRKs are dimers of 39 kDa subunits; however, the prokaryotic PRK are octamers of about 32kDa. Additionally the regulation of this enzyme occurs through two different mechanisms in these two groups (Miziorko, 2000). The prokaryotic enzymes seem to be allosterically regulated, but the activity of the PRK in eukaryotic enzymes seems to be affected by several factors, such as light activation through the ferredoxin/thioredoix-mediated pathway (Buchanan, 1980, Lemaire et al., 2007), inhibition of the chloroplast metabolites (Miziorko, 2000) and protein-protein interactions through the formation of complexes such as GAPDH/CP12/PRK (Figure 1.2) (Miziorko, 2000, Howard et al., 2008, Wedel and Soll, 1998).

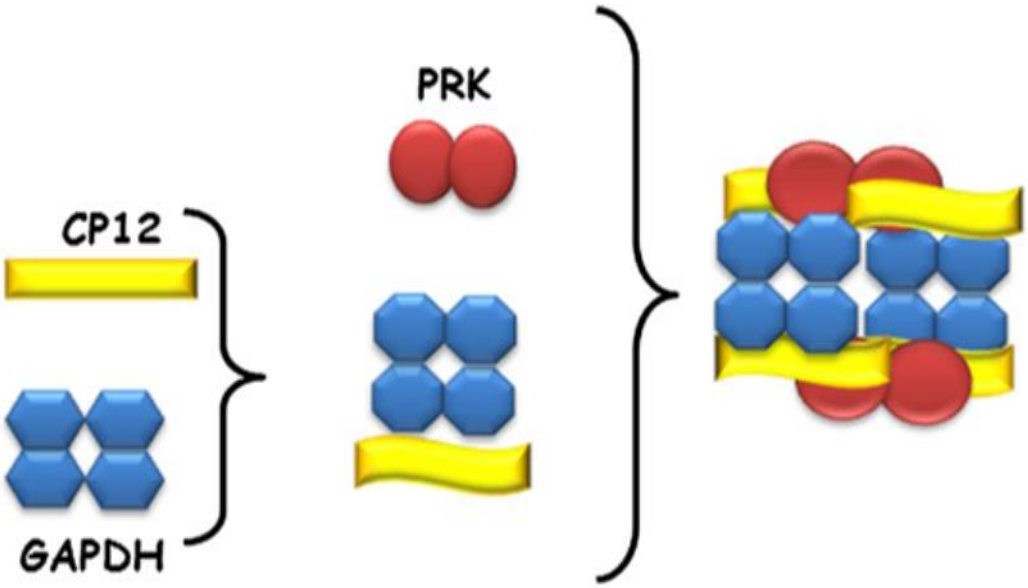

Figure 1.2 Model of the GAPDH/CP12/PRK assembly pathway. GAPDH (tetrameric form) binds CP12, and then PRK (dimeric form) finally binds to them to form the complex. This GAPDH/CP12/PRK unit then dimerises to provide the fully formed supramolecular complex diagram taken from (Gontero and Avilan, 2011).

1.3 Structural details of CP12

CP12 is a small, nuclear-encoded protein of approximately 8 kDa. It was discovered in higher plants by serendipity as a novel protein of 78 amino acids, including a C-terminal sequence which is homologous to the CTE in GAPB subunit. After that, CP12 was found to be widespread in photosynthetic, oxygenic organisms including cyanobacteria (Pohlmeyer et al., 1996, Wedel et al., 1997).

The GAPB subunit of GAPDH enzyme in land plants are now believed to be the result of the event of gene fusion between GAPA and CP12, that must have occurred at the origins of Streptophyte (Petersen et al., 2006) or earlier (Robbens et al., 2007). Both, the C-terminal extension in GAPB and the C-terminal of CP12, show the presence of conserved cysteines, which promote the formation of disulphide bonds and act as targets for thioredoxin regulation (Sparla et al., 2002, Lebreton et al., 2006, Trost et al., 2006, Baalmann et al., 1996, Fermani et al., 2007, Wedel and Soll, 1998). The conserved cysteines in the N-terminal half of CP12 also have the capacity to form disulphide bonds (Wedel et al., 1997, Petersen et al., 2006, Marri et al., 2008). Figure 1.3 shows the secondary structure of mature CP12. Structurally, CP12 proteins have three key primary functional features: an N-terminal cysteine pair, a C-terminal cysteine pair and the core AWD_VEE sequence. These two pairs of conserved cysteine residues have the ability to oxidise, forming two intramolecular disulfide bridges, one between cysteines 1 and 2 at the N-terminal region and the other between cysteines 3 and 4 at the C-terminal region. Studies have shown that these disulfide bridges are important for the complex formation (GAPDH/CP12/PRK) (Wedel and Soll, 1998, Graciet et al., 2003a, Matsumura et al., 2011, Fermani et al., 2012, Wedel et al., 1997) (Figure 1.3).

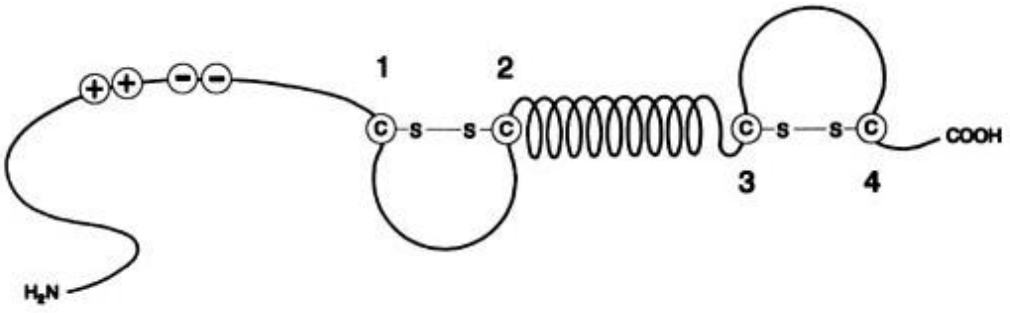

Figure 1.3 Prediction of the mature CP12 secondary structure. The N- and C-terminals of CP12 are indicated by H_2N and COOH. Cysteine residues (numbered) are proposed to form the N- and C-terminal loops (Wedel et al., 1997).

1.4 Discovery of CP12 and genes that code for it

CP12 was first described in 1996 in spinach, as a protein which binds to GAPDH. In 1997, Wedel and collaborators proposed its interaction with PRK. The discovery of CP12 genes and successful experiments involving the cloning of cDNA sequences for CP12, together with the expression of the conserved GAPDH/CP12/PRK complex, suggest that CP12 is conserved in all photosynthetic prokaryotes and eukaryotes (Wedel and Soll, 1998). Several approaches, such as size exclusion and immunoprecipitation, reveal the presence of the multiprotein complex in the stroma of higher plants (Wedel et al., 1997). The occurrence of the regulatory GAPDH/CP12/PRK complex has been commonly found in higher plants. Also, the multimeric forms of GAPDH have been identified in spinach, pea and maize (Scagliarini et al., 1993, Baalmann et al., 1994). The complex of GAPDH/CP12/PRK has been reported in spinach, pea and maize (Scheibe et al., 2002, Wedel et al., 1997, Wedel and Soll, 1998), in a cyanobacterium (Tamoi et al., 2005) and a number of algal species (Avilan et al., 1997, Boggetto et al., 2007, Oesterhelt et al., 2007).

Lower photosynthetic organisms, such as green algae, generally contain only one copy of the CP12 gene. In plants such as *Arabidopsis thaliana* and rice (*Oryza sativa*) CP12 is coded by small multigene families. In *Arabidopsis thaliana*, three CP12 isoforms are present in different chromosomes: At2g47400 codes for CP12-1 located on chromosome 2, At3g62410 for CP12-2 located on chromosome 3 and At1g76560 for CP12-3 on chromosome 1 (Singh et al., 2008, Groben et al., 2010, Gontero and Maberly, 2012).

A bioinformatics analysis of the protein sequences shows that CP12-1 and CP12-2 are 98% similar in their amino acid composition, whereas the sequence homology is below 50% when CP12-1 or CP12-2 are compared with CP12-3 (Singh et al., 2008).

Sixty-six CP12 proteins were obtained from different organisms, compared for their sequence similarity and divided into six types. CP12-1 and CP12-2 were grouped together under type I, which consists of largely disordered sequences. CP12-3 was categorised under type II, which contains other proteins with lower levels of disorder. *In vitro,* all three isoforms formed a supramolecular complex with GAPDH and PRK (Marri et al., 2010). In *Arabidopsis thaliana*, each CP12 isoform was able to bind with A_4-GAPDH to form the [(A_4-GAPDH)-(CP12)2-(PRK)]2 supramolecular complex (Marri et al., 2010).

1.5 The distribution of CP12

CP12 is distributed universally in all oxygenic photosynthetic organisms (Groben et al., 2010), and is reportedly found in cyanobacteria, diatoms, green and red algae, and higher plants, with the exception of the prasinophyte *Ostreococcus* (Wedel et al., 1997, Graciet et al., 2003a, Tamoi et al., 2005, Boggetto et al., 2007, Oesterhelt et al., 2007, Robbens et al., 2007, Stanley et al., 2013, Wedel and Soll, 1998, Groben et al., 2010, Marri et al., 2005a). Recent research has documented the presence of CP12 in viruses: cyanophages which infect the marine cyanobacteria *Prochlorococcus* and *Synechococcus*, carrying and expressing CP12 (Thompson et al., 2011).

Phylogenetic analysis of CP12 protein was performed by alignments of the amino acid sequences which were obtained from different groups of organisms; cyanobacteria, green and red algae, bryophytes, gymnosperms and angiosperms. The results from this analysis revealed that within the angiosperms and according to the similarity, CP12 can be divided into two groups; firstly CP12-1/CP12-2 like and secondly CP12-3 like (names according to the CP12 genes in *Arabidopsis thaliana*). Only one type seems to be present in Moses and green algae which is CP12-1/CP12-2 like. However, gymnosperm CP12s seem to be similar to CP12-3 like and do not include any of CP12-1/CP12-2 forms (Groben et al., 2010).

In *Arabidopsis thaliana* genome, three CP12 genes have been identified (CP12-1, CP12-2 and CP12-3). CP12-1 and CP12-2 are highly similar and the comparison between them in many species could not differentiate them into separate groups. Also, the expression of CP12-1 and CP12-2 is generally coordinated to the expression of the Calvin-Benson cycle enzymes GAPDH and PRK in different organs and growth stages. CP12-3 however, is less similarity with the other two forms at both the amino

acid sequence and gene expression level which indicate to unrelated and still undefined role (Singh et al., 2008, Groben et al., 2010, Marri et al., 2005a).

In general and based on the structural features, at the C-terminus of CP12 proteins, a pair of conserved cysteine residues are invariably present (Pohlmeyer et al., 1996). Another pair of N-terminal cysteine residues seems to be conserved in most CP12 proteins, but might not be included in a number of photosynthetic organisms, such as the Cyanophora and Synechococcus groups (Petersen et al., 2006, Groben et al., 2010). Finally, the distinctive feature of all CP12 portions is the core sequence of A^{34}WDTVEEL^{41} (the numbers taken from CP12 sequence of mature *Chlamydomonas reinhardtii)*, with the exception of CP12 from cyanophage where this sequence is absent (Thompson et al., 2011, Gontero and Maberly, 2012).

Since CP12 is enriched in disorder-promoting residues (alanine, glutamine and lysine) and depleted in order-promoting residues (phenylalanine, tryptophan, tyrosine, asparagine and leucine), it has been characterised as an intrinsically disordered protein (IDP) (Tompa, 2002, Dunker et al., 2001). These proteins (IDPs) which remain flexible even in their bound sites, have the ability to bind to multiple partners as a sequence of their plasticity (to be described later) (Gontero and Maberly, 2012).

1.6 CP12 gene expression in Arabidopsis

Two main independent studies have focused on the expression of CP12 genes in *Arabidopsis thaliana*. First, Marri et al. (2005a) used northern-blot analysis to investigate the expression of four GAPDH genes: GapA-1 and GapB for photosynthetic GAPDH in the chloroplast, GapC-1 for cytosolic GAPDH and GapCp-1 for plastidial GAPDH. They also conducted a similar analysis with PRK and two CP12 genes: CP12-1 and CP12-2. Their findings showed that the expression of GapA-1, GapB, PRK and CP12-2 is co-ordinately regulated with the same organ specificity (Marri et al., 2005a). These four genes were found to be expressed mainly in leaves and flower stalks, less expressed in the flowers, and with almost no expression in the roots and siliques. On the other hand, the expression of CP12-1 seems to be high in the photosynthetic organs and high expression was detected in flowers (Marri et al., 2005a).

The second study was conducted by Singh et al. (2008), who used transgenic *Arabidopsis thaliana* lines expressing *CP12::GUS* fusion constructs and found that all three CP12 genes displayed different expression patterns. This study revealed that the expression of CP12-2 was similar to the expression of the Calvin-Benson cycle enzyme which is light dependent, and it is expressed in photosynthetic tissues such as cotyledons, vegetative tissues and stalks. The expression of CP12-1 was detected in a range of tissues, including dark grown tissues and non-photosynthetic tissues (seeds and root tips). Finally, CP12-3 was found to have very low expression in the leaf tissue but high expression in the roots. Surprisingly, all CP12 genes were expressed in the floral tissues; CP12-1 and CP12-2 were expressed in the sepals and

style; and the expression of CP12-3 was detected in the stigma and anthers (Figure 1.4) (Singh et al., 2008).

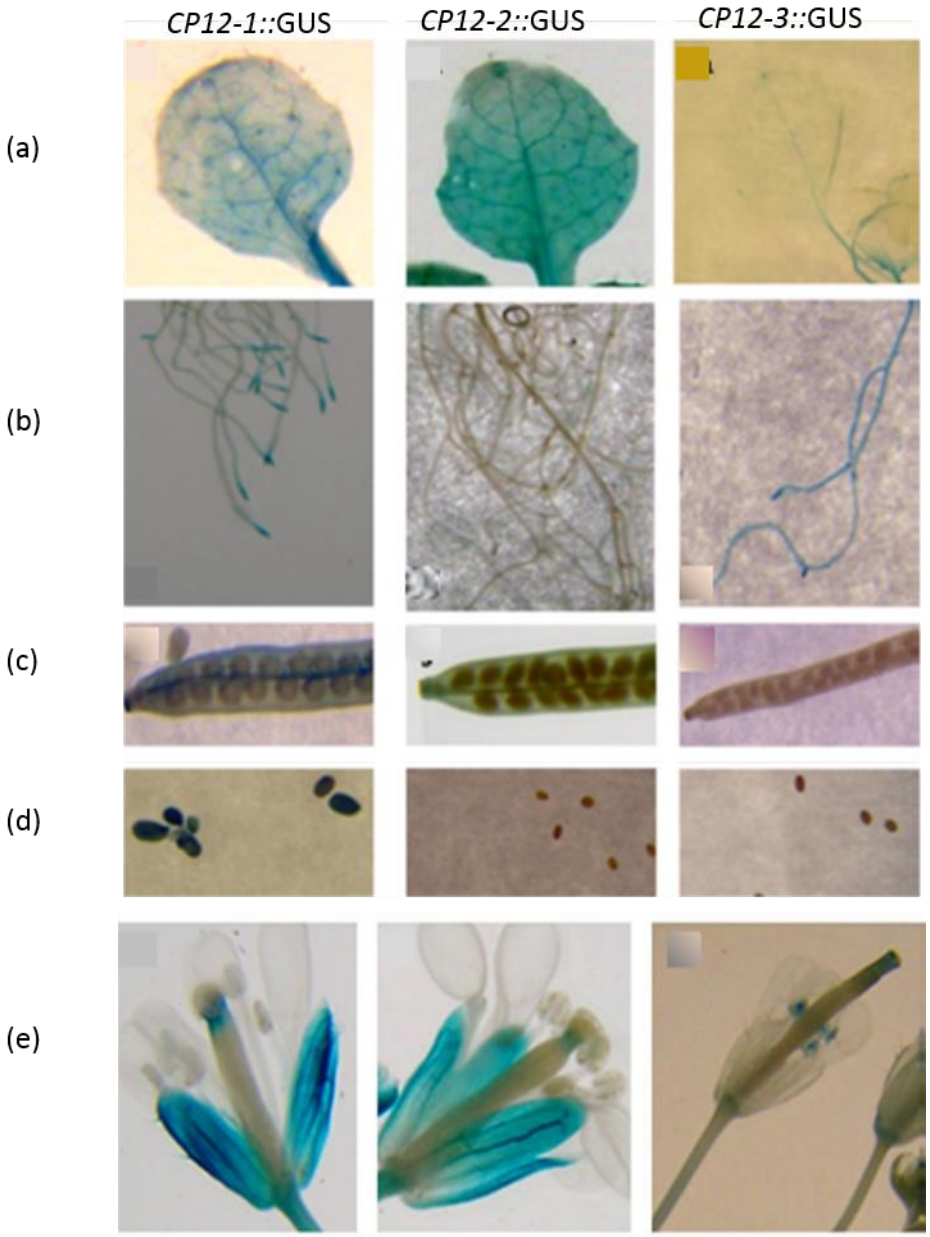

Figure 1.4 Localisation of *CP12-1::GUS*, *CP12-2::GUS* and *CP12-3::GUS* activity of transgenic Arabidopsis plants. **(a)** Leaves, **(b)** roots, **(c)** siliques, **(d)** seeds and **(e)** flowers. Images taken from Singh et al. (2008).

1.7 The role of thioredoxin in the light-modulated dissociation of the GAPDH/CP12/PRK complex

TRXs are small redox-sensitive proteins of approximately 12kDa that are encoded by large gene families in all oxygenic photosynthetic organisms and estimated to have nearly 300 potential targets (Buchanan and Balmer, 2005, Lemaire et al., 2007, Michelet et al., 2014, Lemaire et al., 2003, Florencio et al., 2006, Meyer et al., 2006).

TRXs are considered to be a member of two different redox systems which have been found in a number of cell compartments: firstly, the NADPH-TRX system, which is found in the cytosol and the mitochondria (NTS), and secondly, the ferredoxin-TRX system in the chloroplast (FTS), where they play their role as redox regulators of several targeted enzymes. Within the chloroplast FTS, light energy activates ferredoxin (Fdx), and this in turn reduces oxidised TRX by ferredoxin/thioredoxin reductase (FTR) (Buchanan et al., 2002, Yoo et al., 2011). The ferredoxin/thioredoxin system was identified following the analysis of the molecular mechanism underlying the light dependent activation of Calvin-Benson cycle enzymes was investigated (Buchanan, 1991, Buchanan et al., 2002, Wolosiuk and Buchanan, 1977, Michelet et al., 2013).

In photosynthetic organisms, TRXs can be classified into six general types: *h*, *o*, *f*, *m*, *x* and y. TRX *h* is present in several compartments of the cell, such as the cytosol, nucleus, endoplasmic reticulum and mitochondria, which are involved in oxidative stress defence. They may also be involved in self-incompatibility processes and in the mobilisation of seed reserves during germination (Buchanan and Balmer, 2005,

Lemaire et al., 2007). TRX *o* corresponds to two mitochondrial TRXs in Arabidopsis (Lemaire et al., 2007).

In *Arabidopsis thaliana*, at least 20 genes of TRX proteins have been identified with a conserved WC (G/P) PC motif in the active site (Lemaire et al., 2007, Meyer et al., 2005). Nine of these genes are targeted to plastids (Lemaire et al., 2007, Collin et al., 2003, Collin et al., 2004, Schürmann and Buchanan, 2008). Furthermore, plastidial TRXs have been classified according to their sequence similarities into four types (*f*, *m*, *x* and *y*), each having two or more isoforms. In general, TRXs *x* and *y* seem to serve as hydrogen donors for antioxidant enzymes such as peroxiredoxins (Collin et al., 2003, Collin et al., 2004), while TRXs *f* and *m* are involved in the enzyme regulation of photosynthetic carbon assimilation in the chloroplast.

The early studies of the regulation of two of Calvin-Benson cycle enzymes (FBPase and NADP-MDH) resulted in the identification of these two type of TRX *(f* and *m*) due to their substrate specificity (Jacquot et al., 1978, Wolosiuk et al., 1979). The former one was initially found to activate FBPase, while the latter one appeared to activate NADP-MDH. TRX *f* was found to be more effective than TRX *m* regarding the reduction of all other Calvin-Benson cycle enzymes (Wolosiuk et al., 1979).

In response to light, TRXs *f* and *m* are reduced by photosystem I through ferredoxin and ferredoxin-thioredoxin reductase (Dai et al., 2007, Schürmann and Buchanan, 2008). It has been found that the active sites of reduced TRXs are able to reduce disulphide bridges on target proteins, and enzymes in most cases can be reversibly activated by the reduction (Buchanan and Balmer, 2005).

Additionally, the redox state of TRX can affect the status of the GAPDH/CP12/PRK complex via the reduction of CP12 protein (Howard et al., 2008, Marri et al., 2009). *In vitro,* the breakdown of the complex is mediated by the chloroplastic TRXs *f* and *m* (Marri et al., 2009). High levels of reduced TRXs have the ability to maintain CP12 in a reduced state by the reduction of two cysteine pairs, as a result of which, the complex is dissociated and enzymes are activated. However, in the case of a decreasing level of reduced TRXs, oxidised CP12 increases, and then the complex is formed and the activities of these enzymes decrease (Lopez-Calcagno et al., 2014).

In Arabidopsis the disassociation of the complex GapA/CP12/PRK occurred under several conditions with a different impact on the enzymes activities. Reduced TRX led to complex disruption and also a complete recovery of the activity of PRK enzyme (Marri et al., 2005b).

In peas, TRX *f* is considered a major factor in complex dissociation. This was investigated by Howard et al. (2008) by incubating the stromal extracts from dark-adopted leaves with reduced TRX *f*, resulting in almost total dissociation of the complex. In the same study, two mechanisms were proposed to explain the model of TRX *f*-mediated activation of GAPDH and PRK: directly by the reduction of the disulphide bond in the cysteine residue of these enzymes and indirectly by mediating the dissociation (breakdown) of the complex in response to variations in light intensity.

1.8 The function of CP12 *in vivo*

To date, two studies have documented the importance of CP12 by reducing the level of this protein *in vivo*. The first one studied the knock-out mutant of cyanobacteria *Synechococcus* PCC7942 (Tamoi et al., 2005), and the second one focused on the antisense CP12 plants in tobacco (Howard et al., 2011a). The phenotype which resulted from both studies indicated that CP12 has an important role in the regulation of metabolism. In the cyanobacteria study, the results were consistent with the proposal in which CP12 was essential for the separation of the activities of the Calvin-Benson cycle enzymes from the oxidative pentose phosphate pathway (OPPP) during a day-night cycle.

A recent study, which is in agreement, reported that the cyanobacterial phage exploits the same mechanism by introducing a copy of a CP12-like protein into the cyanobacterial host, leading to down-regulation of enzymes activities of the Calvin-Benson cycle and increasing the flux through the OPPP (Thompson et al., 2011).

In higher plants, the situation is likely to be different to that in cyanobacteria. A number of Calvin-Benson cycle enzymes in higher plants are reductively activated in light; also, TRX *f* reduces the plastidic glucose 6-phosphate dehydrogenase (G6PDH), the first enzyme in OPPP, which leads to the inactivation of G6PDH (Wenderoth et al., 1997, Kruger and von Schaewen, 2003, Née et al., 2009).

Additionally, an analysis of the flux into OPPP in antisense CP12 tobacco plants suggested that the model which was proposed for cyanobacteria cannot be applied in tobacco (Howard et al., 2011a). In this study, no significant impact was detected on the activity of PRK or GAPDH, and no change was found on photosynthetic carbon assimilation. The same study reported a significant change in the growth rate and other dramatic changes, including fused cotyledons, altered leaf morphology, reduced

fertility and a loss of apical dominance (Raines and Paul, 2006, Howard et al., 2011a). The capacity of the malate valve was restricted, and the activity of NADP-malate dehydrogenase decreased (but not the level of the protein) as well as the content of the pyridine nucleotide. The carbon partitioning was also significantly changed with an increased allocation of carbon to the cell wall and a decrease in the allocation of the carbon to starch and soluble carbohydrate. Data from this study indicate that the CP12 protein plays a role in the redox-mediated regulation of carbon partitioning from the chloroplast, providing evidence that CP12 is necessarily required for normal growth and development (Figure 1.5) (Howard et al., 2011a).

Figure 1.5 CP12 antisense tobacco plants with changed phenotypes. Six-week-old plants: from left to right, the control (WT) and the antisense tobacco plants AS1, AS43, AS2/1 and AS6). Image taken from Howard et al. (2011).

1.9 CP12 as an intrinsically disordered protein (IDP)

There are number of proteins that include disordered regions, under physiological conditions, and lack a specific three-dimension structure. These proteins are referred to as IDPs (intrinsically disordered proteins). The absence of a rigid globular structure is considered as a functional advantage enabling one-to-many partners or protein promiscuity (Gontero and Maberly, 2012). Until recently, researchers believed that disordered proteins become ordered upon binding. However, closer inspections of complexes which involve IDPs have revealed that they have the ability to maintain functionally significant disorder in the complex with their binding partner(s); this phenomenon is called 'fuzziness' (Fuxreiter and Tompa, 2012, Gontero and Maberly, 2012).

The crystal structure of the GAPDH-CP12 binary complex from *Synechococcus elongatus* has been analysed (Gontero and Avilan, 2011, Matsumura et al., 2011). The data from this research revealed that the C-terminal region is the only region which is structured of CP12 upon binding, which lies within the groove of the active site of GAPDH. These structural data correlate with the kinetic data from *C. reinhardtii* and reveal that the last residues of CP12 bind to the S-loop of GAPDH, preventing NADPH entry and then down-regulating the chloroplast GAPDH activity (Erales et al., 2011). Additionally, the crystal data agree with the results from EPR, which reveal that CP12 in *C. reinhardtii* remains mobile when bound to GAPDH (Lorenzi et al., 2011).

These data provide evidence that CP12-GAPDH is a fuzzy complex and that the role of CP12 might not be restricted to the regulation of the activity of the Calvin-Benson cycle enzymes (Gontero and Maberly, 2012).

CP12 is considered a conditionally unstructured protein. In the reduced state, CP12 is disordered and inactive; however, under an oxidising state, a more structured active protein is formed through the disulphide bridge and the α helix. The modelling of *C. reinhardtii* CP12 indicates that two α helices are present in the N-terminal and central regions of the proteins (Gardebien et al., 2006). On the other hand, only a single alpha helix is present in the C-terminal region of the GAPDH/CP12 binary complex of cyanobacteria and higher plants, whereas no structure is evident on the N-terminal region, indicating that his region is unstructured (Matsumura et al., 2011, Fermani et al., 2012). As mentioned above, in the reduced state, CP12 loses the conserved α helices and becomes fully unstructured and completely unfolded and is more flexible and mobile than oxidised CP12 (Gardebien et al., 2006, Gontero and Avilan, 2011, Matsumura et al., 2011, Fermani et al., 2012).

In higher plants, CP12 shows an increasing level of disorder compared to eukaryotic algae and cyanobacteria (apart from the green algal class Mesostigmatophyceae). This fact has led to the suggestion that CP12 has evolved to become more flexible, which affects the functionality of this protein and its ability to associate with a wider range of targets. These data indicate that CP12 may have additional roles in higher plants (Marri et al., 2010, Groben et al., 2010). According to the CP12 protein sequence from bioinformatics analysis, some structural similarity has been found with the copper chaperones from Arabidopsis which play many roles in copper homoeostasis (Himelblau et al., 1998, Mira Aparicio et al., 2001, Mira et al., 2001, Delobel et al., 2005). Additionally, *in vitro* metal binding studies have shown that *Chlamydomonas* CP12 can bind to nickel (Ni^{2+}) and copper (Cu^{2+}) ions. Despite the fact that the affinity for nickel is low (Kd11 μM), the affinity for copper (Kd 26 μM) is within the same range of those reported for prion protein (Kd of about 14 μM) and for

copper chaperone proteins (Multhaup et al., 2001, Cobine et al., 2002, Delobel et al., 2005, Erales et al., 2009a). These data revealed that copper ions can assist in the formation of a disulfide bond in reduced CP12 which leads to the recovery of oxidised CP12. This led to the hypothesis that the role of CP12 protein might be linked to the cooper metabolism (Delobel et al., 2005, Gontero and Maberly, 2012). On the other hand, structural studies have revealed that CP12 can bind with PRK and GAPDH in the presence or absence of copper ions. Also, the structure of the backbone of the binary complex GAPDH-CP12 of *Synechococcus elongatus* in both copper-free and copper-bond forms, revealing the same suggestion that copper is not important in terms of the role of CP12 in the GAPDH/CP12/PRK complex (Matsumura et al., 2011, Erales et al., 2009c).

1.10 Sequence of CP12 and CP12-like proteins in Cyanobacteria

A study which was conducted by Stanley et al. (2013) revealed an unexpected diversity of cyanobacterial CP12 proteins. In this study, a bioinformatics analysis of 126 cyanobacterial genomes, including five morphological subsections, reported that all contained one to five CP12 paralogs, with the exception of UCYN-A and *M. product* 3L (Stanley et al., 2013).

A number of 274 genes of CP12 were identified and divided into eight groups according to the key primary structure features. These features are as follows: the N-terminal Cys pair, the C-terminal Cys pair, a core AWD_VEEL sequence and an N-terminal cystathionine-β synthase (CBS) domain (Figure 1.6).

Among the total of 274 cyanobacterial sequences which were analysed, 120 were found to be similar to the higher plant-like CP12 (CP12-N/C). In addition, other types of cyanobacterial CP12 were reported: CP12 lacking both Cys pairs (CP12-0; eight sequences), CP12 containing only an N-terminal Cys pair (CP12-N; two sequences) and CP12 with only a C-terminal Cys pair (CP12-C; 53 sequences).

Interestingly, and unlike any known CP12 homologs in plants or algae, a large subset of 92 cyanobacteria CP12 genes were found to be fused to the CBS domain at the N terminus.

With this, three additional classes of CP12-like proteins were added: CP12-N/C-CBS (14 sequences), CP12-N-CBS (55 sequences) and CP12-0-CBS (23 sequences).

From the three types of fusion in the CP12-CBS domain, an additional layer of complexity in the role of CP12 proteins is present. Each type of fusion contains a single CBS domain. This domain includes regulatory modules in two or four tandem copies per proteins. They are present in functionally diverse proteins in all kingdoms

of life, including channel proteins, kinase, single transduction proteins and membrane proteins (Bateman, 1997, Stanley et al., 2013).

Several studies have shown that the CBS domain can bind to Mg^{2+}, single-stranded DNA and RNA, and double-stranded DNA (Kery et al., 1998, McLEAN et al., 2004, Scott et al., 2004, Hattori et al., 2007, Sharpe et al., 2008, Aguado-Llera et al., 2010, Feng et al., 2010).

To date, the majority of CBS domains have been identified as being able to bind adenine nucleotides as regulatory elements for sensing cellular energy status, resulting in inhibitory or activating roles. This could be a possible role of the CP12 CBS domains; each contains two copies of the nucleotide Rib-OP4-binding motif Ghx (T/S)x(T/S)D (Day et al., 2007). In higher plants, a large family of CBS domains containing protein have been reported; however, there is no evidence for the presence of CP12-CBS fusion (Kushwaha et al., 2009).

The unexpected diversity of CP12 proteins in cyanobacteria together with the presence of the CBS domain fusions including the variation in the distribution of the key structural features indicate an unknown layer of regulatory complexity in the function of CP12. Additionally the fusion of CP12-CBS domain which present in cyanobacteria functionally connect CBS domain and CP12. The findings from this study raise a question whether in plants CBS and CP12 proteins play a redox relay-type role which may act as a metabolic switches. The diversity of cyanobacterial CP12 proteins and the fusion of CBS-CP12 may have evolved to cope with the requirement to trigger different metabolic processes in response to the rapid fluctuating environment (Stanley et al., 2013).

In addition, as other intrinsically disordered proteins (Tompa et al., 2005), several CP12 variants may moonlight, interacting with multiple proteins in various confirmations to enable multiple functions (Stanley et al., 2013).

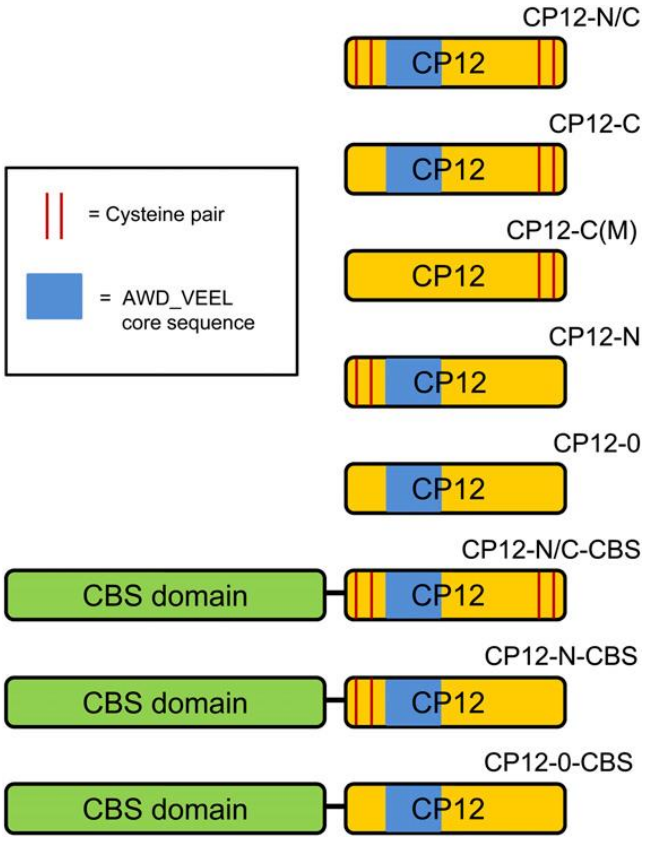

Figure 1.6 Schematic diagram of the different types of cyanobacterial CP12. The yellow rectangles are CP12 sequences, the blue boxes are AWD_VEEL core sequences, the green rectangles are the CBS domain, and red lines are the cysteine pairs. Diagram taken from (Stanley et al., 2013).

1.11 CBS and CBS domains in Arabidopsis

Cystathionine β synthase (CBS) is the first enzyme involved in the reverse transsulfuration pathway in which homocysteine is converted to cysteine via cystathionine (Aitken and Kirsch, 2005). The CBS domain was discovered by Bateman in the archaebacterium genome; *Methanococcus jannaschii* as a conserved domain in a group of proteins (Bateman, 1997). This domain exists in all archaebacterial, eubacterial and eukaryotic proteins and usually occur in tandem repeats (Ignoul and Eggermont, 2005).

Cystathionine β synthase (CBS) domain-containing proteins (CDCPs) comprise a large superfamily of proteins which have conserved CBS domain and they are ubiquitous in all three life's domains; archaea, bacteria and eukaryotes.

Analysis of the functions of different CBS domain containing protein revealed the importance of CBS pair by linking mutations of CBS domain of enzymes and other proteins to different hereditary disease in human including cystathionine β synthase in homocystinuria (Shan et al., 2001), AMP-activated protein kinase in familial hypertrophic cardiomyopathy (Blair et al., 2001, Gollob et al., 2001, Arad et al., 2002) inosine-5'monophosphate dehydrogenase in retinitis pigmentosa (Kennan et al., 2002), and chloride channels in myotonia congenital (Pusch, 2002). According to these studies and based on the structural analysis (Zhang et al., 1999, Mindell et al., 2001), it's now known that a CBS pair binds adenosine-containing ligands such as AMP, ATP or S-adenosylmethionine and the mutations within this domain can affect the functions of these disease-related CDCPs.

However, the significance importance of CBS domain in plants in still obscure, but it has been suggested to have a role in the regulation of different enzymes which in turn can contribute to the maintenance of the intracellular redox balance. In the study conducted by Kushwaha et al. (2009) which was based on the comprehensive analysis of expression pattern using existing transcriptome profile and massively Parallel signature sequences data base, suggested a few CDCPs may involve in the stress tolerance/response and development in the plants. However, the precise functions of both CBS and CDCPs in plants still not identified (Kushwaha et al., 2009).

In the same study, a genome-wide analysis was performed on *Arabidopsis thaliana* and *Oryza sativa,* including identifying and classifying the CDCPs according to their conserved features. Based on the standard bioinformatics tool, a total of 34 proteins (encoded by 33 genes) were identified in Arabidopsis along with 59 proteins (encoded by 37 genes) in Oryza. These proteins were divided into two major groups containing either a single CBS domain or two CBS domains. In Arabidopsis, the single CBS domain containing proteins was classified into six subgroups, whereas in Oryza, the CDCPs were classified into seven subgroups. The two CBS-containing proteins were classified into two subgroups for both Arabidopsis and Oryza (Figure 1.7) (Kushwaha et al., 2009).

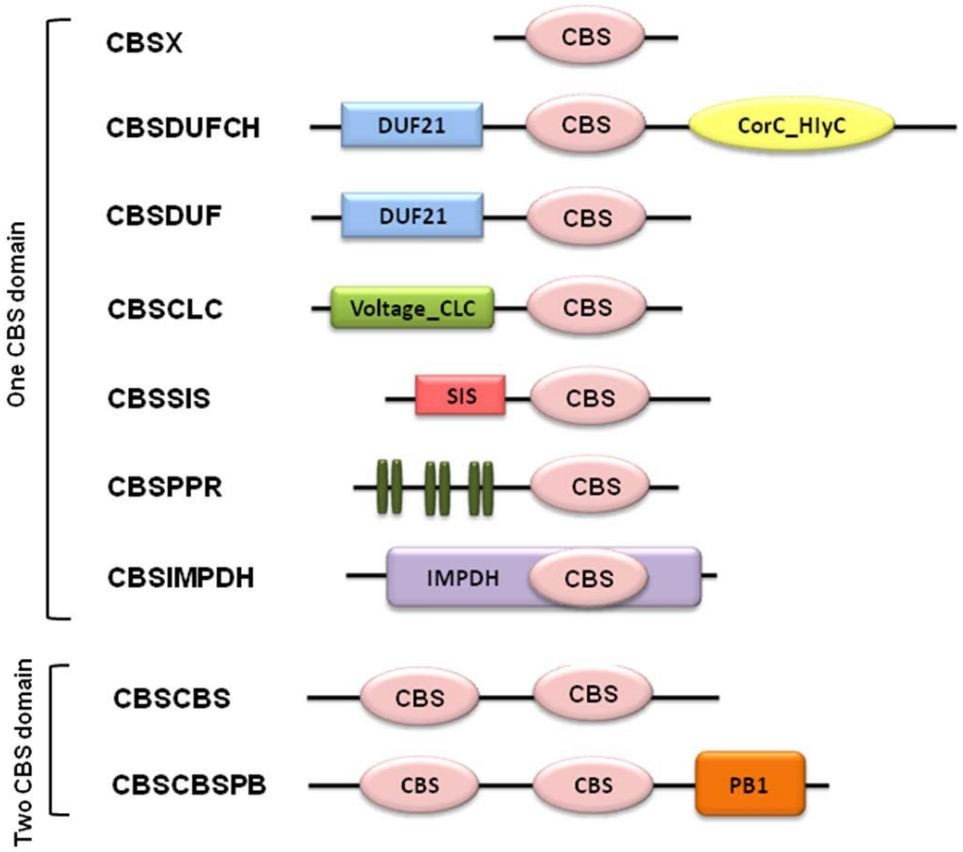

Figure 1.7 The primary domain structure of CBS-domain-containing proteins in *Arabidopsis thaliana* and *Oryza sativa*. CDCPs were classified into two main groups: proteins containing a single CBS domain and two CBS domains. The former group was further divided into six subgroups in *Arabidopsis* based on the other domains present in the protein sequences. The proteins containing a single CBS domain were named CBSX, with the six subgroups being named according to their functional domains (Kushwaha et al., 2009).

The major division of CDCPs containing only one CBS domain is designated CBSX.

Six genes were identified to encode six CBSX proteins in *Arabidopsis thaliana* which localise in different cellular compartments. CBSX1 and 2 were found to be located in the chloroplast, CBSX3 in the mitochondria, CBSX4 in the cytosol, and finally, CBSX5 and 6 in the endoplasmic reticulum.

A study of the chloroplastic single CBS domain containing proteins in Arabidopsis, which was conducted by Yoo et al. (2011), showed that this domain stabilises cellular homeostasis and modulates development via the regulation of the TRX system by sensing change in adenosine-containing ligands. In this study, two of the chloroplast CBSs were identified: CBSX1 and CBSX2 and found to be able to activate all four types of TRX in the ferredoxin-TRX system (FTS). Furthermore, the study revealed that CBSX1 can regulate TRXs and in turn control the level of H_2O_2 which regulates lignin polymerisation in the anther endothecium. In addition, both CBSX1 and 2 were found to form a dimer under oxidative stress conditions, and the level of reduced TRX m and f in these mutants increased (Yoo et al., 2011). This process maintains a high level of reduced CP12, which in turn modulates the Calvin-Benson cycle activity. The CP12 protein may also affect the ability of CBS proteins to dimerise in response to the redox state in the chloroplast through the TRX. No direct evidence has been identified so far to support this idea; however, it is worth considering, given the presence of the fusion of CP12 with CBS in cyanobacteria (Lopez-Calcagno et al., 2014).

1.12 Possible roles of CP12 genes in higher plants

Despite considerable data revealing the importance of CP12 proteins in the regulation of the Calvin-Benson cycle enzymes PRK and GAPDH through the formation of the multienzyme complex, the possibility of wider roles for these proteins in redox regulation mechanisms remains to be investigated. Further questions regarding the role of CP12 proteins need to be addressed (Lopez-Calcagno et al., 2014). As mentioned previously, in higher plants, CP12 is encoded by a multigene family with different patterns of gene expression, which indicates that each isoform may have an individual or overlapping function (Singh et al., 2008, Marri et al., 2005a). A study of antisense CP12 in tobacco resulted in a complex phenotype, which reveals the importance of these proteins for normal growth and development in higher plants (Howard et al., 2011a). A wide diversity of CP12 protein sequences have been identified in about 126 species of cyanobacteria, indicating a wider role of CP12 and CP12-like proteins in this organism (Stanley et al., 2013). Finally, the unique structure of CP12 suggests that it is an IUP (Graciet et al., 2003a, Gardebien et al., 2006). Members of the IUP group have the ability to interact with a number of different molecules in the cell (Tompa, 2002, Dyson and Wright, 2005), which increases the likelihood that CP12 may also be able to interact with other proteins in the chloroplast (Singh et al., 2008). All these data indicate that CP12 proteins may have an additional role in the regulation of metabolism, besides the well-established role of CP12 in the regulation of the Calvin-Benson cycle (Lopez-Calcagno et al., 2014).

The high level of expression of GapA, GapB, PRK, CP12-1 and CP12-2 in photosynthetic tissues (leaves and flower stalks) and the undetectable expression of these genes in *Arabidopsis thaliana* roots and siliques support the role of CP12 in photosynthesis. When *Arabidopsis thaliana* leaves were subjected to prolonged dark

treatment, a rapid decline of GapA, GapB and PRK transcripts was noticed. Among the CP12 transcripts, CP12-2 declined rapidly, but CP12-1 was expressed at a constant level even after five days of exposure to darkness. This shows that in addition to promoting the formation of the multiprotein complex, CP12-1 may perform other vital physiological roles (Marri et al., 2005a).

As mentioned previously, chloroplastic TRX *f* and TRX *m* mediate the formation of the complex of CP12 with PRK and GAPDH via the regulation of the changes in the redox state of the two cysteine pairs. The expression of TRX *f* and *m* in a wide range of non-photosynthetic tissues, such as roots, flowers, seeds and pollen grains, opens the possibility that CP12 may function with TRX isoforms to form a redox network, which in turn may regulate metabolic processes in plastids in response to the varying availability of reducing power (Howard et al., 2008, de Dios Barajas-López et al., 2007, Traverso et al., 2008, Singh et al., 2008).

CP12 has been detected in all photosynthetic organisms. Studies of gene sequences have shown an evolutionary trend towards increased protein disorder in higher plants, which can be correlated with their potency to have multiple partners. Due to its interaction with multiple partners, CP12 may act as a regulatory hub and has been propose to be able to interact with enzymes, including aldolase and malate dehydrogenase (Erales et al., 2008, Gontero and Maberly, 2012). Its interaction with enzymes other than PRK and GAPDH may facilitate functions such as protecting GAPDH from inactivation, regulating stress response and scavenging metal ions, including nickel and copper (Gontero and Maberly, 2012). These findings not only suggest that CP12 can perform multiple functions in addition to regulating the Calvin-Benson cycle but also suggest the need for further research into these multiple roles.

1.13 Aims of the Project

The role of CP12 as an integral component of the GAPDH/CP12/PRK complex has been studied extensively in several species of plants. However, it is not clear whether these three proteins have separate or overlapping roles. This project aims to explore the possibility whether CP12 proteins perform additional functions in higher plants generally and in *Arabidopsis thaliana* specifically. This aim will be achieved by taken several approaches:

- A collection of T-DNA insertional mutant plants, including single, double and triple mutants were used, to investigate the phenotype for slow growth and development.
- RNAi constructs were used to create a null CP12 mutant plant. This is a useful tool which allows researchers to study the gene function.
- Based on the study of cyanobacterial CP12 which demonstrated the fusion of CP12-CBS domain. A question has been raised in higher plants whether CP12 can act with CBS domain. A cross of CBS and CP12 was made to study the possibility of these proteins acting together.

CHAPTER 2

Materials and Methods

2.1 DNA Extraction

Genomic DNA was extracted from plants using the protocol described by (Edwards et al., 1991) with some modifications. The genomic DNA was isolated as follows; a leaf disk was taken, using a 1.5 mL microcentrifuge tube lid. Then, 200 µL of DNA extraction buffer was added (200 mM Tris-HCL pH7.5, 250 mM NaCl, 25 mM EDTA, 0.5% SDS) to the leaf. The leaf was ground using a special pestle and the material was incubated for about two minutes at room temperature, and then centrifuged for 5 minutes at maximum speed in a conventional table top micro centrifuge. Next, the supernatant was carefully removed and placed into a new tube. In the next step, 150 µL of isopropanol was added to the tube and mixed by inverting the tube several times. The tube was centrifuged twice for 10 minutes at maximum speed in a conventional tabletop microcentrifuge. DNA was left for about 10 minutes and allowed to air dry, and then resuspended in 50 µL of TE buffer (10 Mm tris-Cl, Ph 7.5,1 Mm EDTA) and stored at -20° C.

2.2 Primer design

All primers used in this thesis for screening, qPCR and cloning were designed according to the gene sequences of Arabidopsis using available following software:

Primer3 (http://biotools.umassmed.edu/bioapps/primer3_www.cgi),

NCBI tool for primer design (http://www.ncbi.nlm.nih.gov/tools/primer-blast/) and for the qPCR analysis the following website were used: (htt://www.roche-applied-science.com/sis/rtpcr/upl/index.jsp).

2.3 Polymerase chain reaction (PCR)

Polymerase chain reaction (PCR) was performed in 0.2 mL PCR tubes using Dream Taq (Fermentas). For each reaction using Taq DNA polymerase, 0.2 mM dNTPs (0.5 µL of 10 mM stock per each 20 µL PCR reaction) and the recommended amount of enzyme and buffer were added. The forward and the reverse primers were designed and DNA were added to the master mix and volume was made up to 20 µL with RO water. The condition used for the PCR reactions were varied depending on the expected size fragments to be amplified. Appendix 1 and 2 represent information on the annealing temperature and the expected fragments size.

The condition was used in most of the PCR reactions were as following: an initial denaturation at 95 ˚C for 3 minutes; 35 cycle of denaturation at 95 ˚C for 30 seconds, primer annealing at 60 ˚C for 30 seconds and extension at 72 ˚C for 1 minute; final extension at 72 ˚C for 7 minutes.

2.4 Agarose gel electrophoresis of nucleic acids

The PCR products were mixed with 6X DNA loading dye and the DNA was separated for the analysis using gel electrophoresis. The PCR products and the dye were run on 1% agarose gel at 100 volts for 30 minutes alongside the GeneRuler^{TM} DNA ladder Mix from ThermoFisher Scientific. Either Tris-borate buffer (TBE:89mM Tris, 89mM Boric acid, 2 mM EDTA) or Tris-acetate buffer (TAE: 40mMTris ultrapure, 20 mM Acetic acid glacial, 1mM EDTA.Na_2) was used to prepare the gels and running buffer in the tanks. The agarose gel was stained with SafeView and DNA was visualised under UV light using the GeneGenius Bioimaging system.

2.5 Transformation of *E. coli* Component Cells

E. coli chemically competent cells were transformed using heat shock method described by (Sambrook and Russell, 2001). 1-2 µL of the plasmid DNA or TOPO® cloning reaction mixture was added to 50 µL of aliquot of *E. coli* competent cells, this was gently mixed and then incubated on ice for 30 minutes. Heat-shock was performed in water bath at 42 ˚C where the cells incubated for 50-90 seconds and then placed immediately on ice for 2 minutes. After that, 250 µL of Luria-Bertani broth (LB) media was added to the cells and incubated at 37 ˚C with gentle shaking for 1 hour. Finally, the cells were spun and re-suspended in a smaller volume of LB and then spread on selective media and incubated at 37 ˚C for overnight.

2.6 Plasmid DNA preparation

A QIAgen Mini Plasmid preparation kit was used to extract high-purity plasmid DNA from *E. coli* cells according to the manufacturer's instructions. 10 mL of LB media, including antibiotics (50 µg/mL kanamycin, 30 µg/mL hygromycin or other depending on the plasmid) and a colony from a fresh plate, were grown overnight at 37 ˚C. After incubation, 3–10 mL of this culture was spun down and the cells were re-suspended in 250 µL of Buffer P1, which contained RNase A. Following this, 250 µL of Buffer P2 was added and the tube was inverted 4–6 times. Then, 350 µL of Buffer N3 was added and the tube was immediately inverted 4–6 times. The tube was centrifuged for 10 min at maximum speed, and the supernatant was applied to the QIA prep spin column. The column was spun down for 45 seconds at maximum speed, and the flow-through was discarded. The column was washed twice using 500 µL of the PB Buffer for 30–60 seconds, and the flow-through was discarded. Once the column was washed, it was transferred into a clean 1.5 mL tube, and 50 µL EB Buffer (10 mM Tris

Cl, pH 8.5) or water was added to the centre of the column. This was incubated for 1 minute at the room temperature and centrifuged for 1 minute. The purified Plasmid DNA was stored at -20˚C.

2.7 Transformation to *Agrobacterium* using the electroporation technique

The *Agrobacterium tumefaciens* strain GV3101 competent cells were used, and the transformation was performed using the electroporation technique according to the protocol described by (Sambrook and Russell, 2001).

To perform the transformation, 40 µL of the competent cells was gently mixed with 1–2 µL of the plasmid DNA and placed on an ice-cold cuvette. Using the EasyJet Prima electroporator from EQUIBIO, the cells were electroporated at 2500 V. Then, 1 mL of LB was immediately added. Following that, the cells were placed into a 1.5 mL tube and incubated for 2 hours at 28˚C under gentle shaking. After the transformation, 100–200 µL of the culture was spread on LB plates along with the antibiotics and allowed to grow for 48 hours at 28˚C.

2.8 Colony PCR screening

Colony PCR was performed on colonies to confirm the positive transfomants. The PCR mix was set up as mentioned previously and the DNA was added to the mix either by dipping a tip which was already dipped in a middle of a fresh colony or by adding 2-4 µL of quickly washed cells. The washed cells were prepare by centrifuging 20-40 µL of fresh liquid culture at 3000 g for 5 minutes. Next, the pellet was re-suspended in 50 µL of ddH_2O. The PCR products were run on 1% agarose TBE or TEA as mentioned before.

2.9 Screening of mutants

The identification and the confirmation of the Arabidopsis T-DNA insertion mutants was conducted by PCR analysis. For this, the following primers were used to detect the WT and T-DNA insertion alleles.

For screening CP12-1 gene the forward primer 5’ CAAGCTTTATGAAAGCGCATC 3’ and the reverse primer 5’ CGACATCATCAGTCTCAGG 3’ were used. For the insertion of CP12-1 the border primer for SALK mutant was used 5’ GCGTGGACCGCTTGCTGCAACT 3’. To detect the gene for CP12-2 the following primers were used 5’ TCAGCTTTAGGAATCGTGAGC 3’ and the reverse primer was 5’ TACGTCCGATATCCCTCCTTC 3’ and the primer 5’ ATATTGACCATCATACTCATTGC 3’ was used as the boarder primer to detect the insertion. For CP12-3, the gene specific primers which were used were: 5’ TTCATCAGTCAGTATCGATGGG 3’ and 5’ AACACGATGAACAACGGTTTC 3’ as a left and right primers respectively and the insertion specific primer was 5’ GCCTTTTCAGAAATGGTAAATAGCCTTGCTTC 3’.

Four of CBSX T-DNA insertion mutant lines were identified by PCR screening. For this the following primers were used: for CBCX1 SALK_038094 allele the forward primer 5' TCTTCTCTCCTAGGGCGAGTC 3’ and reverse primer 5’ CTAGGCTAAGATCGAATCCCG 3'. For the insertion of this gene the reserve primer was used with the left boarder of the SALK mutant 5' GCGTGGACCGCTTGCTGCCAACT 3'. For CBSX1 GK-050D12-012185 allele forward primer 5' CCATTGGTTTTGCTGAGTAGC 3' and reverse primer 5’ TTGACGAAGACTGGAAATTGG 3' and for the insertion specific primer 5’ GTGGATTGATGTGATATCTCC 3’, were used. For the CBSX2 SALK_136934 the

forward primer was 5' TTTCCAGTACATTGCGTCATG 3’ and the reverse primer was 5' CAGAAGTTCCAACGCTGAAAG 3'. For the CBSX2 SALK_021868 forward primer was 5’ AAAGTCTTCATCTACGCCAAGG 3' and the reverse primer was 5' TGTCTCGGAGTCATGAAATCC 3'. For both CBSX2 insertion reactions the left boarder primer for SALK were used.

2.10 Total RNA and protein extraction

The total plant RNA was isolated using the NucleoSpin® RNA/Protein kit from (MN). Approximately 100 mg of plant tissue was grounded until it became powder, then it was placed in a 1.5 mL tube and used immediately or stored at -80ºC. 350 µL of the lysis buffer and 3.5 µL of β-mercaptoethanol were added to the disrupted tissue and vortexed vigorously. This mixture was placed in the NucleoSpin® Filter and centrifuged for 1 minute at 11,000 x g to clear the lysate. Then, 350 µL of 70% ethanol was added and mixed by pipetting up and down approximately five times. The samples were loaded into the NucleoSpin® RNA/Protein column and centrifuged for 30 seconds, and the flow-through was recovered for the protein assay. Next, 350 µL of the Membrane Desalting Buffer was added and centrifuged for 1 minute. Following this, 95 µL of the rDNase reaction mixture was applied directly to the middle of the silica membrane of the column and incubated for 15 minutes at room temperature. After that, the silica membrane was washed using Buffers RA2 and RA3 and centrifuged for 30 seconds. Finally, the RNA was eluted in 60 µl of RNase-free H_2O and centrifuged for 1 minute.

The RNA was quantified and ascertained by spectrophotometry, using NanoDrop TM ND-100 Spectrophotometer (ThermoFisher Scientific) as the manufacturer’s instructions.

200-500 ng of RNA was taken into a separate tube to convert to cDNA. A mix of Oligo dT, dNTPs and the enzyme RevertAid Reverse Transcriptase was added to each RNA sample and incubate under the following conditions: 25 ˚C for 10 minutes, 42 ˚C for 60 minutes and 70 ˚C for 10 minutes.

2.11 Quantitative reverse transcription PCR (qPCR)

SYBR Green detection chemistry was used to perform quantitative real-time PCR (qRT-PCR). The plate was organized in triplicate reactions on a 96-well plate (Greiner, UK) using the iCycler iQ thermocycler (Bio-Rad). The total volume of each reaction was 15 µL which consisted of 2 µL of cDNA (0.05µg/ µL of RNA), 7.5 µL of the SensiFast SYBR Taq mix and 0.4 µL of primers. Also, for each master mix a blank control were run in triplicate. The conditions for the qPCR were as follows; the first step involved the initial denaturation at 95˚C for 10 minutes to activate the polymerase, followed by 45 cycles of denaturation at 95˚C for 15 seconds, annealing at 60˚C for 30 seconds and extension at 72˚C for 30 seconds. After that, a melting curve analysis was performed while increasing the temperature 0.1˚C every 10 seconds, from 60˚C to 90˚C. The baseline and threshold cycles (Ct) were determined using Bio-Rad iQ software 3.0 to verify the amplification of just a single product.

2.12 Protein Extraction

Leaf tissues approximately 30 mg were collected and stored into -80 °C. Frozen leaf was ground by using liquid nitrogen and cold mortar and pestle into powder. Protein extraction buffer (50 mM 4-(2-Hydroxyethyl) piperazine-1-ethanesulfonic acid (HEPES) pH 8.2, 5 mM MgCl2, 1 mM Ethylenediaminetetraacetic Acid Tetrasodium Salt (EDTA), 10% Glycerol, 0.1% Triton X-100, 2mM Benzamidine, 2mM Aminocaproic acid, 0.5mM Phenylmethanesulfonyl fluoride (PMSF)) was added to the extraction then it was transferred into a cold 1.5 mL microcentrifuge tube. Tubes was spun at 1400 g for 2 minutes at 4°C, then the supernatant was collected and aliquoted to 100µL for Bradford assay and SDS-PAGE analysis. Samples were stored at -80 ˚C.

2.13 SDS-PAGE

Denaturing gel electrophoresis, sodium dodecyl sulphate polyacrylamide gel electrophoresis (SDS-PAGE), was used in order to separate protein for analysis. This method was described by (Laemmli, 1970). Resolving gel used 12% acrylamide in Tris HCl (pH8.8) and stacking gel 5% acrylamide in Tris-HCl (pH 6.8). The gel was run in Tris-Glycine buffer (25 mM Tris, 192 mM Glycine, 0.1% SDS, pH 8.3) for 70 minutes at 110 volts. For reducing SDS-PAGE, samples were mixed previously with 0.3 µL volumes of denaturing buffer (313mM Tris-HCl pH 6.8. 25% Glycerol, 25% β-Mercaptoethanol, 10% SDS) and then the samples were boiled for 5 minutes and centrifuged at maximum speed for 1-5 minutes before loading.

2.14 Western blot

Proteins which were separated by using SDS-PAGE were transferred to PVDF membrane. Then blocking were performed using PBS (137 mM NaCl, 2.7 mM KCl, 10 mM Na_2HPO_4, 2mM KH_2PO_4) + 6% non-fat milk for one hour at room temperature. Three times washing was applied by using PBS +0.05% tween 20 for 10 minutes each. Membrane was incubated with the primary antibody (PBS+30% non-fat milk + antibody) for overnight at 4°C. Washing step was repeated before applying the secondary antibody (0.4 µL/mL anti-rabbit lgG, horseradish peroxidase (HRP) conjugated from Promega) and finally three washes were performed for 10 minutes. For detection, the membrane was incubated for 1 minute in 3 mL of PIERCE ECL Western Blotting substrate. Finally the membrane was exposure by automated western blot imaging system (Fusion FX).

2.15 Plant material and growth conditions

Both T-DNA insertion mutants and the WT from *Arabidopsis thaliana* ecotype Col-0 for CP12-1: SALK_008459.27.80.X (*cp12-1*), CP12-2: GK_397A01_017930 (*cp12-2*) and CP12-3: SAIL_854_F09v2 (*cp12-3*) all in Col-0.

CBSX T-DNA insertion lines from *Arabidopsis thaliana* ecotype Col-0 for CBSX1: SALK__038094 (*cbsx1.2*) and GK-050D12-012185 (*cbsx1.3*) and for CBSX2: SALK_021868 (*cbsx2.1*) and SALK_136934 (*cbsx2.2*). All plants were grown in a growth chamber at 22 ˚C under short day (photoperiod: 8 h light/16 h dark) or long day conditions (photoperiod: 16 h light/8 h dark) and 60% relative humidity (RD), under a photosynthetic photon flux density of about 200 $\mu molm^{-2}s^{-1}$.

For *in vitro* growth of Arabidopsis's seedlings, seeds were surface sterilized and sown on half MS medium without sugar and 0.8% agar. For growth on soil, seeds were

sown (or transferred from plates) into pots containing compost (Levington F2+S, The Scotts Company, Ipswich, UK) of 6 cm diameter plastic pots.

2.16 Seeds sterilization

Arabidopsis seeds were sterilized by the methods described by (Singh, 2007). Seeds were stored at 4 °C for two days before sowing for stratification (to encourage uniform germination). After that, plates were transferred to the growth chamber. In the flow hood, the surfaces of seeds were sterilized by submerging them in a solution of 95% ethanol and 0.1% tween for three minutes. Next, the solution was removed and seeds were rinsed three times with 75% ethanol. Seeds were placed on sterilized filter paper to allow them dry then seed were sown immediately.

2.17 Arabidopsis crosses

The crosses of Arabidopsis was performed under a binocular dissecting microscope. Fine type 7 (T148: TAAB Laboratories Equipment Ltd) forceps were sterilized by 95% ethanol, then washed with RO water and dried before it was used. Crosses were achieved by transferring the pollen to stigma of emasculated flower. 2-5 closed flowers were selected and emasculated. These were fertilized immediately by tapping mature anthers from one line on to a sticky stigma of the other line until it was covered with pollen. The fertilized inflorescence were placed inside small plastic bag which made of cling film wrap to protect them from drying. Plants were kept in long day growth conditions and the siliques were allowed to develop. Fully developed siliques containing hybrid seeds were obtained within 25 days. After that, in order to confirm the crossing, DNA was extracted and plants from F1, F2, F3 and F4 generations were

screened for the presence of the WT and the mutant allele by PCR using DreamTaq polymerase.

2.18 Arabidopsis plant transformation

The *Arabidopsis thaliana* transformation was conducted using a floral inoculating method according to the protocol described by (Bent and Clough, 1998, Narusaka et al., 2010) with some modifications. First, the plants were grown in the short-day chamber with 8 hours light and 16 hours dark for four weeks. Then, they were moved to the long-day chamber (16 hours light and 8 hours dark) for four weeks until they were flowering. To enable the proliferation of many secondary blots, the first bolts were cut and the plants were inoculated a week later. After that, 10 mL of LB with required antibiotics (rifampicin (Rif) 50 μg mL^{-1}, gentamicin (Gen) 25 μg mL^{-1}, kanamycin (Kn) 50 μg/mL and approximately 33 μg mL^{-1} hygromycin (Hg)), were grown overnight at 28˚C.

The bacteria were then spun down at 3000 g for about 20 minutes and re-suspended in 5% sucrose solution to an OD of about 0.8. Prior to inoculating, 0.05% (500 μL/L) Silwet L-77 was added and 5 μL of the *Agrobacterium* inoculum was put on each flower bud. Each plant was inoculated with approximately 30–50 μL of the *Agrobacterium* inoculums. The plants were covered with a plastic autoclave bag and were kept in the dark for 24 hours at 18 ˚C. The plants were then moved into the greenhouse, and the seeds were harvested. The transformants were selected by growing them in plates containing antibiotics for 15–20 days, and then the plants were potted into individual pots and allowed to grow and produce seeds.

2.19 Gas exchange analysis

The assimilation rate response of CO_2 (*A*) to the concentration of the intercellular CO_2 (C_i) was determined at saturating light level (1000 µmol photon m^{-2} s^{-1}) with a leaf temperature of 25 ± 1.5 ˚C, by using an open infrared gas analyser (IRGA) (CIRAS-1;PP-System, Hitchin, Herts. UK). Before using IRGA, it was calibrate against standard of known CO_2 (Linde Gas Ltd, Stratford, London, UK).

Photosynthetic carbon fixation rate was determined at a range of CO_2 concentrations (from 0 to 1150 µmol mol^{-1}). The measurement started with 400 µmol mol^{-1} of CO_2 concentration which is the ambient concentration which plants had grown. Next, it was decreased to 250, 150, 100, and 50 and then increased to 400, 550, 700, 900, and 1150 µmol mol^{-1}. The data obtained from these measurements was used to calculate the *A* and C_i using the equations of (Von Caemmerer and Farquhar, 1981).

2.20 Fluorescence imaging

Chlorophyll fluorescence imaging (CF imaging) was performed by the FluorImager analytical instrument as described by (Barbagallo et al., 2003). Images were processed using version 2.229 FluorImager application software (Technologica Ltd., Colchester, Essex, UK). For this, seedlings of different ages (14, 18, 20 and 22 days) were grown in a controlled environment chamber at 130 µmol mol^{-2} s^{-1} and ambient (400 µmol mol^{-1}) CO_2, and were imaged directly in ½ MS agar plates. The operating efficiency of photosystem II (PSII) photochemistry, *F*q *′*/*F*m*′*, was calculated from measurements of steady-state fluorescence in the light (*F′*) and maximum fluorescence in the light (*F*m′) was obtained after a saturating 800 ms pulse of 6200

µmol m^{-2} s^{-1} PPFD using the following equation $Fq'/Fm' = (Fm'-F')/Fm'$. Images of *Fq′/Fm′* were taken under stable PPFD of 130 and 300 µmol m^{-2} s^{-1} PPFD.

2.21 Rosette area calculations

Rosette area of plants at different ages was determined from images which were captured through digital camera. After that, images were processed using ImageJ image processing software (htt://rsb.info.nih.gov/ij/index.htmil). All processed images were statistically tested by Kruskal-Wallis followed by Mann-Whitney tests ($P< 0.05$) using SPSS (Statistical Product and Service Solutions) from IBM in order to determine the significance among certain lines.

2.22 Rosette fresh and dry weight

At the end of the growth analysis and prior to the flowing (bolting), the fresh and the dry weight were determined by weighing freshly detached rosette on scale. After that, each rosette was place individually in a paper bag and kept in an oven at 80 ˚C until stable weight was reached (approximately one week).

2.23 Root growth analysis

Plants were grown in square Petri dishes and positioned vertically in the growth chamber of long day conditions in order to determine the primary root length and the number of lateral roots.

All plates were scanned and the length of the primary root were measured using ImageJ software. The number of the lateral root were determined by counting them in each time point.

2.24 H_2O_2 determination

Frozen leaves (100 mg) were ground on ice with 100 Mm HCl solution and centrifuged at 12000 *g* for 10 min at 4 °C. Activated charcoal columns were used to purify the supernatants. Homovanillic acid (HVA; #306-08-1, Sigma-Aldrich®; (Guilbault et al., 1967)) was used to measure the H_2O_2 concentration. Briefly, 45 μL of a buffer containing 1 mM of HVA, 48.5 mM of HEPES and 20 U ml^{-1} of horseradish peroxidase (#P8375, Sigma-Aldrich®) was added to 5 μL of each extract. An HPLC system was used to measure H_2O_2 at an excitation of 315 and emission of 425 nm. A standard curve of known H_2O_2 concentrations was used to determine H_2O_2 for each sample.

2.25 Measurement of Chlorophyll

100 mg of leaf tissue was collected in 1.5 mL of centrifuge tube and frozen on dry ice to measure the level of Chlorophyll a and Chlorophyll b. the samples were ground in 1 mL of 80% Acetone using a mortar and pestle and placed on ice. After that, the samples were centrifuged at 10000 *g* for 5 minutes at 4 ˚C. 200 μL of the supernatant was used to measure the absorbance at 663 nm and 646 nm using a SPECTROstar Omega microplate reader (BMG LABTECH). Chlorophyll a and b were calculated per fresh weight using the following for

$$\text{Chlorophyll a} = \frac{(12.15 \times A_{663}) - (2.55 \times A_{646})}{\text{Fresh Weight}}$$

$$\text{Chlorophyll b} = \frac{(18.29 \times A_{646}) - (4.58 \times A_{663})}{\text{Fresh Weight}}$$

CHAPTER 3

Molecular analysis of the CP12 protein family in *Arabidopsis thaliana* plants

Introduction

CP12 was originally characterized as a small redox-sensitive chloroplast protein which has the ability to interact with two enzymes of the Calvin-Benson cycle PRK and GAPDH, forming a multi enzyme complex. This complex has been identified in a number of higher plants (Wedel et al., 1997, Scheibe et al., 2002, Howard et al., 2011b, Wedel and Soll, 1998) and algal species (Avilan et al., 1997, Boggetto et al., 2007, Oesterhelt et al., 2007). In higher plants there are three CP12 proteins, two that are highly similar, CP12-1 and CP12-2, and CP12-3 which has much lower amino acid similarity to the other two. Expression patterns of these three genes have been shown by both RT-PCR and promoter GUS fusions to have both overlapping and distinct features. Interestingly, these lines expressing *CP12::GUS* constructs displayed different expression patterns through *Arabidopsis thaliana* tissues. The most unexpected finding from this study was that all CP12 genes were expressed in the floral tissues. CP12-1 and CP12-2 were expressed in the sepals and styles, however, the expression of CP12-3 was detected in the stigma and the anthers (Singh et al., 2008, Marri et al., 2005a). The role of CP12 in the regulation of Calvin-Benson cycle within the complex has been well studied, however, it is still not clear whether these proteins have separate or overlapping functions in higher plants. Considering that there has been no previous comprehensive study focusing on the role of the individual Arabidopsis CP12 proteins *in vivo,* we decided to exploit the availability of tools generated in the lab previously together with the development of new ones, allowing us to study and to understand each form of CP12 protein individually.

The aim of this chapter is to create tools which will enable the study of the role of CP12 protein family in Arabidopsis.

T-DNA insertion mutant lines of *cp12-1*, *cp12-2* and *cp12-3* were selected previously using the TAIR database. These lines were then identified and characterised to confirm the T-DNA insertions. Crossings were made among these lines with the aim of producing multiple mutant lines which were *cp12-1/2*, *cp12-1/3*, *cp12-2/3* and *cp12-1/2/3* (Lopez-Calcagno, 2013). In this chapter, first of all we performed a molecular characterisation of the T-DNA insertion lines which include the single mutant lines, double and the triple mutant CP12 lines by PCR analysis.

The previous analysis of the T-DNA insertion mutant lines revealed that CP12-1 and CP12-3 were a knock out (KO) lines. However, CP12-2 insertion line was a knockdown (KD) with about 50% reduction in the transcript level (Lopez-Calcagno, 2013). Because *cp12-2* mutant line is a knock down and not a knock out, we have used the RNAi technique with a view to obtaining a knock out line.

Additionally because we have only one mutant allele for each CP12 gene, we have taken a complementation approach in order to provide evidence that an insertional mutation is the only reason which may cause a phenotype.

Results

3.1 Identification and characterisation of *Arabidopsis thaliana* CP12 insertion lines

The identification and the characterisation of the T-DNA insertion mutant lines as well as producing the double and the triple mutant were conducted in the lab previously by Patricia Lopez –Calcagno (Lopez-Calcagno, 2013).

For this, The Arabidopsis Information Resource (TAIR) data base was used to search the T-DNA insertion mutant lines for all three CP12 genes; CP12-1 (At2g47400), CP12-2 (At3g62410) and CP12-3 (At1g76560).

Four lines were selected according to the position of the insertion also based on the possibility of the insertion to interfere the expression of the genes.

In order to screen for the homozygous lines, two types of primers were used; gene specific primers (GSP) and insertion specific primers (ISP). The former primers were used to amplify the fragments of WT allele and the latter primers were designed to amplify the T-DNA insert in the mutant lines.

Our analysis confirms that all lines were homozygous lines for the expected T-DNA insertion.

3.1.1 Confirmation of the CP12 single insertion lines *cp12-1*, *cp12-2* and *cp12-3*

In this study, we have focused on three of the T-DNA insertion lines, one line for each CP12 gene. These lines were identified from the TAIR database according to the previously described criteria. For each CP12 gene, one T-DNA mutant line was selected as followed; CP12-1 SALK 008459.27.80.X (*cp12-1*), CP12-2 GK_397A01_017930 (*cp12-2*) and CP12-3 SAIL_854_F09.v2 *(cp12-3).*

PCR analysis was undertaken for each line to confirm that plants were homozygous for each insertion.

A combination of gene specific primers and insertion specific primers were used to confirm the WT and the homozygous plants. In the WT plant a band of WT allele was amplified with the gene specific primers for all CP12 genes, however, no fragments were amplified with the insertion specific primers (Figure 3.1 a).

For the single CP12 mutant lines *cp12-1*, *cp12-2* and *cp12-3* a band was shown with the insertion specific primers for each CP12 gene, however, no band was observed with the gene specific primers which confirm the presence of the T-DNA insertion (Figure 3.1 b, c and d).

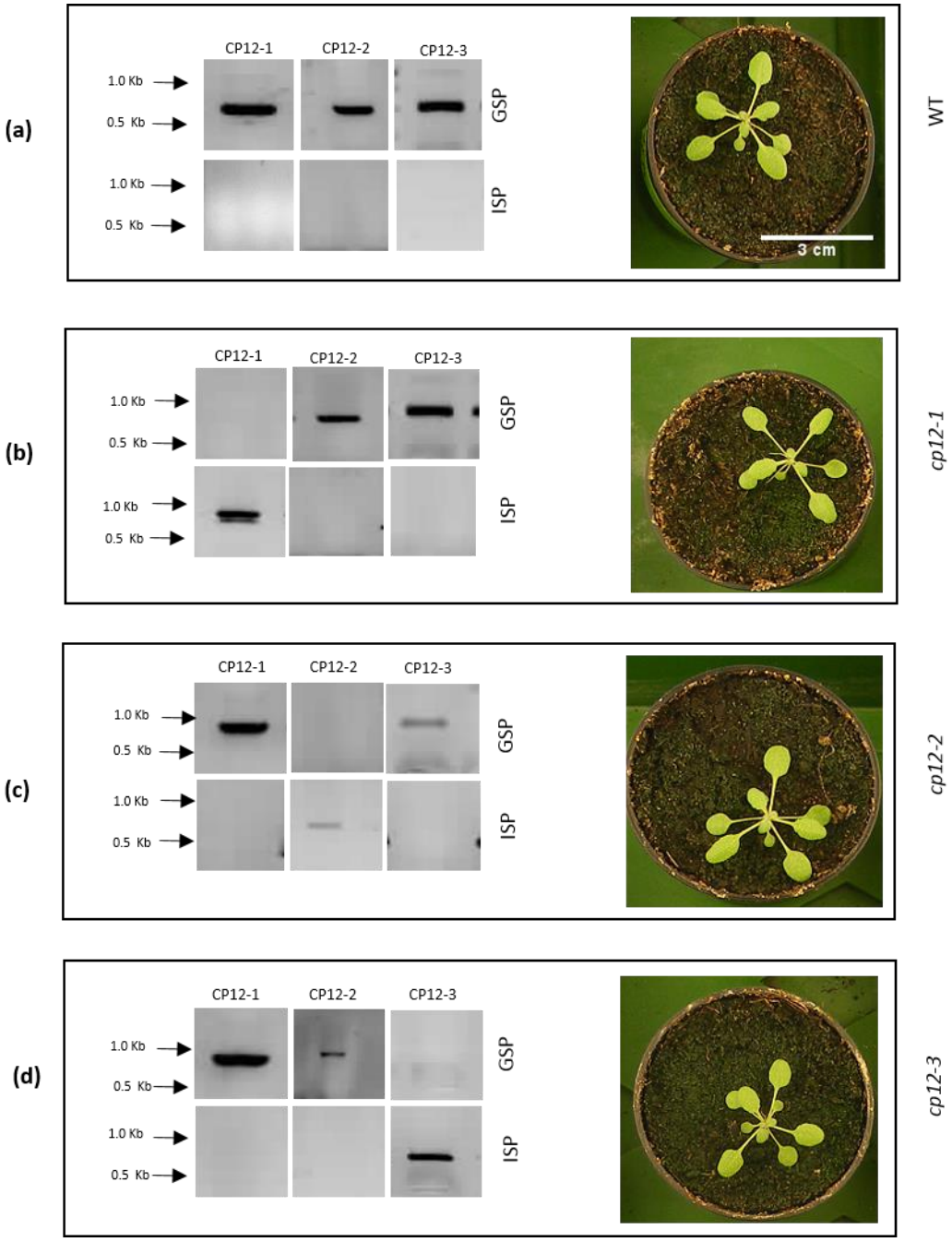

Figure 3.1 Identification and characterisation of the single insertion mutant lines. PCR analysis was used to confirm the presence of CP12 WT allele and the T-DNA insert in the single insertion lines. Gene specific primers (GSP) were used for detection of WT allele (upper gel) and insertion specific primers (ISP) were used to detect the T-DNA insert (lower gel). **(a)** WT plant. **(b)** *cp12-1* plant. **(c)** *cp12-2* plant. **(d)** *cp12-3* plant. Plants were grown for 23 days in soil under 8 h light/ 16 h dark conditions in controlled-environment room. White scale represents 3 cm. PCR products run alongside molecular weight marker (1kb DNA ladder from Invitrogen).

3.1.2 Confirmation of the CP12 double insertion lines *cp12-1/2*, *cp12-1/3* and *cp12-2/3*

In order to study the function of CP12 in Arabidopsis, it was important to generate lines with reduction in more than one gene of CP12. For this, double mutant lines were produced in the lab by crossing single homozygous mutant lines to produce all the possible combination of the double lines *cp12-1/2*, *cp12-1/3* and *cp12-2/3*.

PCR analysis was used to confirm the double homozygous lines. WT allele as well as T-DNA insert were checked by using the combination of gene specific primers and the insertion specific primers respectively. With the gene specific primers all WT allele of CP12 genes were observed in the WT plant but not with the insertion specific primers (Figure 3.2 a).

For the double mutant lines, bands of the T-DNA insertion were observed only with the insertion specific primers, which confirm the presence of the T-DNA insert. However, no bands were shown with the gene specific primers with each insertion line (Figure 3.2 b, c and d).

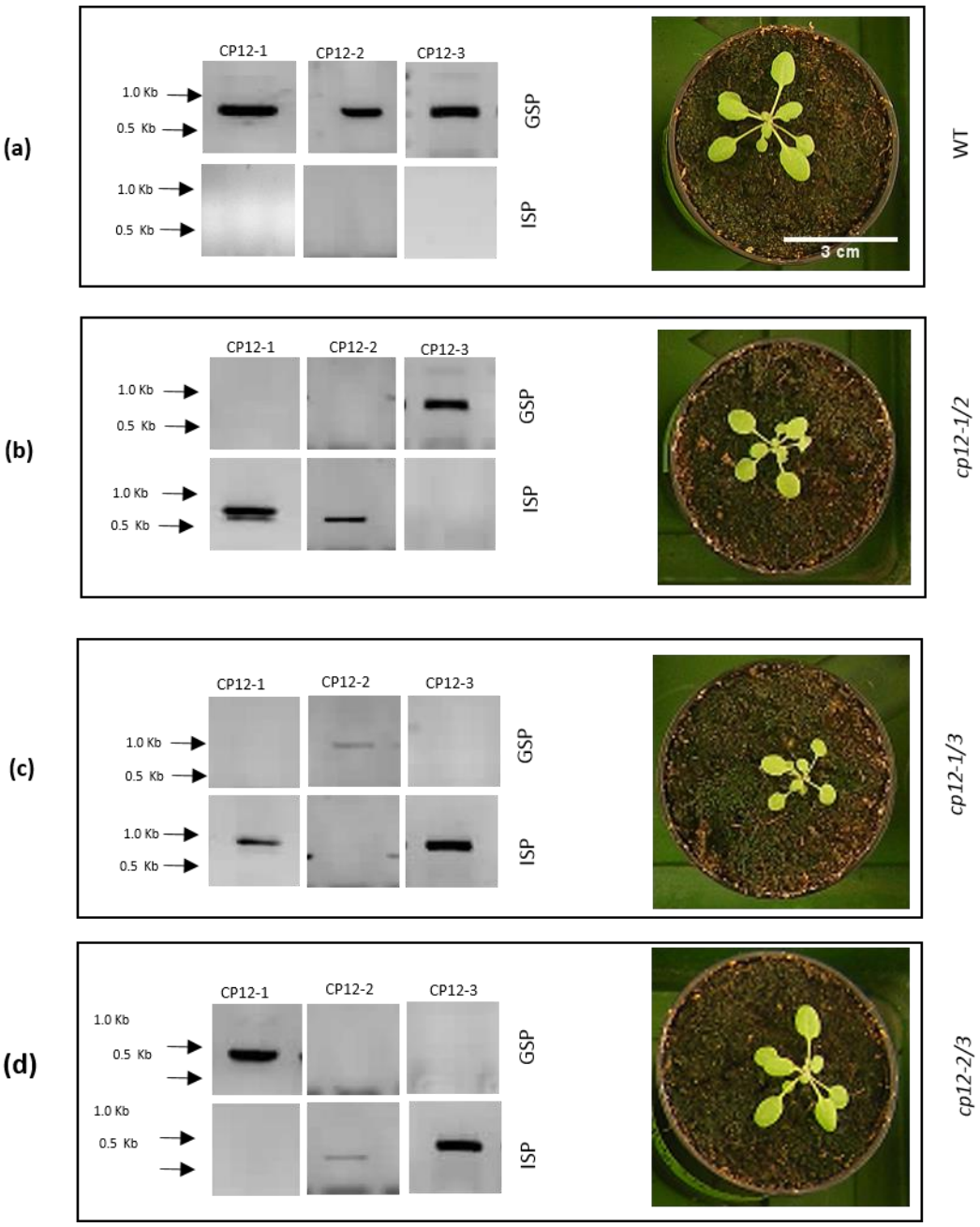

Figure 3.2 Identification and characterisation of the double insertion mutant lines. PCR analysis was used to confirm the presence of CP12 WT allele and the T-DNA insert in the double insertion lines. Gene specific primers (GSP) were used for detection of WT allele (upper gel) and insertion specific primers (ISP) were used to detect the T-DNA insert (lower gel). **(a)** WT plant. **(b)** *cp12-1/2* plant. **(c)** *cp12-1/3* plant. **(d)** *cp12-2/3* plant. Plants were grown for 23 days in soil under 8 h light/ 16 h dark conditions in controlled-environment room. White scale represents 3 cm. PCR products run alongside molecular weight marker (1kb DNA ladder from Invitrogen).

3.1.3 Confirmation of the CP12 triple insertion line *cp12-1*/2/3

In order to study the effect of loss all CP12 genes in plants, triple mutant were produced by crossing two plants of the double mutant *cp12-1/2* and *cp12-1/3*.

The confirmation of the homozygous triple plant *cp12-1/2/3* was checked by PCR analysis. Gene specific primers and insertion specific primers for all CP12 genes were used to amplify the WT allele and the T-DNA insert respectively. In the triple mutant line *cp12-1/2/3*, bands were produced by using the insertion specific primers in all three CP12 genes, however, no products were yield in any of the CP12 genes by using the gene specific primers (Figure 3.3).

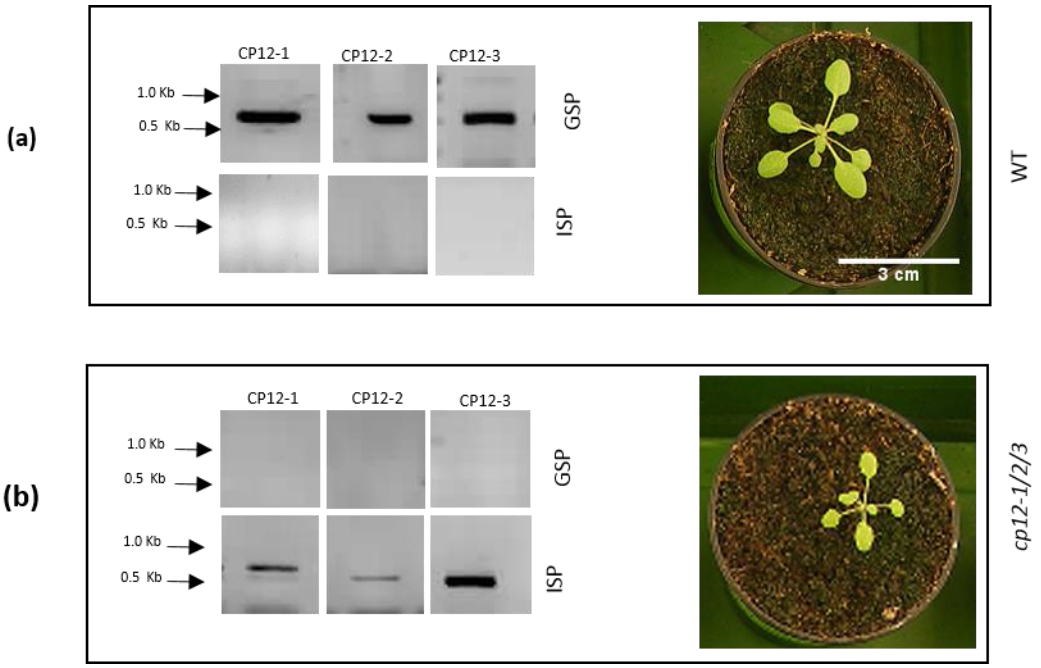

Figure 3.3 Identification and characterisation of the triple insertion mutant line. PCR analysis was used to confirm the presence of CP12 WT allele and the T-DNA insert in the triple insertion lines. Gene specific primers (GSP) were used for detection of WT allele (upper gel) and insertion specific primers (ISP) were used to detect the T-DNA insert (lower gel). **(a)** WT plant. **(b)** *cp12-1/2/3* plant. Plants were grown for 23 days in soil under 8 h light/ 16 h dark conditions in controlled-environment room. White scale represents 3 cm. PCR products run alongside molecular weight marker (1kb DNA ladder from Invitrogen).

3.2 Building and analysing stable *Arabidopsis thaliana* plants expressing RNAi constructs

The position of the T-DNA insertion for the *cp12-1* and *cp12-3* mutant lines were either in the upstream from the ATG or in the exon which resulted in two knock out lines. However, *cp12-2* mutant lines was a knock down line with about 50% reduction on the transcript level.

In order to explore the function of CP12 genes and the effect of lacking all CP12 genes on plant growth and development, RNAi approach was used to create a null CP12 transgenic plants. Golden gate technology was used to build three different constructs (Engler et al., 2009). A generic construct that targets all CP12 isoforms and two specific constructs which target CP12-2 only.

The generic one, which was coded as 52, was designed by performing multiple sequence alignment for all CP12 sequences and selecting the most similar region among them. Additionally, the specific ones, which were coded by 53 & 54, were designed by performing multiple sequence alignment for CP12-1 and CP12-2 sequences and selecting the most unique region for CP12-2. It is important to note that these two specific constructs were very similar, the only difference between them was the length of the selected fragment which was 126 bp for 53 specific construct and 180 bp for the 54 specific construct (Figure 3.4).

After that, DNA fragments were synthesized for each construct. These included two copies of the CP12 fragment in opposite direction, separated by intron 8 from Arabidopsis Plastid Terminal oxidase (236 bp).

Following that, all these parts were assembled together with promoter (cauliflower mosaic virus CaM35S) and NOS terminator (tNOS) in a plant expression vector, using

Golden gate technology according to the protocol described in (Engler et al., 2008, Engler et al., 2009) (Figure 3.4).

Finally, after transformation into *Agrobacterium*, these three construct were introduced by floral inoculation dipping method into WT, *cp12-1/2* and *cp12-1/2/3* plants in order to achieve single mutant of *cp12-2* RNAi transgenic line, double mutant of *cp12-1/2* RNAi transgenic lines and triple mutant of *cp12-1/2/3* RNAi transgenic lines (Narusaka et al., 2010) (Figure 3.5).

Plants were allowed to grow and then the T1 seeds were collected for the screening on selective media of Hygromycin for positive transformants (Figure3.6). The potential positive plants were moved to individual pots, tissue was collected and then the presence of the transgene was confirmed by PCR analysis. Also, the impact on the CP12-2 transcript level was evaluated by performing qPCR.

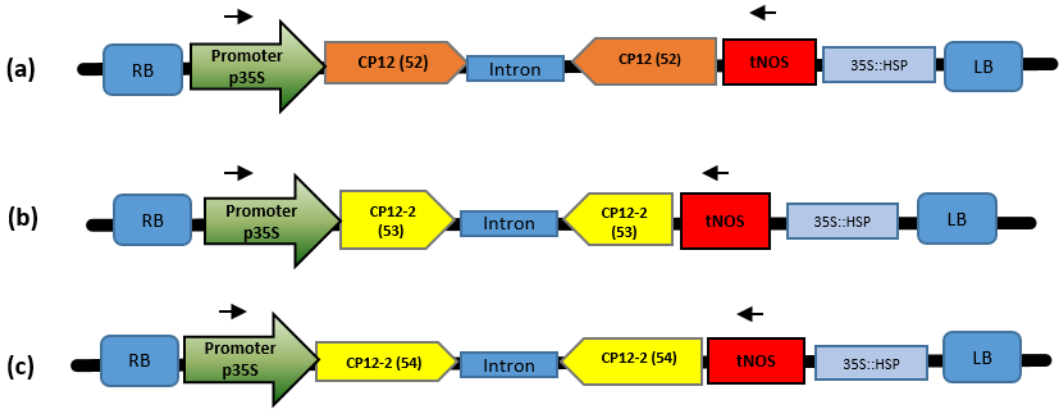

Figure 3.4 Silencing CP12 using RNAi. Schematic diagram of generic CP12 RNAi constructs. CP12 fragment and inverted CP12 fragment were separated by an intron and assembled into the expression vector using Golden gate technology. 35S cauliflower mosaic virus promoter and tNOS terminator were used. RB and LB indicate to the right and the left border. **(a)** Generic RNAi construct 52 using a fragment of 140 bp length. **(b**) Specific RNAi construct 53 using a fragment of 126 bp length. **(c)** Specific RNAi construct 54 using a fragment of 180 bp length. Black arrows indicate to the location primers were used for the screening.

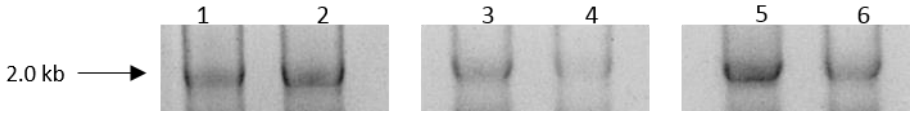

Figure 3.5 Colony PCR of CP12 RNAi constructs in *Agrobacterium*. The presence of the fragment of interest was checked by PCR analysis using the forward primer which located on the promoter and the reverse primer on the terminator. 1 and 2 generic RNAi construct 52 transgene. 3 and 4 specific RNAi construct 53 transgenes. 5 and 6 specific RNAi construct 54 transgenes. Samples run alongside a molecular weight marker from Invitrogen.

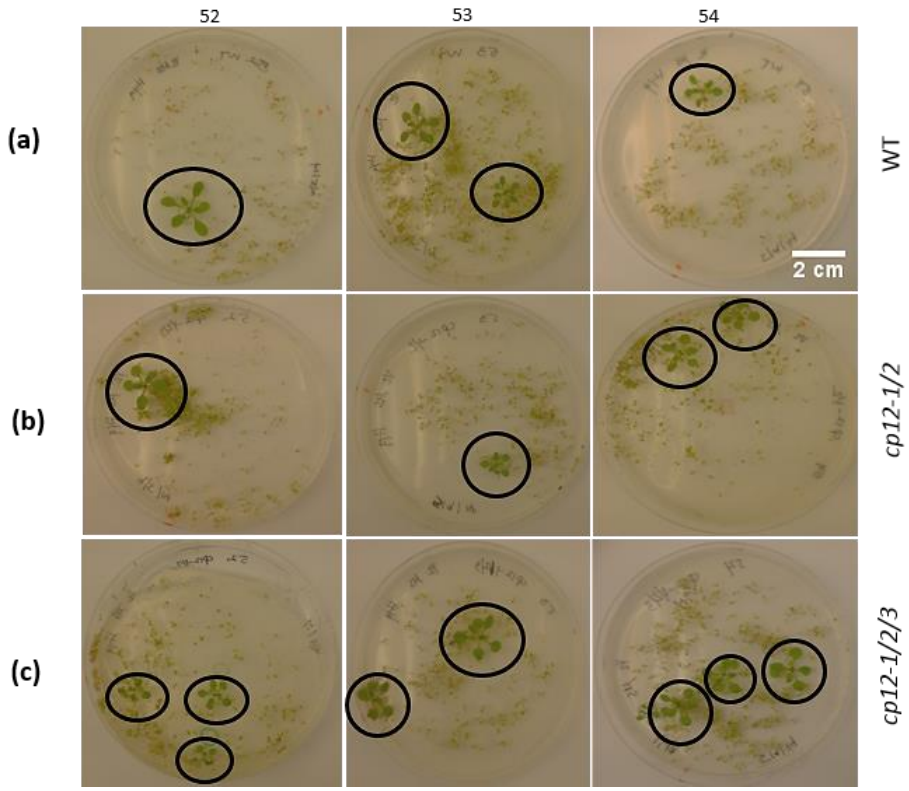

Figure 3.6 Identification of transformed RNAi lines generated using the floral inoculating protocol. Screening of T1 seedlings transformed with the RNAi constructs in selective media. Seeds were sown in half MS media containing 10 µg mL $^{-1}$ Hygromycin. The generic CP12 RNAi construct (52) and the specific CP12-2 constructs (53 and 54) were transformed in **(a)** WT backgrounds **(b)** *cp12-1/2* backgrounds **(c)** *cp12-1/2/3* background. Scale bar represents 2 cm.

Constructs	Backgrounds	Hg Resistant plants	PCR positive plants
Generic CP12 52	WT	1	1
	cp12-1/2	3	3
	cp12-1/2/3	2	2
Specific CP12-2 53	WT	4	3
	cp12-1/2	1	1
	cp12-1/2/3	2	2
Specific CP12-2 54	WT	3	3
	cp12-1/2	6	6
	cp12-1/2/3	5	5

Table 3.1 Antibiotic selection for RNAi construct of *Arabidopsis thaliana* transgenic plants.

3.2.1 Identification and characterisation of T1 generation of RNAi plants

In order to confirm the presence of the transgene in the T1 generation, DNA extraction from leaf tissue of *Arabidopsis thaliana* rosette was made and used in PCR analysis. The fragment of interest was checked by using the forward primer which located in the promoter and the reverse primer which designed on the terminator (Figure 3.4). The expected fragment of the PCR reaction were 2157 bp, 2129 bp and 2273 bp for the generic RNAi construct (52), specific RNAi construct (53) and specific RNAi construct (54) respectively (Figure 3.7).

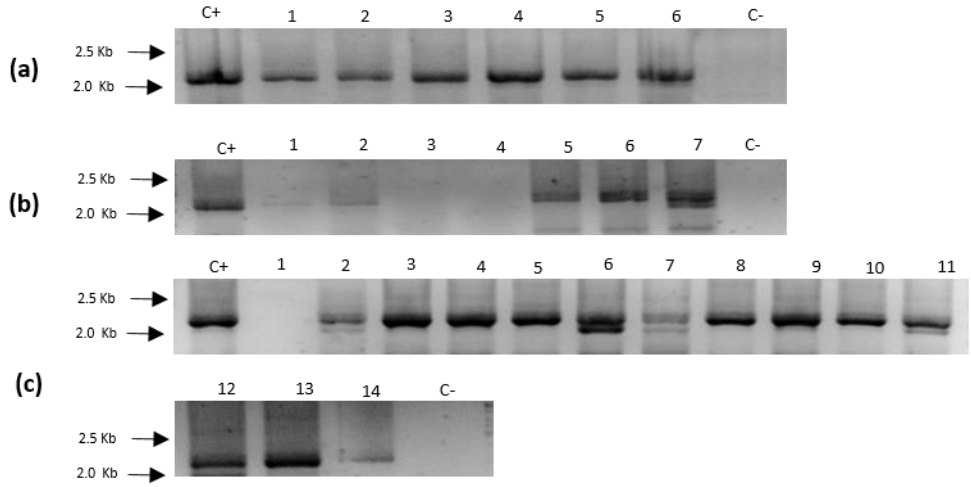

Figure 3.7 PCR screening for the presence of the RNAi transgene in the T1 generation putative transformants. The presence of the RNAi transgene for all lines was checked with PCR analysis using the forward primer located on the promoter and reverse primer located on the terminator. **(a)** Generic RNAi (52) transgene in the WT background (1), *cp12-1/2* background (2-4) and *cp12-1/2/3* background (5&6). **(b)** Specific RNAi (53) transgene in the WT background (1-4), *cp12-1/2* background (5) and *cp12-1/2/3* background (6&7). **(c)** Specific RNAi (54) transgene in the WT background (1-3), *cp12-1/2* background (4-9) and *cp12-1/2/3* background (10-14). WT DNA was used as a negative control (C-). Plasmid DNA containing the gene of interest was used as a positive control (C+). 1 kb DNA ladder was used as a molecular marker from Introvigen.

3.2.2 Quantification of the expression of the CP12 genes in T1 generation

To investigate the impact of the expression of the RNAi constructs on the CP12 genes, the transcript level of all three CP12 genes for each construct was checked by qPCR analysis in all positive transformants. T1 RNAi transgenic lines were germinated on half MS media plates containing 10 µg mL^{-1} Hygromycin and were grown under long day condition of 16 h light / 8 h dark in controlled-environment room. At 14 days, plants were moved to individual pots and adult rosette from each line were sampled at 47 days.

Following this, total RNA was isolated using the NucleoSpin® RNA/Protein kit from (MN), then cDNA was produced which was used to quantify the expression of the transcript for individual CP12 gene in all transgenic lines for each construct.

The results in figure 3.8 present the expression of the CP12 genes in the RNAi transgenic lines with generic construct (52). The generic RNAi construct in the WT background resulted in strong decrease in the CP12-2 transcript level about 96% of the expression compared to the WT. The level of the expression of CP12-1 was slightly affected with a reduction of about 13%. However, the expression level of CP12-3 in the same plant was increased significantly by about 63%. The expression of the generic RNAi construct (52) in the triple *cp12-/2/3* backgrounds displayed lack of expression for CP12-1 and CP12-3 genes due to the T-DNA insert, however, the expression of CP12-2 was still detected with the range of 10-30% of the expression. In the specific construct for CP12-2 (53), the expression of CP12-2 was reduced significantly in both backgrounds (WT and *cp12-1/2/3*), but the expression of CP12-1 and CP12-3 showed complementary increase in most of the WT background lines

and in the *cp12-1/2/3* background the expression of CP12-1 and CP12-3 was not detected since they are (KO) lines (Figure 3.9).

The expression of the second specific construct of CP12-2 (54), led to a dramatic reduction in the CP12-2 expression in the most of the lines of WT background, while the level of transcript of CP12-3 was increased (*WT.R.1, 2, 3*). Also, the expression of CP12-1 was increased in two lines of the WT backgrounds (*WT.R.1, 2*).

As expected, the triple mutant plants (*TM.R.1, 2, 3, 4, 5*) showed lack of expression for CP12-1 and CP12-3 genes. Additionally, the transcript level of CP12-2 was further declined significantly in all lines except (*TM.R.3)* which was slightly elevated compared with the triple mutant *cp12-1/2/3* (TM) control (Figure 3.10).

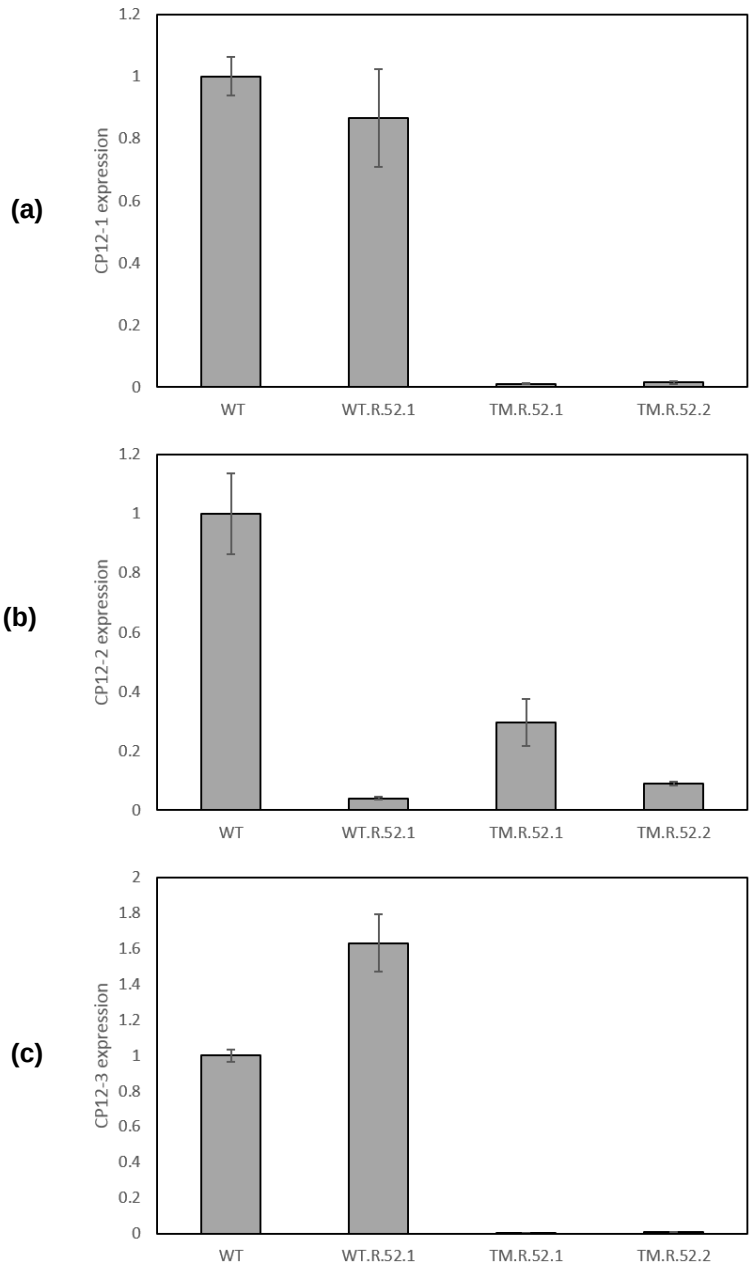

Figure 3.8 Quantitative PCR (qPCR) analysis of the expression of the generic RNAi construct (52). Total RNA was extracted from the leaf tissue of adult rosettes and used to estimate the relative levels of expression of CP12 genes in the RNAi transgenic lines with respect the WT levels of expression. **(a)** Expression of the CP12-1 gene in the WT background (*WT.R.52.1*) and in the *cp12-1/2/3* background (*TM.R.52.1&2*) relative to the WT control. **(b)** Expression of the CP12-2 gene in the WT background (*WT.R.52.1*) and in the *cp12-1/2/3* background (*TM.R.52.1&2*) relative to the WT control. **(c)** Expression of the CP12-3 gene in the WT background (*WT.R.52.1*) and in the *cp12-1/2/3* background (*TM.R.52.1&2*) relative to the WT control. The results are normalised with the actin and cyclophilin genes. The error bars represent the SE, calculated using the relative expression software tool (REST) for group-wise comparison and statistical analysis of relative expression results in real-time PCR. Version 2009 (Pfaffl et al., 2002).

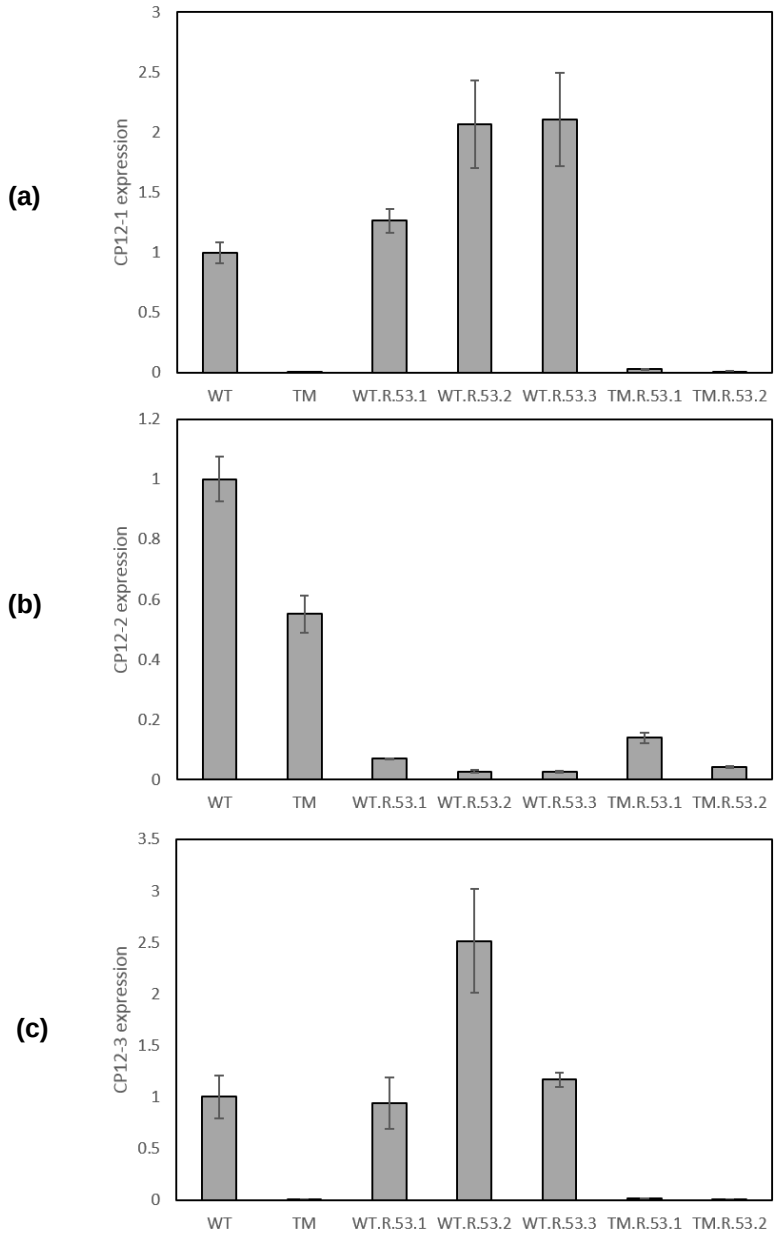

Figure 3.9 Quantitative PCR (qPCR) analysis of the expression of the specific RNAi construct (53). Total RNA was extracted from the leaf tissue of adult rosette and used to estimate the relative levels of expression of CP12 genes in the RNAi transgenic lines with respect the WT levels of expression. **(a)** Expression of the CP12-1 gene in the WT background (*WT.R.53.1,2&3*) and in the *cp12-1/2/3* background (*TM.R.53.1&2*) relative to the WT control. **(b)** Expression of the CP12-2 in the WT background (*WT.R.53.1,2&3*) and in the *cp12-1/2/3* background (*TM.R.53.1&2*) relative to the WT control. **(c)** Expression of the CP12-3 gene in the WT background (*WT.R.53.1,2&3*) and in the *cp12-1/2/3* background (*TM.R.53.1&2*) relative to the WT control. The results are normalised with the actin and cyclophilin genes. The error bars represent the SE, calculated using the relative expression software tool (REST) for group-wise comparison and statistical analysis of relative expression results in real-time PCR. Version 2009 (Pfaffl et al., 2002).

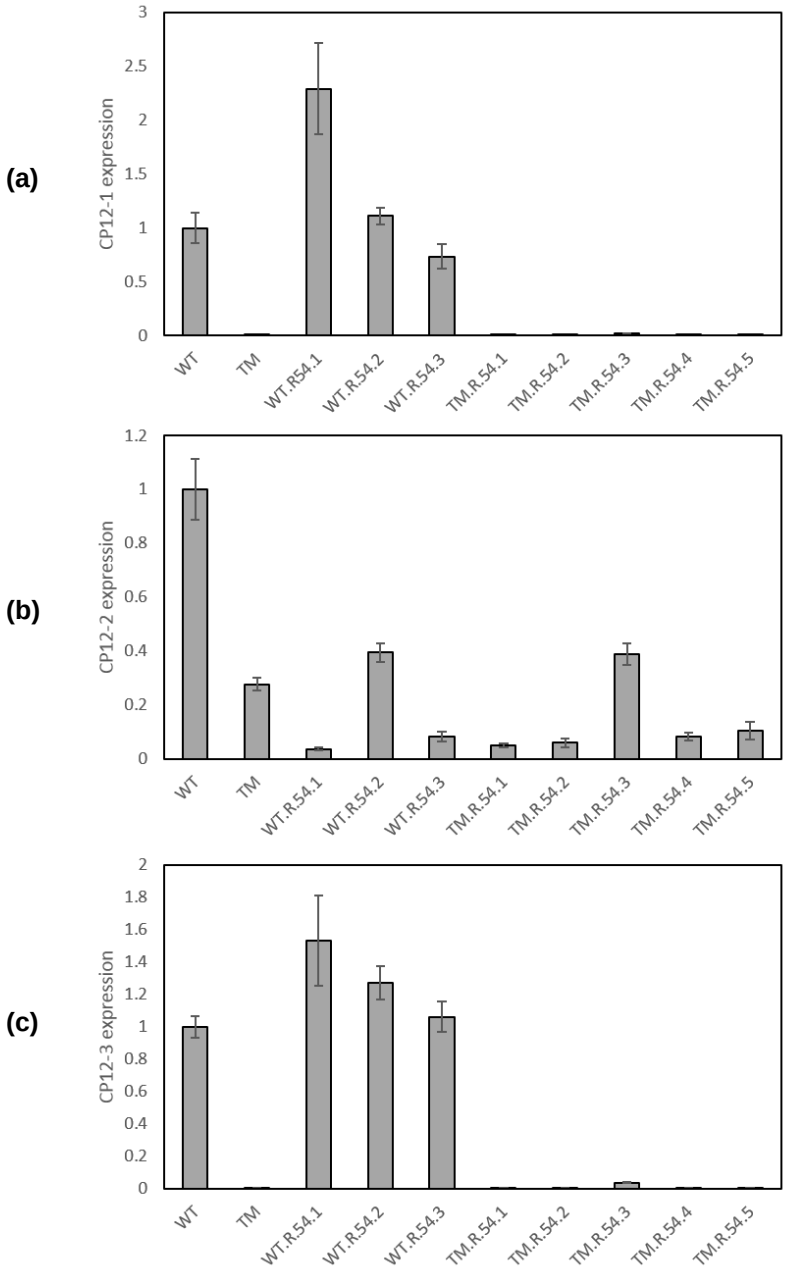

Figure 3.10 Quantitative PCR (qPCR) analysis of the expression of the specific RNAi construct (54). Total RNA was extracted from the leaf tissue of adult rosettes and used to estimate the relative levels of expression of CP12 genes in the RNAi transgenic lines with respect the WT levels of expression. **(a)** Expression of the CP12-1 gene in the WT background (*WT.R.54.1,2&3*) and in the *cp12-1/2/3* background (*TM.R.54.1,2,3,4&5*) relative to the WT control. **(b)** Expression of the CP12-2 gene in the WT background (*WT.R.54.1,2&3*) and in the *cp12-1/2/3* background (*TM.R.54.1,2,3,4&5*) relative to the WT control. **(c)** Expression of the CP12-3 gene in the WT background (*WT.R.54.1,2,&3*) and in the *cp12-1/2/3* background (*TM.R.54.1,2,3,4&5*) relative to the WT control. The results are normalised with the actin and cyclophilin genes. The error bars represent the SE, calculated using the relative expression software tool (REST) for group-wise comparison and statistical analysis of relative expression results in real-time PCR. Version 2009 (Pfaffl et al., 2002).

3.3 Analysis of the complementation of the CP12-1 in the triple mutant *cp12-1/2/3* background

To investigate the role of CP12-1 *in vivo*, a chimeric gene construct was produced in the lab previously with CP12-1 fused to the epitope-tag FLAG. The expression of this gene fusion construct was driven by the CP12-1 native promoter as described in Singh et al. (2008). This construct was built using Gateway technology and introduced in the triple mutant plants *cp12-1/2/3* using floral dipping method (Bent and Clough, 1998). Plants were allow to grow and seeds were collected for the T1 generation.

3.3.1 Identification and characterisation of T1 *Arabidopsis thaliana* plants expressing CP12-1::FLAG under the native promoter

The T1 generation of the *Arabidopsis thaliana* plants expressing CP12-1::FLAG in the *cp12-1/2/3* background were sown on half MS media containing 10 μg mL^{-1} Hygromycin under long day conditions of 16 h light/ 8 h dark in controlled-environment room. Four positive transformants were identified on the selective media and moved to individual pots. After that, plants were allowed to acclimate and then tissue was collected form each positive line in order to check the presence of the transgene by PCR analysis (Figure 3.11 a and b).

In the PCR reaction the position of the forward primer was in the promoter and the reverse primer was located in the FLAG-tag. The size of the expected fragment was 952 bp.

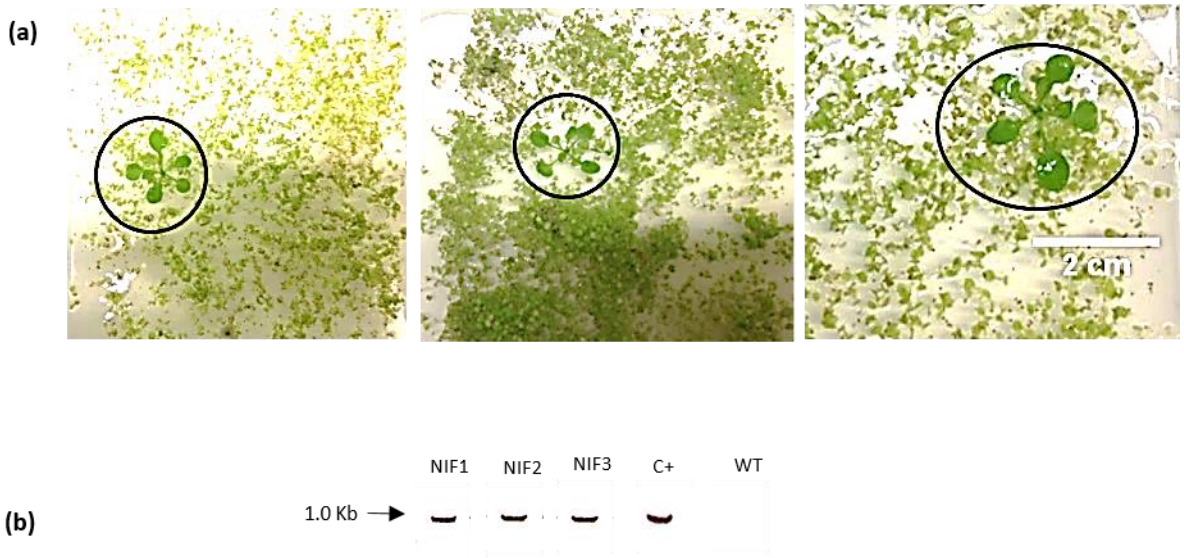

Figure 3.11 Analysis of T1 generation native promoter NP-CP12-1:: FLAG in the *cp12-1/2/3* background. (a) Antibiotic selection of CP12-1::FLAG stable transgenic plants. Seeds were sown in half MS media containing 10 µg mL^{-1} Hygromycin. **(b)** PCR screening for presence of the NP-CP12-1::FLAG transgene in *cp12-1/2/3* putative transformants. The presence of the NP-CP12-1::FLAG transgene was checked by PCR analysis using a forward primer in the CP12 gene and a reverse primer in the FLAG-tag. WT and plasmid DNA containing the gene of interest were used as negative and positive controls respectively. Molecular weight marker was run with the PCR products (1Kb DNA from Invitrogen). Scale represents 2 cm.

3.3.2 Identification and characterisation of T2 *Arabidopsis thaliana* plants expressing CP12-1::FLAG under the native promoter

Seeds for the next generation of the native promoter CP12-1 FLAG (NP-CP12-1::FLAG) lines T2 were grown in half MS media under long day conditions of 16 h light / 8 h dark in controlled-environment room. Following by that plants were moved to individual pots and tissue was collected in order to check the presence of the transgene by PCR analysis using the same combination of primers which were used to check the previous generation. Also, the expression of the transgene was evaluated in these positive plants by western blot (Figure 3.12 a, b).

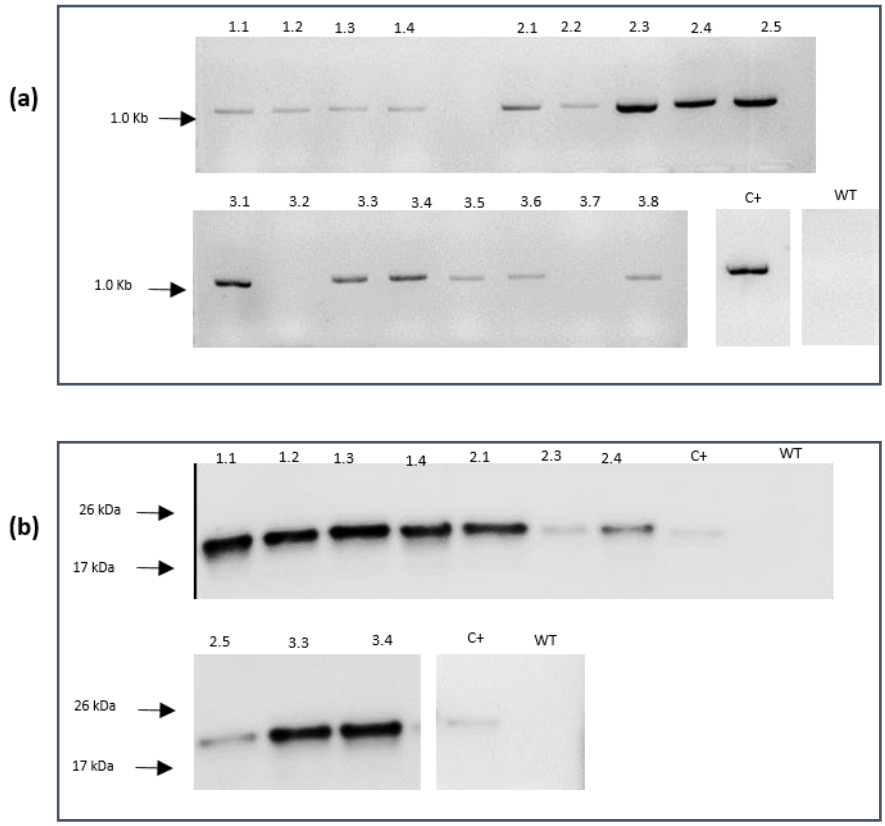

Figure 3.12 Analysis of T2 generation native promoter NP-CP12-1::FLAG in the *cp12-1/2/3* plants. (a) PCR screening for presence of the NP-CP12-1::FLAG transgene in *cp12-1/2/3* putative transformants. The presence of the NP-CP12-1::FLAG transgene was checked by PCR analysis using a forward primer in the CP12 gene and a reverse primer in the FLAG-tag. WT and plasmid DNA containing the gene of interest (C+) were used as negative and positive controls respectively. PCR products were run with molecular weight markers (1 Kb ladder from Invitrogen). **(b)** Western blot of NP-CP12::FLAG in the *cp12-1/2/3* plants. Expression of CP121::FLAG was checked in the T2 generation by western blot using antibodies against FLAG in protein extracts from leaf tissue. WT extract was used as a negative control. Pervious positive T1 sample was used as a positive control (C+). Samples were run with a PageRuler ^{TM} Protein Ladder from Fermentas.

Discussion

To date and since CP12 protein was first identified, the vast majority of work have focused on the characterisation of CP12 proteins in the complex of GAPDH and PRK in the Calvin-Benson cycle *in vitro*. However, evidences from a number of studies suggest that these proteins may have additional functions outside the Calvin-Benson cycle regulation. This includes the fact that CP12 in higher plant is encoded by a small gene family which show different expression patterns (Singh et al., 2008, Marri et al., 2005a), in 2011 Howard et al. (2011a) showed the complex phenotype which resulted from the antisense suppression of CP12 in tobacco and in 2013 Stanley et al. (2013) presented the diversity of CP12 protein in cyanobacteria (Stanley et al., 2013, Howard et al., 2011a). Taken together these data strongly indicate that CP12 gene family might have a wider role throughout the plant life cycle.

To explore further the roles of the individual CP12 proteins, it is crucial to develop a number of tools. The results in this chapter present the development of the molecular tools that have been used in the subsequent chapters to study the function of the three members of CP12 in *Arabidopsis thaliana*.

T-DNA insertion mutant lines including single, double and triple lines were produced previously and in this chapter analysis of these mutants is presented. PCR analysis confirmed that homozygous lines for the single insertion mutants of *cp12-1*, *cp12-2* and *cp12-3*, double mutant lines of *cp12-1/2*, *cp12-1/3* and *cp12-2/3* and triple mutant line of *cp12-1/2/3* were identified.

In previous study of these T-DNA insertion lines, qPCR analysis revealed a complete lack of expression for *cp12-1* and *cp12-3*, however, some expression of *cp12-2* was still detectable (Lopez-Calcagno, 2013).

RNA interference (RNAi) was first descried by Fire et al and it can be used as an effective experimental tool to reduce the expression of a target gene and in turn elucidate the function of this gene. It is a conserved mechanism in wide range of eukaryotic organisms and it inactivates the expression of the gene in sequence-specific manner (Fire et al., 1998, Hirai and Kodama, 2008).

As mentioned previously, the T-DNA insertion line for CP12-2 was a knock down with about 50% reduction of the transcript level, relative to wild type plants. Based on that, RNAi approach was used as a gene silencing technology to reduce the expression in all CP12 genes generally and CP12-2 specifically. Three different constructs were built and introduced to into the different background plants in order to produce single transgenic line for *cp12-2*, double transgenic line for *cp12-1/2* and triple transgenic line for *cp12-1/2/3*. These RNAi transgenic lines should be able to provide further information on the effect of losing all isoforms of CP12 gene in Arabidopsis.

With the specific constructs, which targets CP12-2 gene, we successfully managed to produce a number of lines for each background; 6 lines for the WT background, 7 lines for the *cp12-1/2* background and 7 lines for the *cp12-1/2/3* background. Introducing the generic CP12 construct to target all CP12 isoforms, resulted in 6 transgenic lines; one line for the WT background, 3 lines for the *cp12-1/2* background and 2 for the *cp12-1/2/3* background (Table 3.1).

qPCR results revealed some alterations in the expression level of CP12 transcript when the expression of one or more member of the family was affected by the

silencing of RNAi construct. The expression of WT plants of the specific constructs, which considered as *cp12-2* transgenic lines, revealed that in some cases when the level of CP12-2 decreased, the expression of CP12-1 and CP12-3 increased, showing a compensating affect in these cases. In addition, the expression level of all CP12-2 isoforms seemed to be decreased significantly in the *cp12-1/2/3* plants carrying of the specific constructs.

In order to demonstrate that an insertional mutation is the only reason which may cause a phenotype, one of the two following procedures must be conducted; either to identify additional mutant allele for the locus or to introduce a wild-type copy to the mutant line by using transgenic technology in an assay called complementation (Krysan et al., 1999).

Since only one mutant allele was identified for each CP12 gene, it was necessary to consider the complementation approach in this research to provide an evidence that CP12 gene is responsible for a phenotype which may appear in the T-DNA insertion mutant lines.

In this chapter, we have experimentally tested the triple mutant line *cp12-1/2/3* which complement with CP12-1 derive by the native promoter. Since CP12 proteins in plants are highly similar and it is difficult to be recognized by antibodies, an antigenic epitope tag (FLAG) was attached to the protein to enable us to discriminate the different isoforms of these three proteins. This transgenic line is one of the collection which have been generated in the lab previously. These transgenic lines should help to complement a phenotype which believed to be caused by a member of CP12 gene. In addition, these transgenic lines could be a useful tool to explore the possibility of CP12 proteins, forming other complexes by using different approaches such as co immunoprecipitation.

These single T-DNA insertion mutant lines could be used in further study of the effect of lacking one isoform of CP12 in Arabidopsis growth and development. Additionally, having the multiple mutant lines with the all possible combinations will help to study the effect of the absence of more than one isoform of CP12s gene.

We have identified a number of positive independent lines, three of them were fully characterized and used in further studies.

CHAPTER 4

Phenotypic analysis of lack of CP12 in *Arabidopsis thaliana*

Introduction

CP12 is a small redox-sensitive protein consisting of approximately 80 amino acids that was originally described by Pohlmeyer et al. (1996). It is found in most photosynthetic organisms, such as higher plants, green and red algae, and cyanobacteria with the exception of ultrasmall green algae *Ostreococcus* (Wedel et al., 1997, Wedel and Soll, 1998, Graciet et al., 2003a, Tamoi et al., 2005, Oesterhelt et al., 2007, Marri et al., 2005a, Robbens et al., 2007, Groben et al., 2010, Stanley et al., 2013) .

In eukaryotic organisms, CP12 is a nuclear-encoded protein that is transported into the chloroplast, where it plays its only currently identified role. CP12 regulates the enzymes involved in the Calvin-Benson cycle by forming a multienzyme complex with glyceraldehyde-3-phosphate dehydrogenase (GAPDH) and subsequently, phosphoribulokinase (PRK) (Avilan et al., 1997, Wedel et al., 1997, Wedel and Soll, 1998, Howard et al., 2008, Marri et al., 2009). Within this multienzyme complex, the GAPDH and PRK activity is decreased, which results in the down regulation of the enzyme activity of Calvin-Benson cycle. This effect has been demonstrated in *Chlamydomonas reinhardtii,* plants and cyanobacteria (Wedel et al., 1997, Graciet et al., 2003b, Tamoi et al., 2005, Marri et al., 2005b).

The presence of the GAPDH/CP12/PRK complex has been reported in several higher plants (Wedel et al., 1997, Wedel and Soll, 1998, Scheibe et al., 2002, Howard et al., 2011b) and algal species (Avilan et al., 1997, Boggetto et al., 2007, Oesterhelt et al., 2007). Previous research has suggested that the association and disassociation of the GAPDH/CP12/PRK complex occur via changes to the NADP(H):NAD(H) ratio in

the chloroplast (Wedel et al., 1997, Wedel and Soll, 1998, Tamoi et al., 2005, Trost et al., 2006). However, more recent studies have shown that the redox state of thioredoxin regulates the status of the complex (Howard et al., 2008, Marri et al., 2009).

Thioredoxin consists of a group of well-known proteins that all play a key role in regulating various cellular processes in plants, algae and cyanobacteria (Meyer et al., 2009, Buchanan et al., 2012). In the 1970s, two types of thioredoxin, namely *f* and *m*, were identified in higher plants as activators of the enzymes involved in the Calvin-Benson cycle in the chloroplast (Buchanan, 1980, Buchanan and Balmer, 2005). Furthermore, both types of thioredoxin have been found to be able to mediate the status of the GAPDH/CP12/PRK complex by reducing the two cysteine pairs in the CP12 protein (Marri et al., 2009).

Genome sequencing and data obtained from expressed sequence tags (EST) have demonstrated that the CP12 protein in higher plants is encoded by a small multigene family. In Arabidopsis, the CP12 family is formed by 3 genes: CP12-1, CP12-2 and CP12-3. A comparison of the amino acid sequences of these three proteins determined that CP12-1 and CP12-2 exhibit approximately 98% similarity; however, CP12-3 exhibits less than 50% similarity to the other two proteins (Singh et al., 2008).

Further analysis focused on the expression of the CP12 gene family has revealed that CP12 genes are expressed differently in *Arabidopsis thaliana* (Singh et al., 2008, Marri et al., 2005a). The expression patterns of CP12-2 are similar to those of the Calvin-Benson cycle enzymes GAPDH and PRK, which are light-dependent and highly expressed in photosynthetic tissues such as cotyledon, vegetative leaves and

stalks. CP12-1 is expressed in dark-grown tissues and it is abundantly expressed in photosynthetic tissues. It is also expressed in a range of other tissues, including flowers, seeds and root tips. On the other hand, CP12-3 has a very low expression level in leaf tissue, while it is highly expressed in root tissue. Surprisingly, all three CP12 genes are expressed in floral tissues. CP12-1 and CP12-2 are expressed in the sepals and styles of the flowers; however, the expression of CP12-3 has been detected in the stigmas and anthers (Singh et al., 2008). These data, which demonstrate that the CP12 genes are expressed in non-photosynthetic tissues, indicate that the CP12 proteins may have a wider role than only involving in the regulation of the Calvin-Benson cycle.

Further support for this hypothesis can be found in a study of CP12-transgenic antisense tobacco, which results in a complex phenotype that includes altered leaf morphology, reduced fertility and a loss of apical dominance (Howard et al., 2011a). Furthermore, only a slight effect on PRK and GAPDH activity and photosynthetic carbon fixation was found in these transgenic antisense plants (Howard et al., 2011a).

The role of CP12 as an integral component of the GAPDH/CP12/PRK complex has been studied extensively *in vitro*. However, it remains unclear whether these three proteins play separate or overlapping roles *in vivo*. This chapter will therefore use the tools which produced and described in the previous chapter to explore whether the different forms of CP12 have additional functions in Arabidopsis. This will be accomplished by focusing on different aspects. The collection of T-DNA insertion mutant plants, including single, double and triple mutants, was studied to investigate the phenotype of slow growth and development. In addition, since CP12-2 is a

knockdown mutant, the RNAi construct was used to create a nearly-null CP12 mutant plant.

This is a useful tool for reducing the level of gene expression and thus facilitate the study of gene function. Finally, a complementation study was performed to rescue the slow growth phenotype and confirm that lack of CP12 causes it.

Results

4.1 The analysis of the T-DNA insertion mutant lines

4.1.1 Growth analysis of T-DNA insertion mutant lines' rosette area, fresh and dry weight, and leaf number

As described in the previous chapter, the T-DNA insertion mutant lines of all *Arabidopsis thaliana* CP12 members were identified from TAIR. Then, crosses were made to produce all possible combinations of these multiple mutant lines. As a result, along with the three single mutant lines that have been identified (*cp12-1*, *cp12-2* and *cp12-3*), three double lines (*cp12-1/2*, *cp12-1/3* and *cp12-2/3*) and one triple line (*cp12-1/2/3*) were generated.

In order to evaluate the effect of the lack of CP12 on the growth and development of *Arabidopsis thaliana*, a growth analysis of all the T-DNA insertion mutant lines and the WT was performed. First, the seeds of all the lines were placed in a cold room (temperature of 4˚C) for three days to synchronize the germination. Then, the seeds were sown in soil under short-day conditions of 8 h light and 16 h dark. The plants were allowed to grow for six weeks and the total rosette area of the WT, single lines, double lines and triple line was determined over the duration of the experiment. For each line, ten biological replicates were included and the plants were distributed in a random way in order to avoid any effects due to the position of the tray. Additionally, the number of leaves was counted at several time points during the study. Finally, the fresh and dry weights of the 36-day-old plants were determined.

No phenotype was evident in the single mutant lines *cp12-2* and *cp12-3*. However, *cp12-1* showed a mild phenotype and a small reduction in the rosette area when

compared with the WT. At 16 days, *cp12-1* showed a slow growth rate with a reduction of 24% in the rosette area, however, it is still not significantly different from the WT.

Recording the growth rate of the multiple mutant lines revealed notably slow growth in the double mutant lines *cp12-1/2* and *cp12-1/3* with a 30% and 31% reduction in the rosette area, respectively (at the 16-day time point). Furthermore, the triple mutant *cp12-1/2/3* also showed a slow growth phenotype as the rosette reached to only 65% of that of the WT.

As the growth rates of a number of the insertion mutant lines were affected, it was likely that the fresh and dry weights (biomass), as well as the number of leaves, are also impacted. In order to evaluate the fresh weight, the rosette of each plant was cut and weighed on a scale immediately after the final time point of the growth analysis. Then, to determine the dry weight, each rosette was placed in a paper bag and put in an oven at 80˚C for approximately a week before weighing for a second time.

The fresh and dry weights results revealed the same tendency. Specifically, the weights of the *cp12-1/2, cp12-1/3* and *cp12-1/2/3* lines were significantly lower than those of the WT. Furthermore, the *cp12-1* single mutant line showed a small reduction in the fresh and dry weights of approximately 26% and 15%, respectively (Figure 4.3).

The number of leaves were counted at several time points throughout the growth analysis. All single mutant lines including *cp12-1*, *cp12-2* and *cp12-3* were not significantly different from the WT, with a slight reduction in the *cp12-1*. In addition, results showed a significant reduction in the number of leaves in the *cp12-1/2* and *cp12-1/2/3* lines compare to the WT (Figure 4.4).

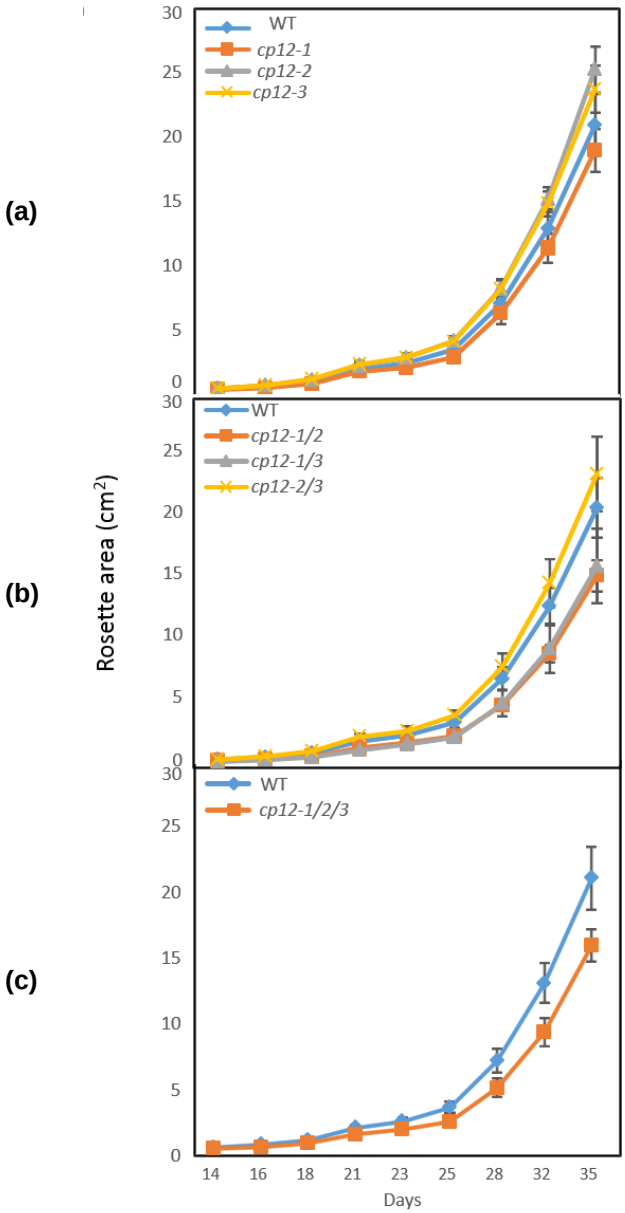

Figure 4.1 Comparison of the growth rates of the WT and the CP12 insertion mutant lines. The plants were grown in soil under identical conditions in a controlled environment (22°C, 8 h light and 16 h dark cycle). Pictures were taken at weeks 2, 3, 4 and 5, and the photographs were used to calculate the rosette area. **(a)** *Arabidopsis thaliana* (Col-0) WT and CP12 single mutant lines (*cp12-1*, *cp12-2* and *cp12-3*). **(b)** *Arabidopsis thaliana* (Col-0) WT and CP12 double mutant lines (*cp12-1/2*, *cp12-1/3* and *cp12-2/3).* **(c)** *Arabidopsis thaliana* (Col-0) WT and triple mutant line (*cp12-1/2/3*). The error bars represent SE n=10 replicates.

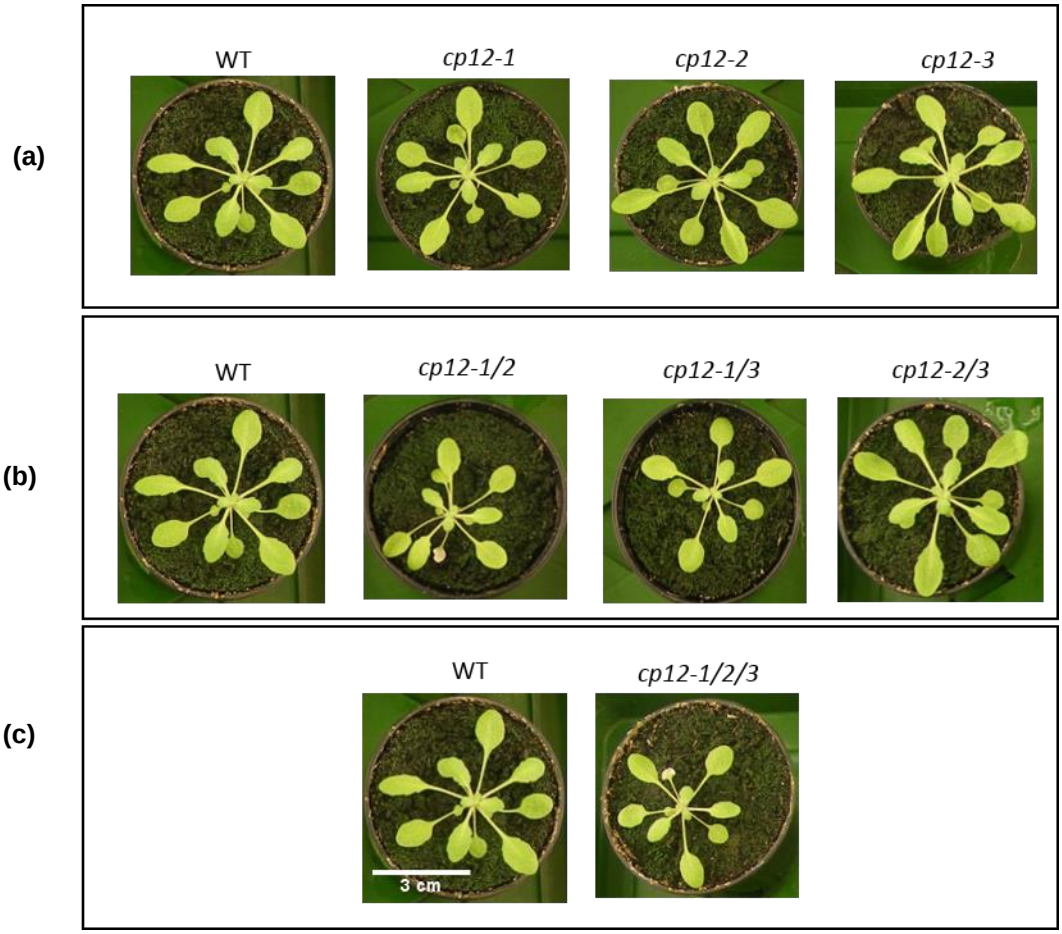

Figure 4.2 Comparison of the WT and CP12 insertion mutant plants grown in soil. The plants were grown for seven weeks under identical conditions in a controlled environment (22°C, 8 h light and 16 h dark cycle). Pictures were taken at weeks 2, 3, 4, 5, and the photographs were used to calculate the rosette area. **(a)** *Arabidopsis thaliana* (Col-0) WT and CP12 single mutant lines (*cp12-1*, *cp12-2* and *cp12-3*) of 28 days. **(b)** *Arabidopsis thaliana* (Col-0) WT and CP12 double mutant lines (*cp12-1/2*, *cp12-1/3* and *cp12-2/3)* of 28 days. **(c)** *Arabidopsis thaliana* (Col-0) WT and triple mutant line (*cp12-1/2/3*) of 28 days. The white scale bar represents 3 cm.

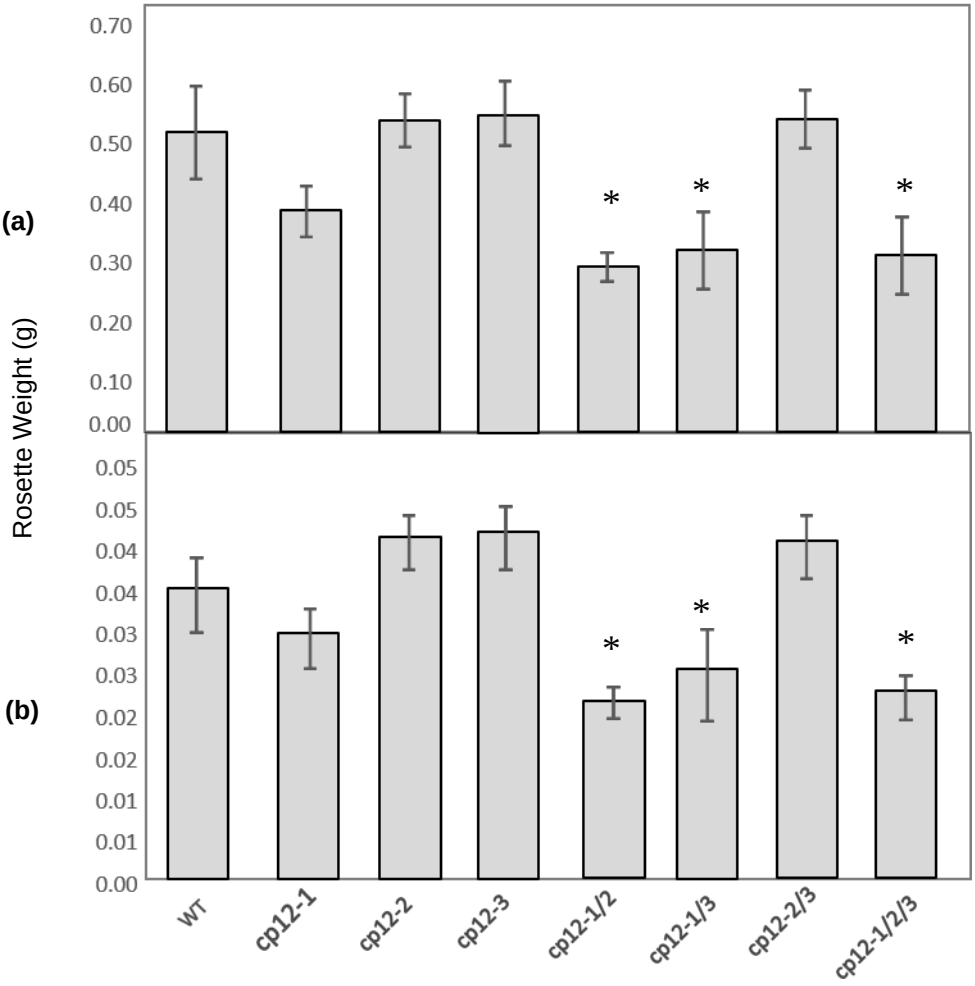

Figure 4.3 *Arabidopsis thaliana* CP12 mutant rosette fresh and dry weights at five weeks. The plants were grown in soil for five weeks and then their fresh and dry weights were determined by weighing the rosettes before and after they were placed in an oven to dry. **(a)** Fresh weight for the WT and CP12 mutant lines. **(b)** Dry weight for the WT and CP12 mutant lines. The error bars represent SE n=10 replicates. Significant differences was determined by Kruskal-Wallis followed by Mann-Whitney test using SPSS, (P<0.05).

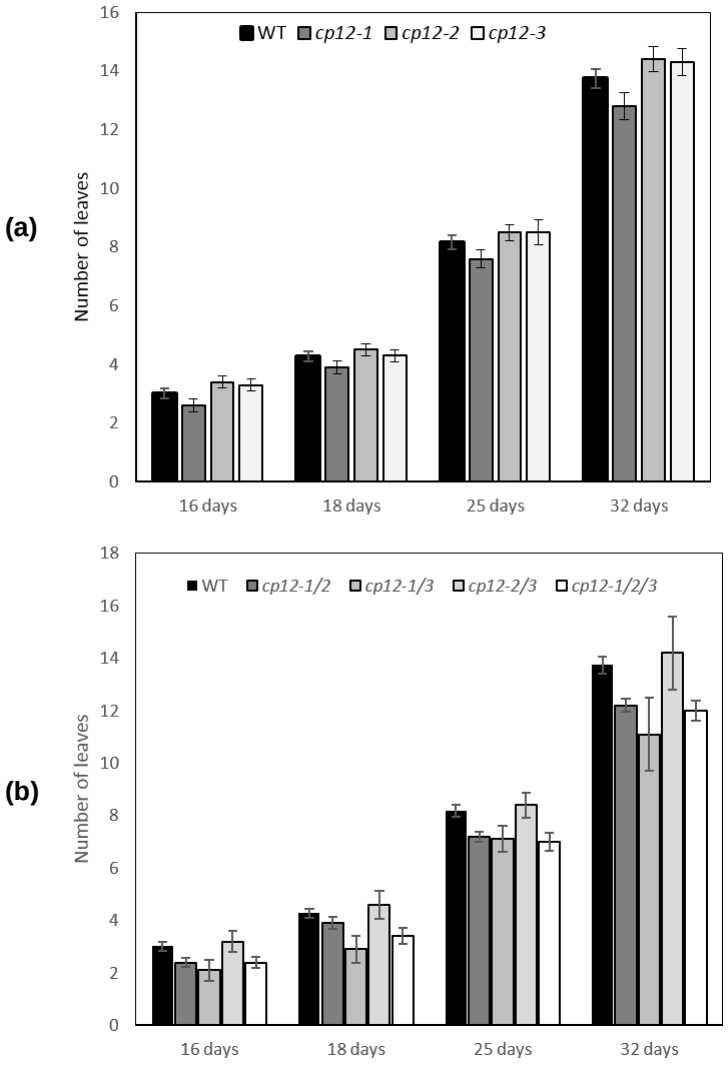

Figure 4.4 Variation in leaf numbers of *Arabidopsis thaliana* CP12 mutant lines. The plants were grown in soil for five weeks and then the number of leaves were counted in weeks 3, 4 and 5. **(a)** Leaf number of the WT and single CP12 mutant lines (*cp12-1*, *cp12-2* and *cp12-3*). **(b)** Leaf number of the WT and multiple CP12 mutant lines (*cp12-1/2*, *cp12-1/3*, *cp12-2/3* and *cp12-1/2/3*). The error bars represent SE n= 10 replicates.

4.1.2 Analysis of the photosynthetic carbon assimilation rate of the WT, *cp12-1/2*, *cp12-1/3* and *cp12-1/2/3* lines

In order to explain the phenotype described in the growth analysis, the carbon assimilation rates of those lines with the most severe phenotype (*cp12-1/2*, *cp12-1/3* and *cp12-1/2/3*) were determined. This was achieved by calculating the assimilation rate under an increasing intercellular CO_2 (net CO_2 assimilation rate [*A*] versus the calculated substomatal CO_2 [*Ci*] response curve). The plants were grown under short-day conditions of 8 hours light and 16 hours dark.

At very high *Ci* values, the *cp12-1/2* and *cp12-1/2/3* lines seem to have the lowest assimilation rate when compared with the WT. However, no significant difference was found between the WT and the mutant lines (Figure 4.5).

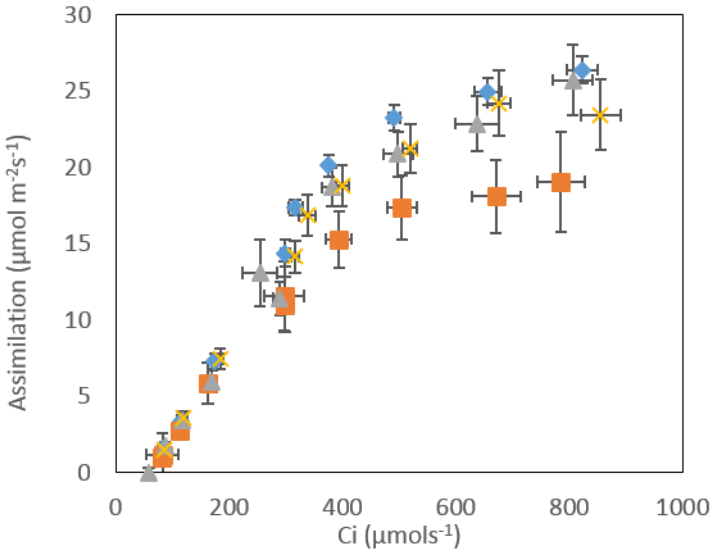

Figure 4.5 Photosynthetic carbon assimilation rate of the WT and CP12 insertion mutants. The carbon assimilation rate for the WT and the *cp12-1/2*, *cp12-1/3* and *cp12-1/2/3* lines at different CO_2 concentrations. The blue diamond is the WT, the orange square is the *cp12-1/2* line, the grey triangle is the *cp12-1/3* line and the yellow cross is the *cp12-1/2/3* line. The error bars represent SE n=9–12 replicates.

4.1.3 Photosystem II (PSII) operating efficiency (*Fq'/Fm'*) of the T-DNA lines

Further analysis of the T-DNA insertion lines was performed in order to further elucidate the slow growth phenotype, two different lights were used to estimate the photosystem II operating efficiency (F*q*'/F*m*').

The F*q*'/F*m*' parameter was used to estimate the operating efficiency of PSII for the insertion mutant lines and the WT. The experiment was conducted on young seedlings of 14–22 days of growth, sown in half MS and grown under long-day conditions of 16 h light and 8 h dark.

A comparison between the T-DNA insertion lines and the WT showed that the *cp12-1/2* and *cp12-1/2/3* lines had significantly lower F*q*'/F*m*' values than the WT. However, no significant difference was found between the single mutant lines *cp12-1*, *cp12-2* and *cp12-3* and the WT.

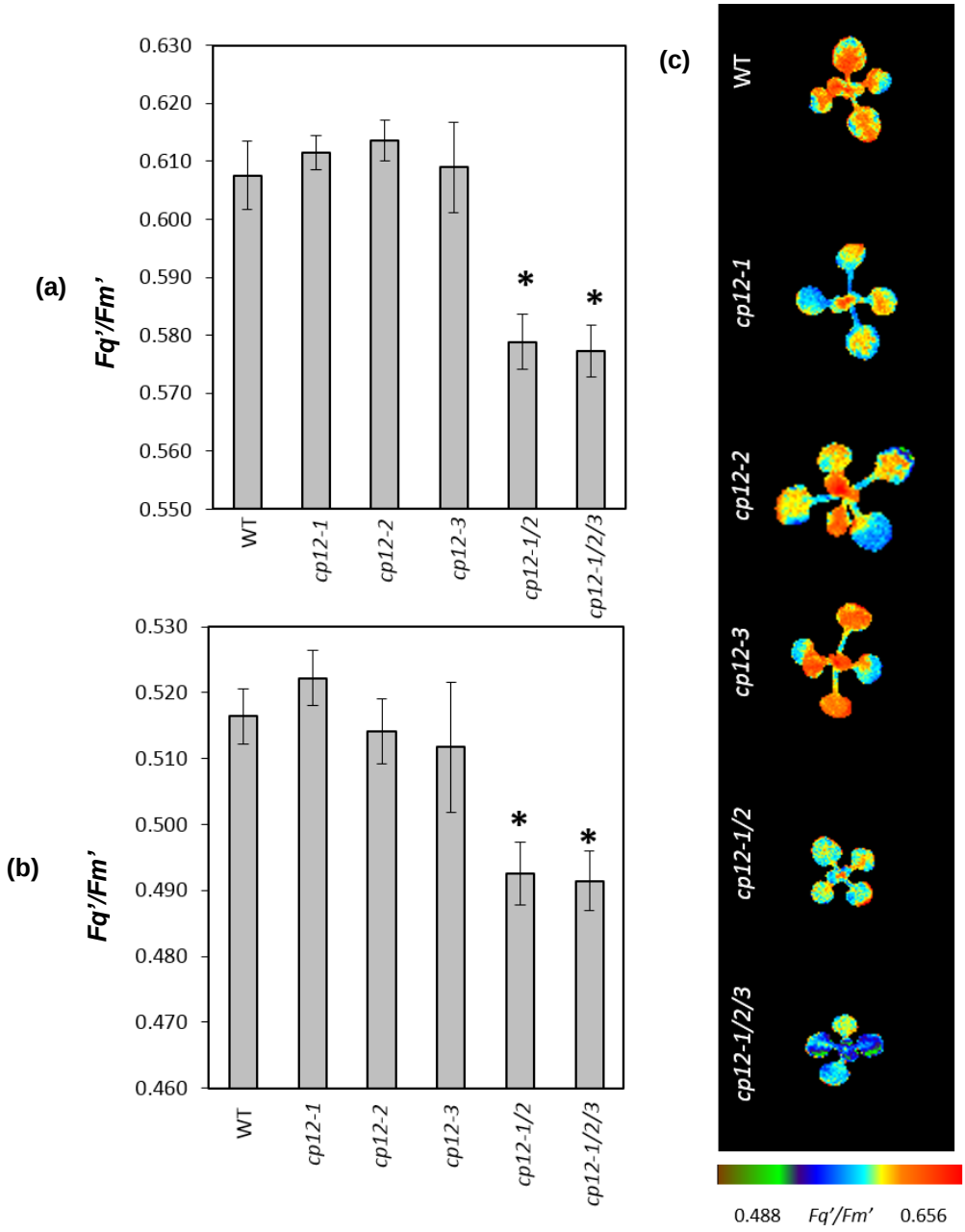

Figure 4.6 Photosystem II operating efficiency of the CP12 T-DNA insertion mutant lines plants when compared with the WT plants. The WT and mutant plants were grown in controlled environmental conditions with a light intensity of 130 µmol m^{-2} s^{-1} and a 16/8 h light/dark cycle for 14 days. Chlorophyll fluorescence was used to determine the *F*q′/*F*m′ (PSII operating efficiency) at two light intensities: **(a)** 130, **(b)** 300 and **(c)** 130 µmol m^{-2} s^{-1}. The scale bar represents an *F*q′/*F*m′ of 0.488–0.656. All data are means (± SE). The error bars represent SE n=3-5 replicates.

4.1.4 Fluctuating and square light regimes

To further extend the analysis of the phenotype observed from the growth analysis, three different lines, namely the WT, *cp12-1/2* and *cp12-1/2/3* (these lines were selected due to the severe phenotype that was previously observed), were exposed to different light regimes.

For this, seeds from these lines were chilled for about three days in order to promote germination and then sown in soil. The plants were transferred to a growth room. When the plants were two weeks old, they were moved to one of two different light regimes: one was a square wave light regime and the other was a fluctuating light regime. Both regimes had short-day conditions of 8 h light and 16 h dark, a temperature of about 22^{o}C and the same amount of light.

As anticipated, under the square light regime a slow growth rate is observed in the double mutant *cp12-1/2* and the triple mutant *cp12-1/2/3*. However, under the fluctuating light regime, the slow growth phenotype was disappeared, showing no difference between the WT and the mutant lines (Figure 4.7).

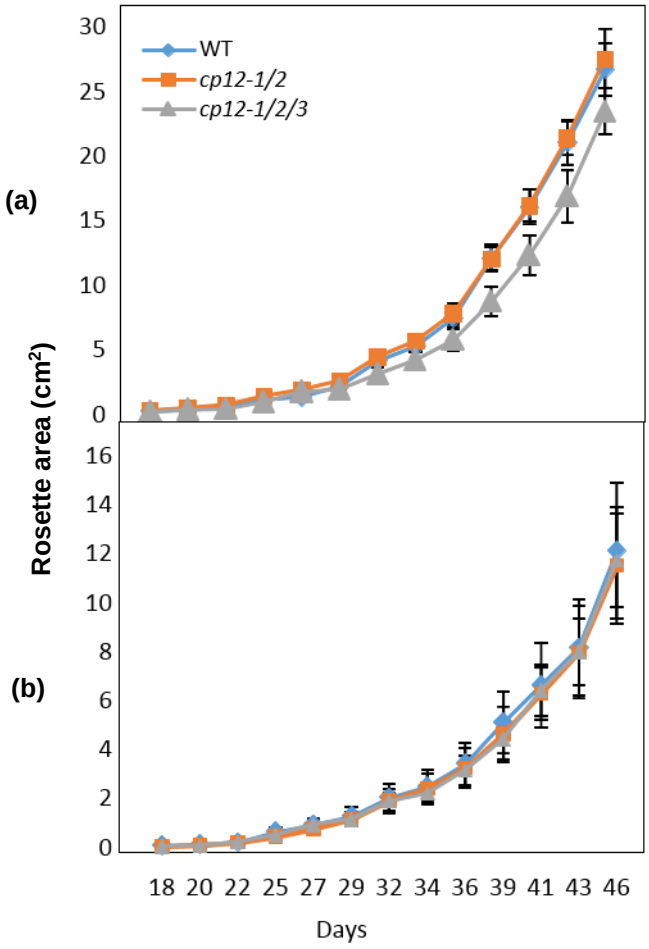

Figure 4.7 Comparison of the leaf area of the WT, *cp12-1/2* and *cp12-1/2/3* lines under the fluctuating and square light regimes. The plants were grown under identical conditions of 8 hours light and 16 hours dark and a temperature of 22˚C. **(a)** *Arabidopsis thaliana* WT, double mutant *cp12-1/2* and triple *cp12-1/2/3* under a square (control) light. **(b)** *Arabidopsis thaliana* WT, double mutants *cp12-1/2* and triple mutant *cp12-1/2/3* under a fluctuating light. The error bars represent SE n=3-6.

4.2 Complementation

In order to confirm that the slow growth phenotype of the T-DNA *cp12-1/2/3* is due to the absence of CP12 gene, and since only one mutant allele for each CP12 gene was identified, a complementation testing strategy was adopted. For this, a construct of flag-tagged CP12-1 driven by the native promoter was introduced into the *cp12-1/2/3* (Singh et al., 2008). Four independent lines were identified and then genetically checked to confirm the presence of the construct and the production of the flag-tagged protein. Based on the results of the PCR and Western bolt analysis, three independent lines were selected to study the phenotype. Furthermore, a qPCR analysis was conducted to evaluate the transcript level of the entire CP12 gene family. As shown in Figure 4.8, the CP12-1 gene in all three lines (*1.1*, *2.1* and *3.3*) appears to be complemented because the mRNA is clearly detected. Similarly, the expression of the CP12-2 gene was also detected as the T-DNA insertion only leads to a 50% reduction of the expression (knockdown line). On the other hand, the T-DNA insertion in CP12-3 knocks out the expression of the gene; therefore, as expected, no expression was detected in any of the lines.

Following this, a growth analysis was conducted to monitor the rosette area at several time points. The transgenic lines NP-CP12-1::FLAG *1.1*, *2.1* and *3.3*, as well as the WT and *cp12-1/2/3*, were grown in a controlled environment for 6–7 weeks under short-day conditions of 8 h light and 16 h dark.

The results of the growth analysis revealed that two out of three lines of the NP-CP12-1::FLAG seemed to partially complement the phenotype by showing no significant difference between the transgenic lines (*1.1* and *2.1*) and the WT.

However, line *3.3* showed a slow growth phenotype which seemed to be significantly different to that of the WT. The statistical analysis from this experiment revealed that triple mutant *cp12-1/2/3* seemed to be significantly different from the WT and the complemented lines (*1.1* and *2.1*), which indicate that in these lines the phenotype is rescued by the expression of the CP12-1::FLAG transgene.

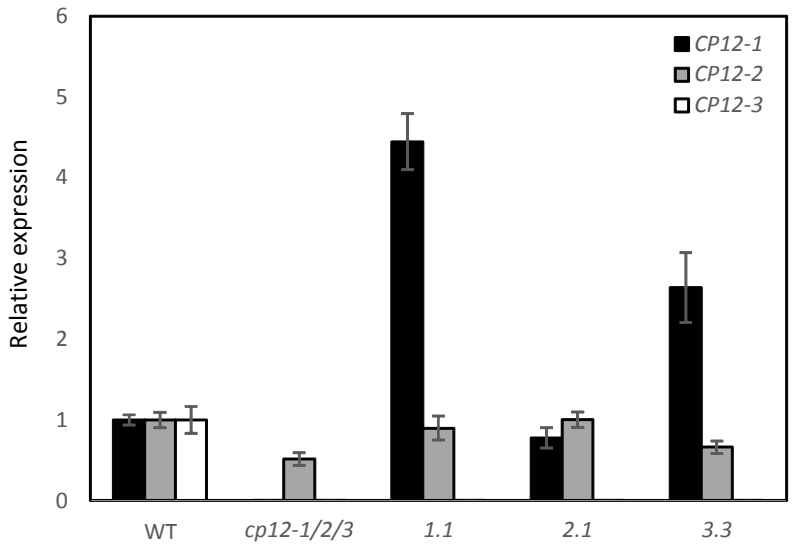

Figure 4.8 Quantitative PCR (qPCR) analysis of the expression of the complementation lines of native promoter CP12-1-FLAG. The total RNA was extracted from the leaf tissue of adult rosettes**.** Black bars indicate the expression of CP12-1, grey bars represent the expression of CP12-2 expression and white bars indicate the CP12-3 expression. All results are normalised with the actin and cyclophilin genes. The error bars represent SE n=3-10.

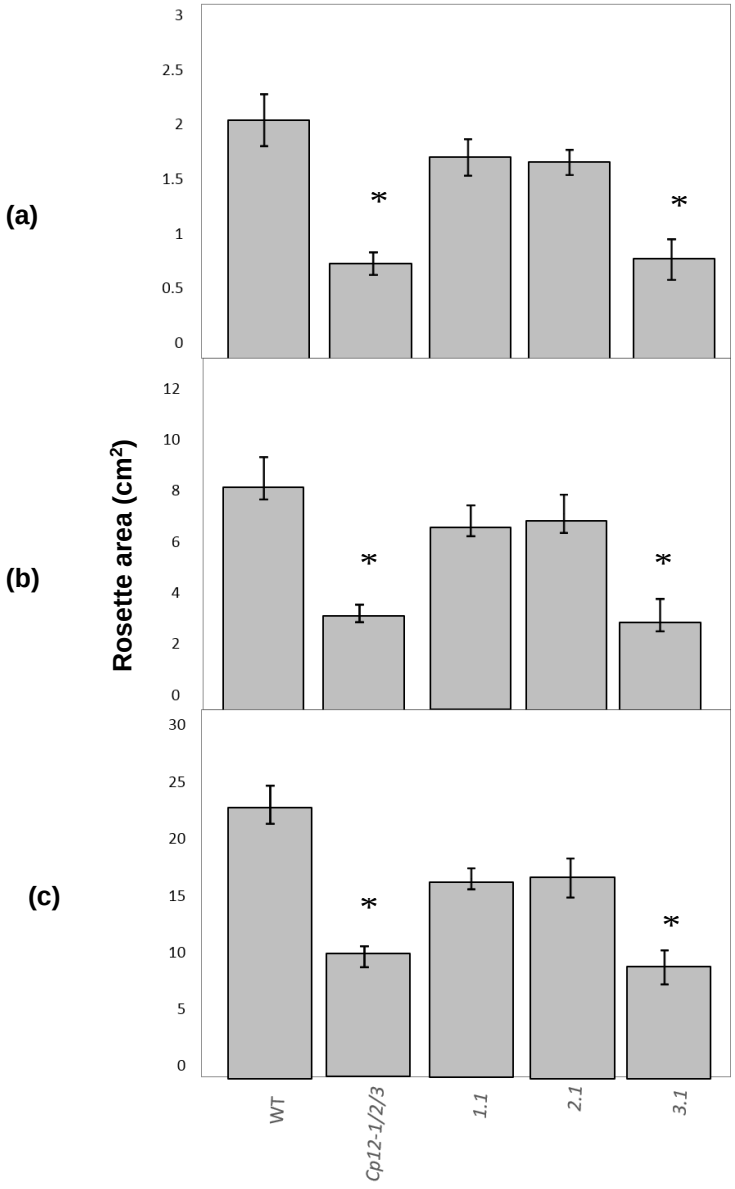

Figure 4.9 Comparison of the leaf area of the WT*, cp12-1/2/3* and three independent lines of NP-CP12-1::FLAG in a *cp12-1/2/3* background. The plants were grown in soil under identical conditions of 8 h light and 16 h dark at 22˚C. **(a)** Leaf area analysis of the WT, *cp12-1/2/3, 1.1*, *2.1* and *3.3* at 22 days **(b)** Leaf area analysis of the WT, *cp12-1/2/3*, *1.1*, *2.1* and *3.3* at 29 days **(c)** Leaf area analysis of the WT, *cp12-1/2/3*, *1.1*, *2.1* and *3.3* at 36 days. The error bars represent SE n=4-10. * indicates significant differences compared to the WT. Significant determined by Kruskal-Wallis followed by Mann-Whitney tests (*P*<0.05).

(a)

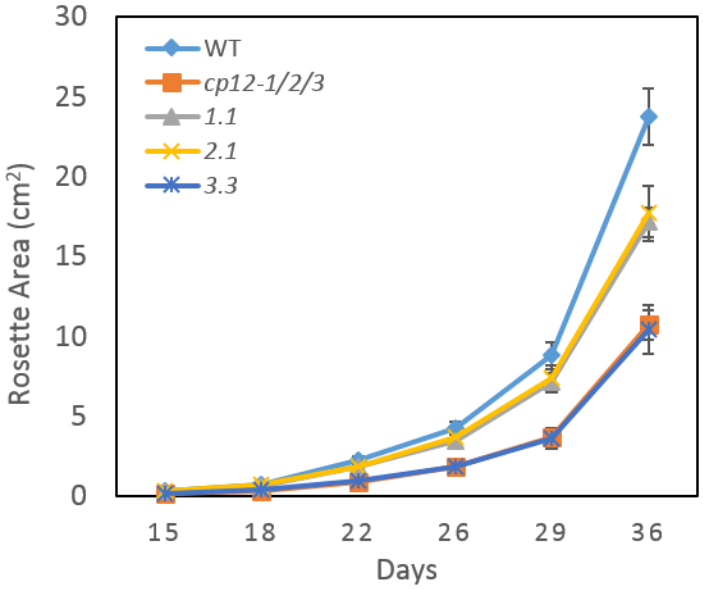

(b)

Figure 4.10 Complementation of the triple mutant *cp12-1/2/3* by the native promoter-CP12-1::FLAG. (a) Comparison of the growth rate of the WT and NP-CP12-FLAG in the triple mutant *cp12-1/2/3.* The plants were grown in soil under identical conditions in a controlled environment (22°C, 8 h light and 16 h dark cycle). Pictures were taken at weeks 2, 3, 4 and 5, and the photographs were used to calculate the rosette area. **(b)** *Arabidopsis thaliana* WT, *cp12-12/3* and NP-CP12-1::FLAG (*2.1*). Plants at 34 days. The error bars represent SE n=4-10 replicates.

4.3 Analysis of the RNAi transgenic lines

4.3.1 Quantification of the expression of CP12 in the RNAi transgenic lines

The qPCR results of tests previously conducted on the T-DNA insertion lines revealed that the *cp12-2* line was only a knockdown, with an approximately 50% reduction of the CP12-2 transcript level. The RNAi approach was used to reduce the level of CP12-2 transcript in the WT, *cp12-1/2* and *cp12-1/2/3* in order to produce the single *cp12-2 WT.RNAi (WT.R)*, the double *cp12-1/2 DB.RNAi (DB.R)* and the triple *cp12-1/2/3 TM.RNAi (TM.R)* transgenic lines with further reduced CP12-2 expression.

To study the effect of the RNAi construct on the expression of the CP12-2 gene, the transcript levels of plants with a *cp12-1/2/3* background (*TM.R.53.1*, *TM.R.53.2*, *TM.R.54.1*, *TM.R.54.2* and *TM.R.54.4*) were evaluated via qPCR analysis.

The plants were grown in soil under short-day conditions of 8 h light and 16 h dark. Leaf tissues were sampled from an adult rosette and collected from three biological replicates. cDNA was produced via RNA extraction, which was then used to quantify the expression of CP12-2.

While the expression of CP12-2 in the triple mutant *cp12-1/2/3* was only reduced to around 47% when compared to the WT, it is clearly evident that there is a further reduction in the transcript level of CP12-2 due to the RNAi-specific constructs.

The results presented in Figure 4.11 showed that the RNAi-specific construct in the triple T-DNA insertion lines clearly reduced the level of CP12-2 expression to 33% and 34% in lines *TM.R.53.1* and *TM.R.53.2* respectively of the WT level. Additionally, the transcript level of CP12-2 was decreased to 28% and 27% in lines *TM.R.54.1* and

TM.R.54.2 respectively. Finally the line *TM.R.54.4* had the most dramatic reduction in CP12-2 transcript, with less than 20% WT transcript level.

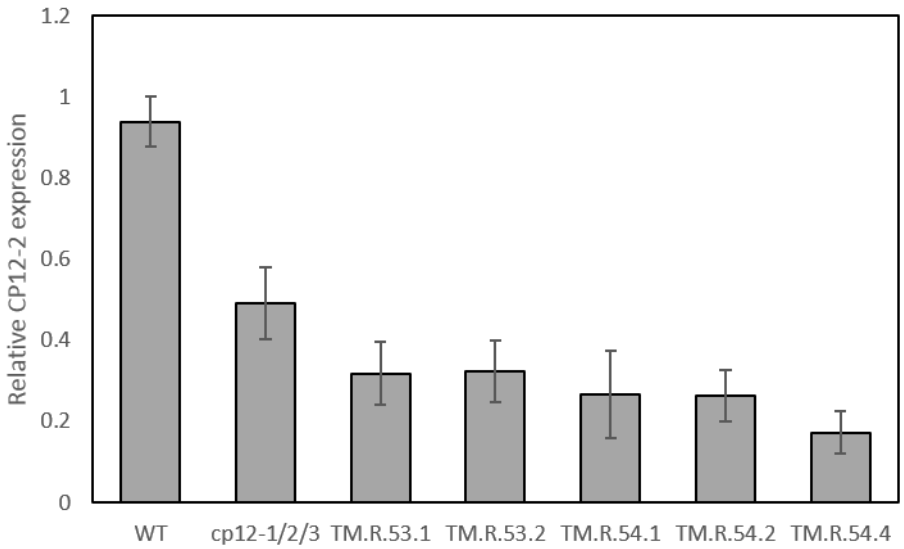

Figure 4.11 qPCR analysis of the expression of CP12-2 in the RNAi transgenic plants. Total RNA was extracted from the leaf tissues of an adult rosette and then used in quantitative RT-PCR to estimate the relative level of expression of the CP12-2 gene in the RNAi transgenic lines with respect to the WT level of expression. The error bars represent SE. All results were calculated using the relative expression software tool (REST) for group-wise comparison and the statistical analysis of the relative expression results in real-time PCR (2009 version) (Pfaffl et al., 2002).

4.3.2 Change observed in rosette area over time and seed yield

In order to evaluate the impact of further reductions in CP12-2 transcript on plant development, a growth analysis of the T2 generation was performed for all the transgenic RNAi lines of WT and *cp12-1/2/3* background and their controls. As mentioned in the previous chapter, two different RNAi-specific constructs targeting CP12-2 were introduced in the WT and *cp12-1/2/3* to produce single *cp12-2* and triple *cp12-1/2/3*. Six individual lines were used for the WT background (*WT.R.53.1*, *WT.R.53.2*, *WT.R.53.3*, *WT.R.54.1*, *WT.R.54.2* and *WT.R.54.3*) and five individual lines for the *cp12-1/2/3* background (*TM.R.53.1*, *TM.R.53.2*, *TM.R.54.1*, *TM.R.54.2* and *TM.R.54.4*). These lines were grown along with the *cp12-2, cp12-1/2/3* and WT. Seeds were sown in soil under short-day conditions of 8 h light and 16 h dark for 45 days. Ten replicates were included for each line.

With both specific constructs (53 and 54), no significant differences were found in the RNAi transgenic lines with the WT background when compared with the *cp12-2* and WT. Figure 4.12 shows the rosette area and barely any differences between the *WT.RNAi* transgenic lines and the WT.

However, recordings of the growth rate demonstrated a considerable slow growth phenotype of the RNAi transgenic lines with the *cp12-1/2/3* background. At 15 days after sowing, lines from both RNAi-specific constructs (53 and 54) showed clear evidence of the slow growth phenotype, since the rosette area for lines *TM.R.53.1* and *TM.R.53.2* was only 51% and 58%, respectively, of the WT. In addition, the lines from construct 54 showed a reduction of 53%, 64% and 52% for lines *TM.R.54.1*, *TM.R.54.2* and *TM.R.54.4* respectively.

Figure 4.13 shows how the RNAi-specific constructs significantly impacted on the plant's growth and development and that in most of the lines, especially with the 54 construct, further reduction in the CP12-2 transcript level led to increase the phenotype of the slow growth rate compare to the *cp12-1/2/3* (Figure 4.13 and Figure 4.15). The most dramatic phenotype was in the line *TM.R.54.2* which with further reduction of about 27% compare to the *cp12-1/2/3.*

As the rosette area and the growth rate of the RNAi transgenic plants were both affected, the seed yield might also be impacted. In order to assess this, the plants were allowed to flower before being individually bagged and allowed to produce seeds. The seeds that were produced by each plant were collected and weighed to estimate the seed yield. As expected, there was a reduction in the total seed yield of the RNAi transgenic lines with the *cp12-1/2/3* background *(TM.RNAi)* lines when compared with the WT. However, the transgenic RNAi in the WT background did not exhibit any difference in terms of seed yield when compared with the WT and the *cp12-2* (Figure 4.16.a).

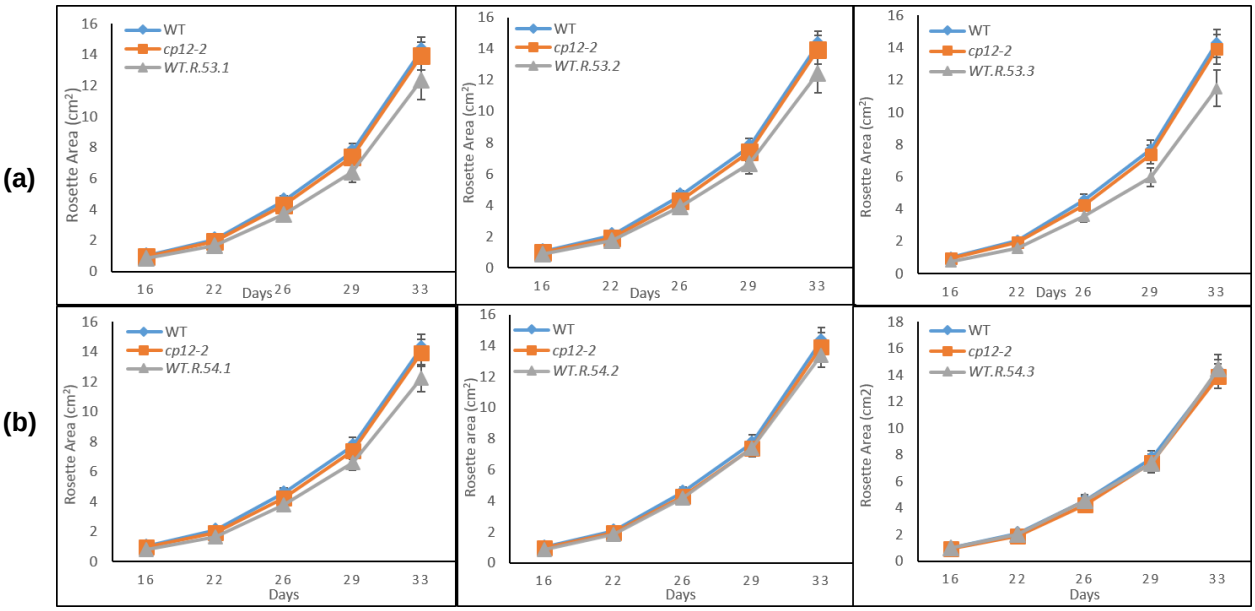

Figure 4.12 Comparison of the growth rates of the WT, T-DNA *cp12-2* and single RNAi transgenic lines. The plants were grown in soil under controlled environment conditions of 8 hours of light and 16 hours of dark at a temperature of 22˚C and a light level of about 200 µmol m^{-2} s^{-1}. Photographs were taken at weeks 3, 4, 5 and 6, and the rosette area was calculated from those photographs. **(a)** *Arabidopsis thaliana* WT, T-DNA *cp12-2* and RNAi transgenic for specific construct 53 (*WT.R.53.1*, *WT.R.53.2* and *WT.R.53.3*). **(b)** *Arabidopsis thaliana* WT, T-DNA *cp12-2* and single RNAi transgenic line for specific construct 54 (*WT.R.54.1*, *WT.R.54.2* and *WT.R.54.3*). The error bars represent SE n=14-15 replicates.

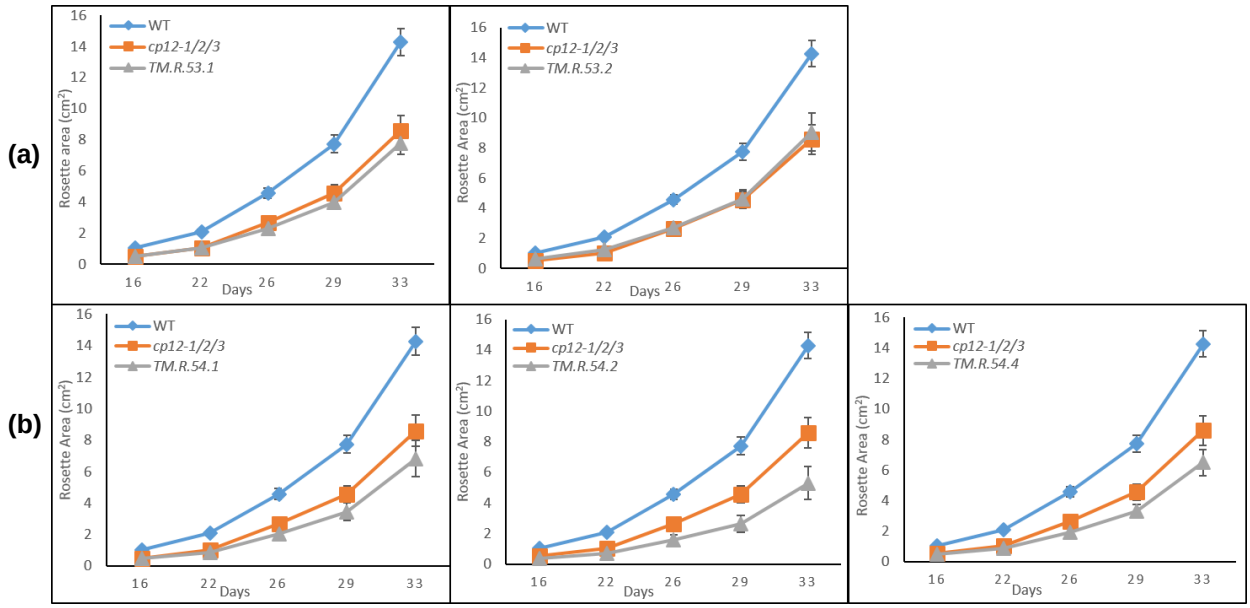

Figure 4.13 Comparison of the growth rates of the WT, *cp12-1/2/3* and triple RNAi transgenic lines. The plants were grown in soil under controlled environment conditions of 8 hours of light and 16 hours of dark at a temperature of 22˚C and a light level of about 200 µmol m^{-2} s^{-1}. Photographs were taken at weeks 3, 4, 5 and 6, and the rosette area was calculated from those photographs. **(a)** *Arabidopsis thaliana* WT, T-DNA *cp12-1/2/3* and triple *cp12-1/2/3* RNAi transgenic line of specific construct 53 (*TM.R.53.1* and *TM.R.53.2*). **(b)** *Arabidopsis thaliana* WT, T-DNA *cp12-1/2/3* and triple *cp12-1/2/3* RNAi transgenic line of specific construct 54 (*TM.R.54.1*, *TM.R.54.2* and *TM.R.54.4*). The error bars represent SE n=14-15 replicates.

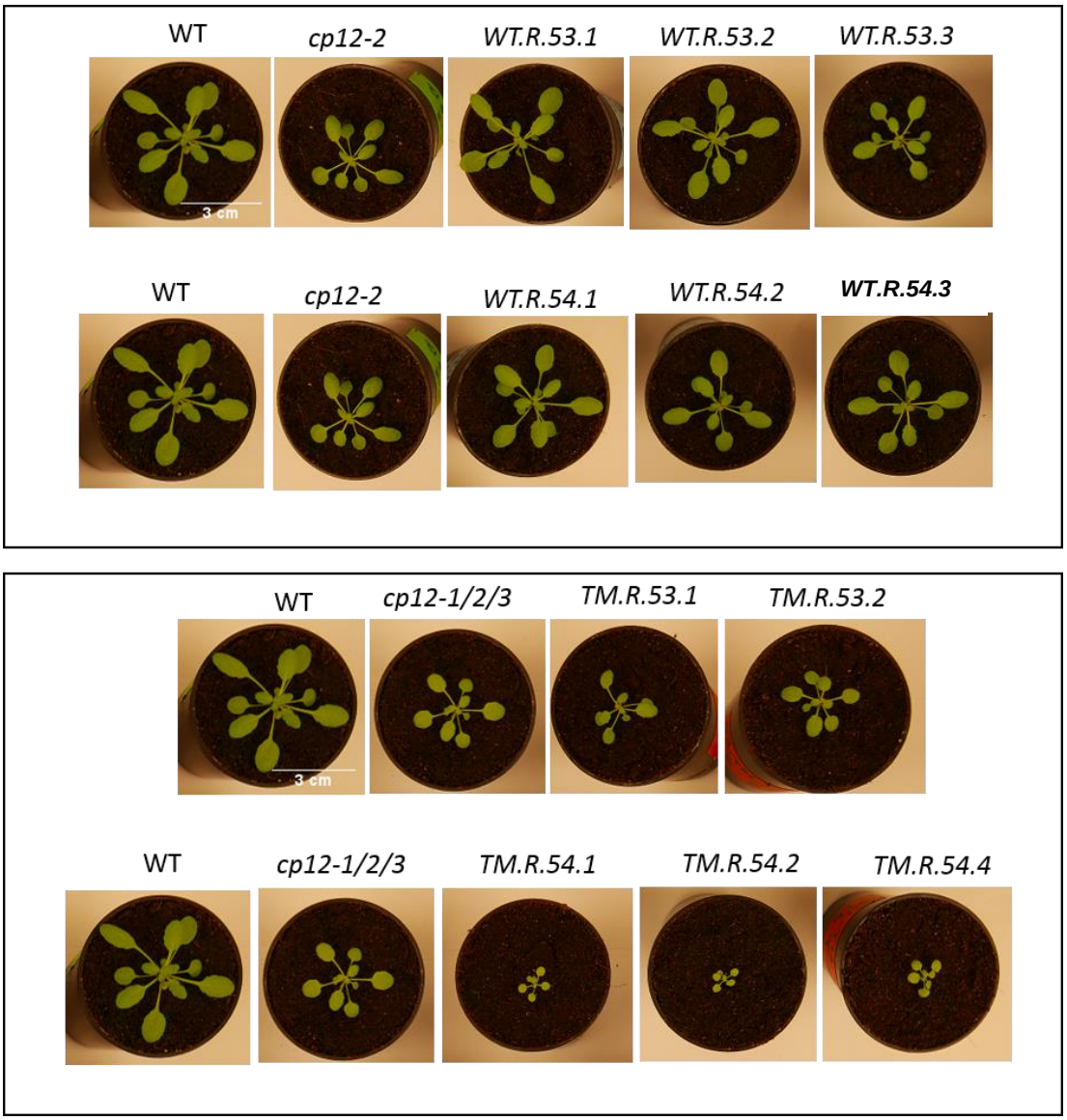

Figure 4.14 Comparison of the WT and RNAi transgenic lines in soil. The plants were grown in soil under controlled environmental conditions of 8 hours of light and 16 hours of dark at a temperature of 22˚C and a light level of about 200 µmol m^{-2} s^{-1}. **(a)** *Arabidopsis thaliana* WT, T-DNA *cp12-2* and single *cp12-2* RNAi transgenic lines in the WT background of 26 days. **(b)** *Arabidopsis thaliana* WT, T-DNA *cp12-1/2/3* and triple *cp12-1/2/3* RNAi transgenic lines with *cp12-1/2/3* background of 26 days. The white scale bar represents 3 cm.

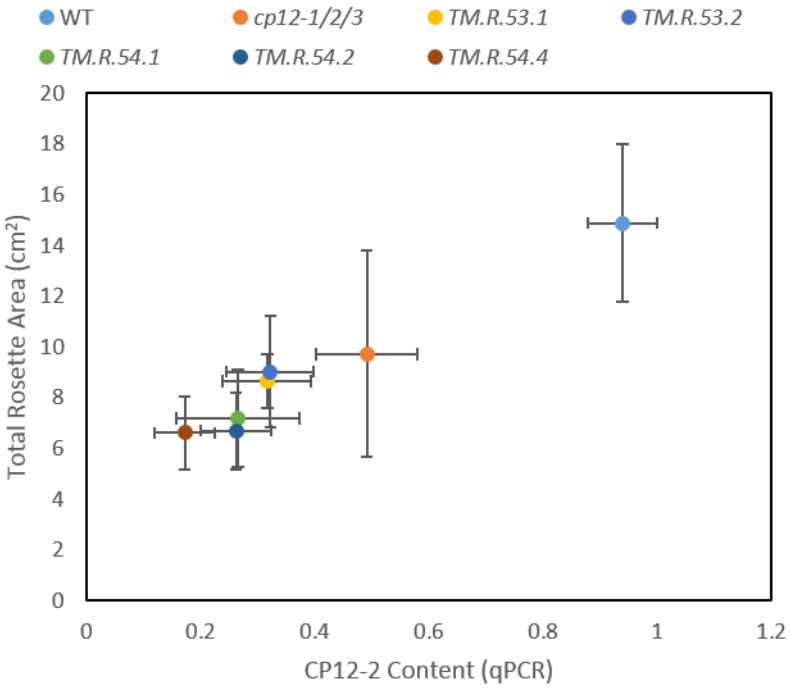

Figure 4.15 Comparison of total CP12-2 content (qPCR) and the total rosette area. *Arabidopsis thaliana* WT, *cp12-1/2/3* and triple RNAi transgenic lines *(TM.R.53.1, TM.R.53.2, TM.R.54.1, TM.R.54.2* and *TM.R.54.4).* Plants of 34 days. The errors bars represent SE n=3-8 replicates.

(a)

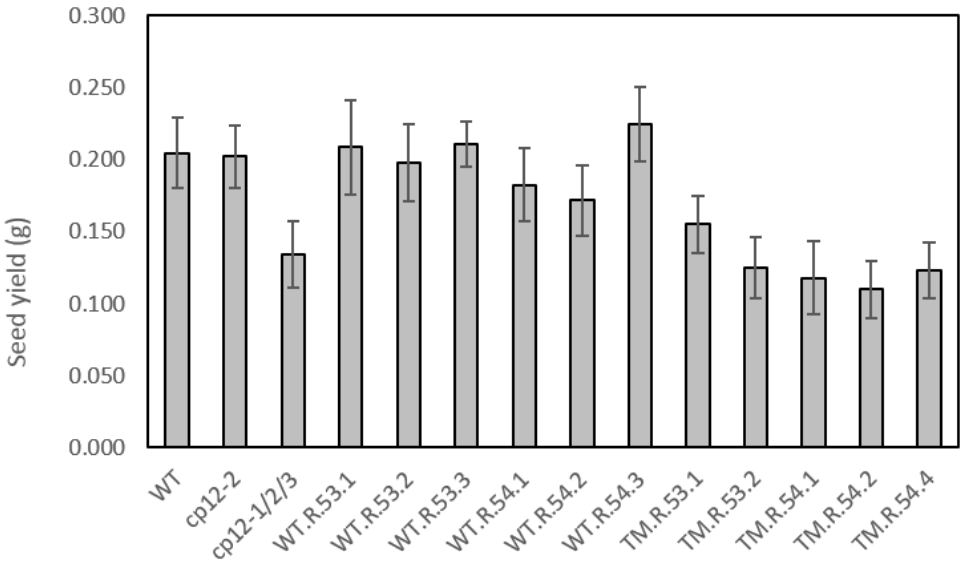

(b)

Figure 4.16 Seed yield of WT and RNAi transgenic plants. (a) Total seed yield produced by WT and the RNAi transgenic lines. Error bars represents SE n=14-15 replicates. **(b)** *Arabidopsis thaliana* WT, *cp12-1/2/3* and triple RNAi transgenic lines *(TM.R.54.1* and *TM.R.54.2).* Plants of 77 days.

4.3.3 PSII operating efficiency (*Fq'/Fm'*) for the RNAi lines

In order to investigate whether the severe growth phenotype the RNAi transgenic lines is caused by a reduction in photosynthesis in these plants, *Fq'/Fm'* was used to estimate the PSII operating efficiency at 14–23 days of growth. All the T2 segregating RNAi transgenic lines, including the single, double and triple lines, were grown in half MS media for 23 days under long-day conditions of 16 hours light and 8 hours dark.

The single lines of RNAi *WT.R.53.1*, *WT.R.45.1* and *WT.R.54.3* were tested at light intensities of both 130 and 330 µmol $m^{-2}s^{-1}$. Although there was a slight decrease in these lines, there was no significant difference between the RNAi transgenic lines and the *cp12-2* T-DNA insertion line or the WT.

Additionally, in the double RNAi transgenic lines, *Fq'/Fm'* revealed that the double lines *DB.R.54.2* and *DB.R.54.5* had an increased level when compared to the *cp12-1/2*.

In the triple RNAi transgenic lines, there is a clear reduction in the *Fq'/Fm'* for lines *TM.R.53.1*, *TM.R.54.1*, *TM.R.54.2* and *TM.R.54.4* when compared to the WT and the T-DNA insertion line *cp12-1/2/3.*

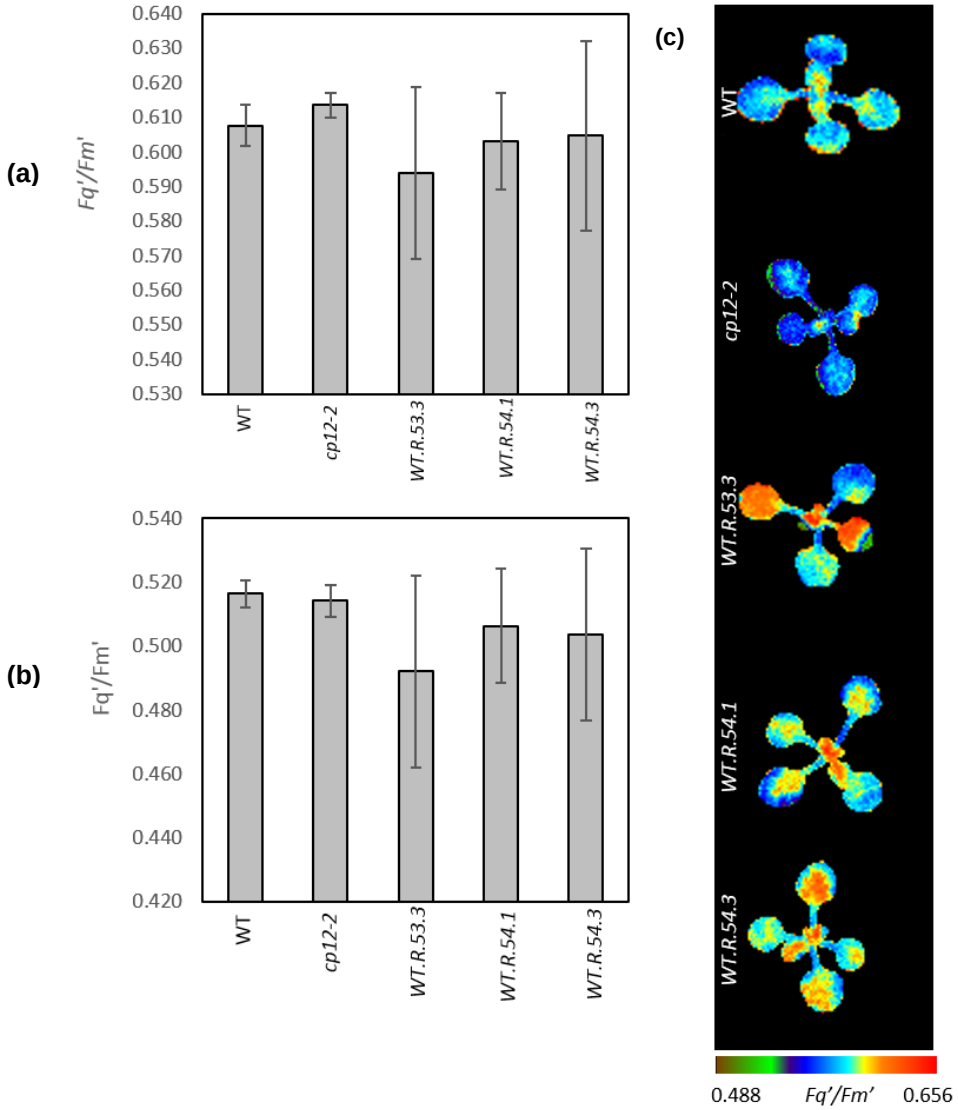

Figure 4.17 Photosystem II operating efficiency of the CP12 single RNAi transgenic lines plants when compared with the WT plants. The WT and single RNAi transgenic plants were grown in controlled environmental conditions with a light intensity of 130 µmol m^{-2} s^{-1} and a 16/8 h light/dark cycle for 14 days. Chlorophyll fluorescence was used to determine the *F*q′/*F*m′ (PSII operating efficiency) at two light intensities: **(a)** 130, **(b)** 300 and **(c)** 130 µmol m^{-2} s^{-1}. The scale bar represents an *F*q′/*F*m′ of 0.488–0.656. All data are means (± SE) 3-5 replicates.

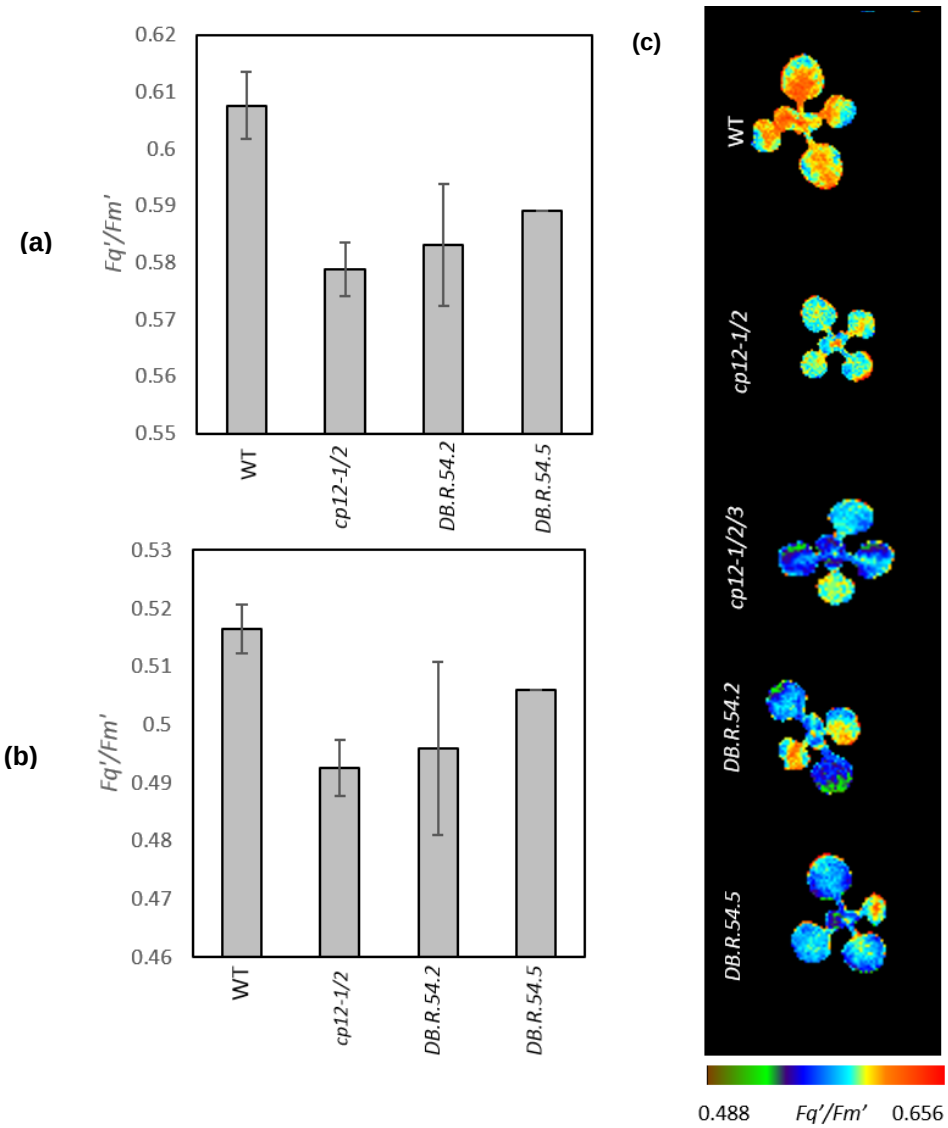

Figure 4.18 Photosystem II operating efficiency of the CP12 double RNAi transgenic lines plants when compared with the WT plants. The WT and double RNAi transgenic plants were grown in controlled environmental conditions with a light intensity of 130 µmol m^{-2} s^{-1} and a 16/8 h light/dark cycle for 14 days. Chlorophyll fluorescence was used to determine the *F*q′/*F*m′ (PSII operating efficiency) at two light intensities: **(a)** 130, **(b)** 300 and **(c)** 130 µmol m^{-2} s^{-1}. The scale bar represents an *F*q′/*F*m′ of 0.488–0.656. All data are means (± SE) 1-5 replicates.

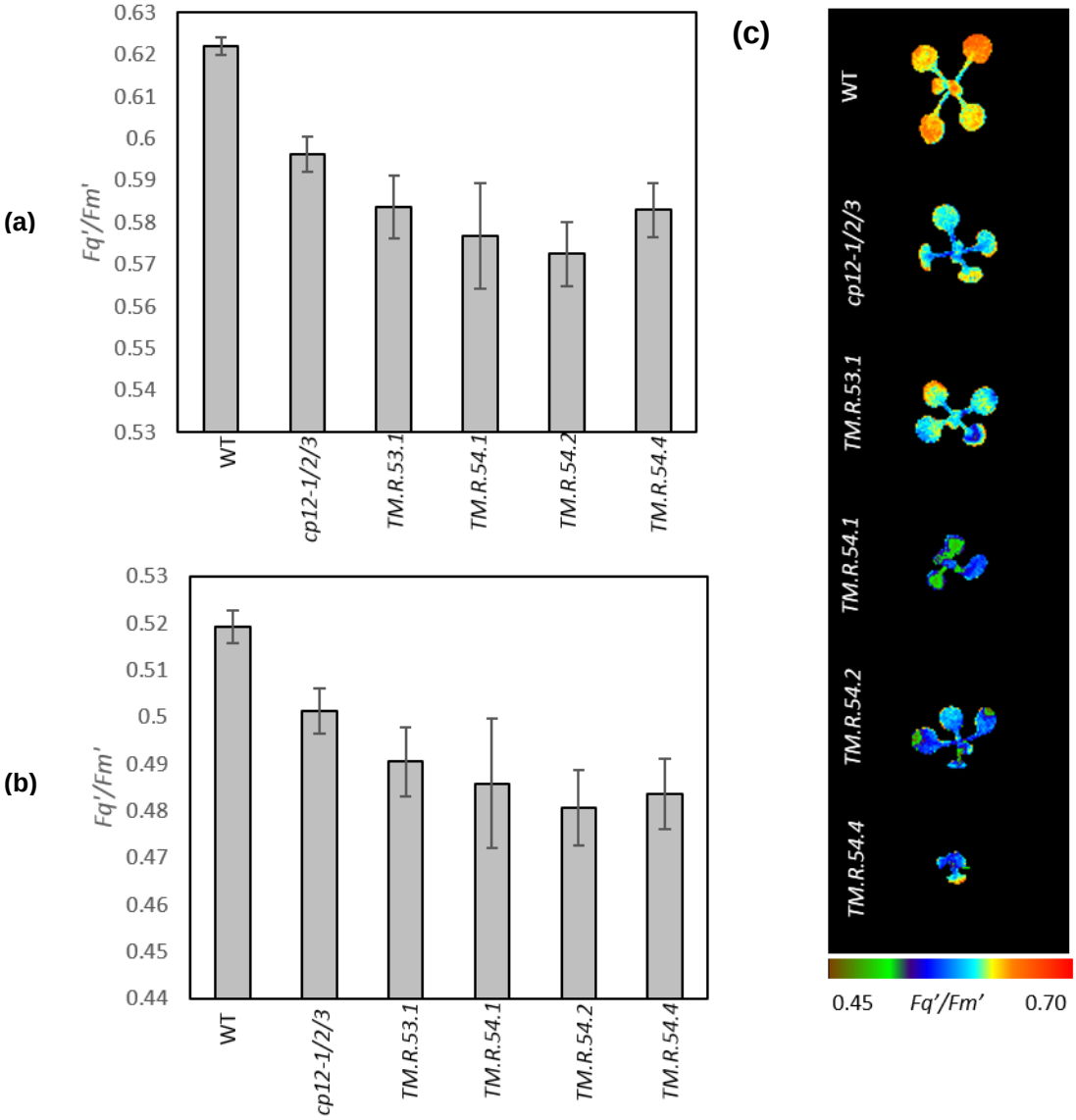

Figure 4.19 Photosystem II operating efficiency of the CP12 triple RNAi transgenic lines plants when compared with the WT plants. The WT and triple RNAi transgenic plants were grown in controlled environmental conditions with a light intensity of 130 µmol m^{-2} s^{-1} and a 16/8 h light/dark cycle for 14 days. Chlorophyll fluorescence was used to determine the *F*q′/*F*m′ (PSII operating efficiency) at two light intensities: **(a)** 130, **(b)** 300 and **(c)** 130 µmol m^{-2} s^{-1}. The scale bar represents an *F*q′/*F*m′ of 0.488–0.656. All data are means (± SE) 3-5 replicates.

4.3.4 Analysis of the root growth and the lateral roots in the RNAi transgenic lines

In order to further analyze the phenotype identified in the growth analysis of the RNAi lines, and since it has been found that the redox state of the leaves can affect the development of the lateral roots, a root growth experiment was performed to monitor the root development and check whether reduced levels of CP12 expression would lead to an abnormal root development phenotype. This experiment targeted the root length in addition to the number of lateral roots for each line. Two lines of the RNAi transgenic lines *TM.R.53.1* and *TM.R.54.1* as well as *cp12-1/2/3* and the WT, were included in the experiment.

Seeds from the four lines were sown in half MS media in square plates. After that, the plates were orientated vertically and incubated in a growth chamber under long-day conditions. The root length was measured and the number of lateral roots was counted using Image J software twice a week.

During early seedling growth, the RNAi lines and the T-DNA *cp12-1/2/3* showed a slow rate of root growth, as well as fewer lateral roots, than the WT plants (Figure 4.20).

Additionally, since the formation of the lateral root is highly influenced by Auxin, auxin1- Naphthalene acetic acid (NAA) was added to the MS in two concentrations (10^{-9} and 10^{-8} mM of NAA) to test whether the phenotype of the lateral roots would be affected. The treatment with NAA increased the root length and the number of lateral roots for the *cp12-1/2/3* and *TM.R.54.1* lines, however, an inhibitory effect seemed to be found in the RNAi line *TM.R.53.1*, which seemed to exhibit a reduction in both root length and the number of lateral roots.

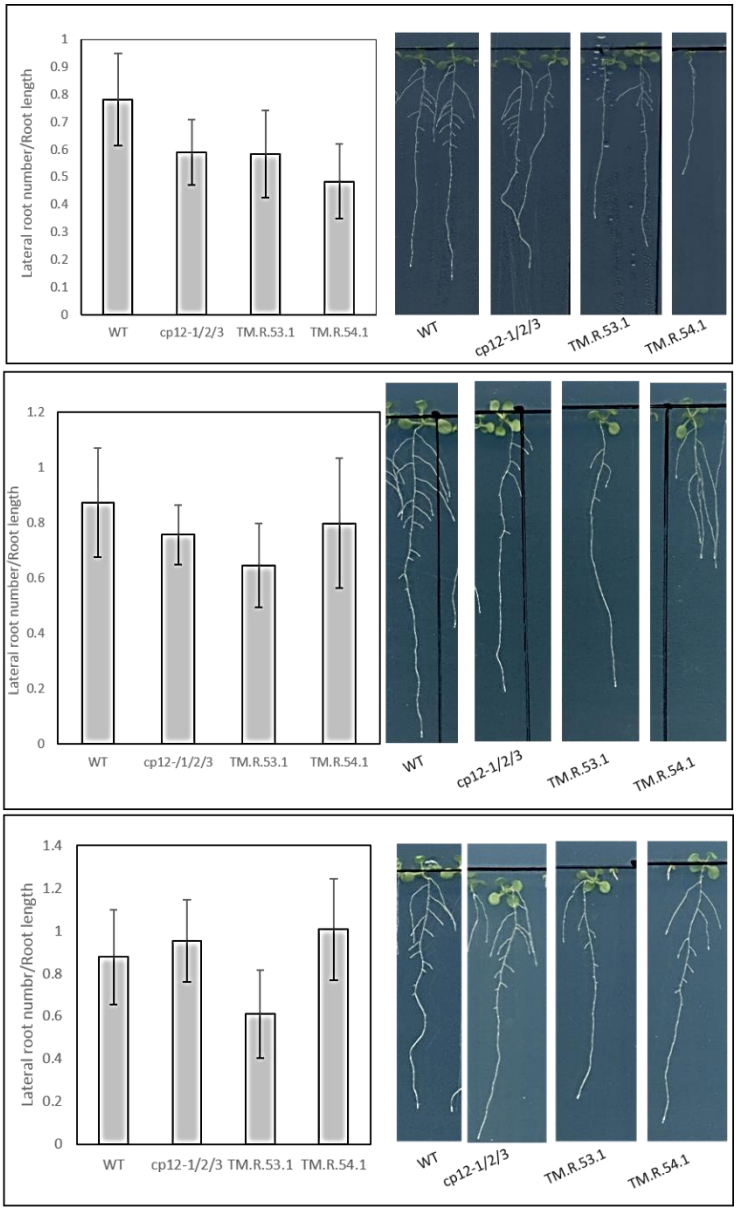

Figure 4.20 Comparison of the root growth of the WT and *cp12-1/2/3* RNAi transgenic plants under different NAA concentrations. Images of 14-day-old wild-type (WT), T-DNA *cp12-1/2/3* and triple RNAi transgenic lines (*TM.R.53.1* and *TM.R.54.1*) grown under long-day conditions. Quantification of the number of lateral roots related to the root length of seedlings of different *Arabidopsis* varieties. **(a)** Controls without NAA treatment. **(b)** 10^{-9} of NAA. **(c)** 10^{-8} of NAA. The error bars represent SE n=11-20 replicates.

4.3.5 H_2O_2 measurement

Since the CP12 protein family is known to be a redox regulator, and in order to investigate the impact of reducing the level of CP12 on the metabolism of the leaves, a H_2O_2 assay was performed on selected lines of the transgenic RNAi plants along with the WT and *cp12-1/2/3*. Five lines of transgenic RNAi and three technical replicates were included.

For this, 100 mg of adult rosette leaf tissue was ground with HCl and passed through an activated choral column in order to purify the supernatant. A master mix containing homovanilic acid and peroxidase was added to each extract and the H_2O_2 level was measured using a HPLC system.

The results of this analysis revealed that there is a significant reduction in H_2O_2 levels in the triple mutant *cp12-1/2/3* and one line of the RNAi lines, namely *TM.R.53.1*, of about 61%. Furthermore, there is also a notable decrease in lines *TM.R.54.2* and *TM.R.54.4* of 36% and 40% respectively, when compared to the WT. Transgenic line *TM.R.54.1* presented no change in the H_2O_2 level (Figure 4.21).

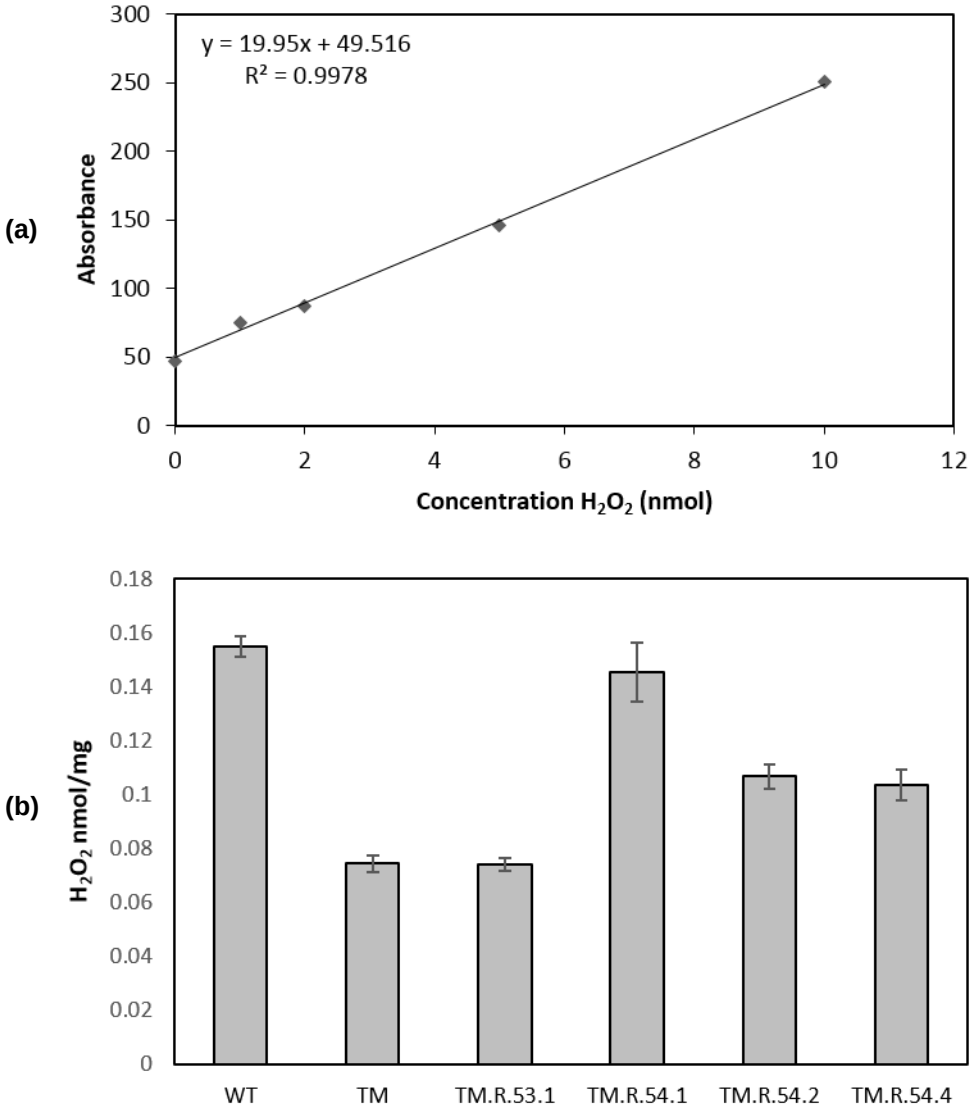

Figure 4.21 H_2O_2 content of the WT, T-DNA *cp12-1/2/3* and triple RNAi transgenic plants. **(a)** Standard curve for H_2O_2. **(b)** H_2O_2 content of fresh weight WT, *cp12-1/2/3* (TM) and triple RNAi plants (*TM.R.53.1, TM.R.54.1, TM.R.54.2* and *TM.R.54.4*). The error bars represent SE n=3 replicates.

4.3.6 Chlorophyll measurement

During the growth analysis of the RNAi transgenic lines, leaves with a chlorotic phenotype were observed in several plants with a severe growth phenotype. To investigate this phenomenon, the chlorophyll content of these lines was checked in order to determine whether a lack of CP12 has an impact on the chlorophyll content of *Arabidopsis thaliana*. Chlorophyll was extracted from the leaves with 80% acetone and then quantified by measuring the absorbance at 646 and 663 nm. Five lines of the RNAi transgenic lines were included, along with the WT and the T-DNA insertion line *cp12-1/2/3*. Two to three biological replicates were included for each line.

The results clearly showed that there is no significant difference in the chlorophyll content between the WT and the plants with the reduced levels of CP12 expression in both the T-DNA *cp12-1/2/3* and the RNAi transgenic lines. Nevertheless, although they are not statically significant, RNAi lines showed a tendency to slightly lower chlorophyll content compare to the WT (Figure 4.22).

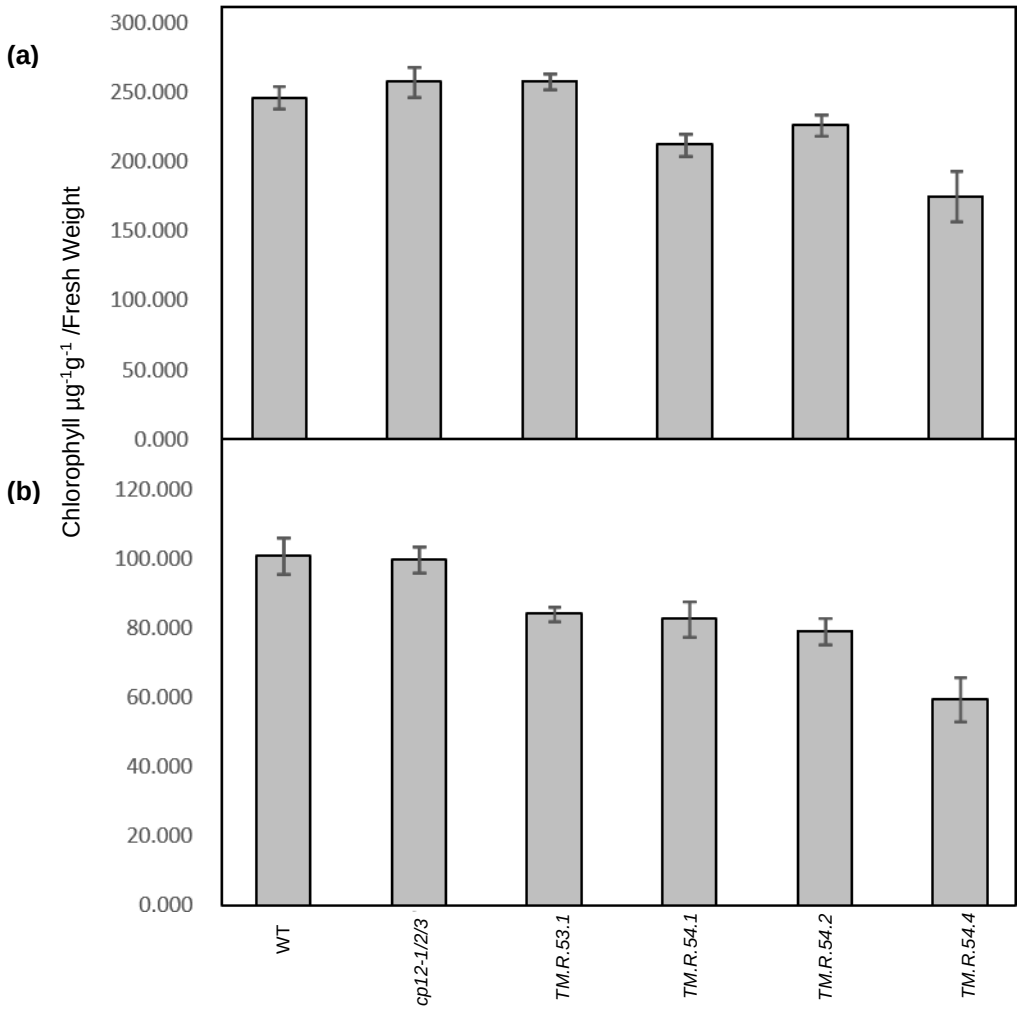

Figure 4.22 Chlorophyll content of the WT, T-DNA *cp12-1/2/3* and triple RNAi transgenic plants. Amount of chlorophyll content per fresh weight of the WT, *cp12-1/2/3* and triple RNAi plants *(TM.R.53.1*, *TM.R.54.1*, *TM.R.54.2* and *TM.R.54.4*). **(a)** Chlorophyll A**. (b)** Chlorophyll B. The error bars represent SE n=2-10 replicates.

4.4 *Arabidopsis thaliana* CP12 gene family expression analysis obtained from GENEVESTIGATOR database

Genevestigator is a database and web-browser which can be used to retrieve the expression patterns of individual genes throughout chosen environmental conditions, growth stages or organs (Zimmermann et al., 2004).

Here in the results, the developmental tool in genevestigator was used to summarise the expression of the three CP12 genes across different developmental stages in *Arabidopsis thaliana* from seed germination to senescence.

In order to develop this, first of all a selection of data must be performed by choosing plant and *Arabidopsis thaliana* as an organism and sample. After that, the gene of interest is selected; in this step a list of genes must be entered with their specific numbers CP12-1 (AT2G47400), CP12-2 (AT3G62410) and CP12-3 (AT1G76560). The plot is automatically generated and indicates the expression of the three genes of CP12 in *Arabidopsis thaliana*.

The microarray gene expression database showed that CP12 genes display different levels of expression throughout the 10 developmental stages of *Arabidopsis thaliana*. CP12-1 shows the highest level of expression, followed by CP12-2, whereas CP12-3 is expressed at a very low level compared with the other two genes. Interestingly, the expression level of CP12-3 increases dramatically at the late stage of development (senescence stage), which occurs simultaneously with the reduction in the expression level of CP12-2, indicating that these genes may be involved in this specific developmental stage (Figure 4.23).

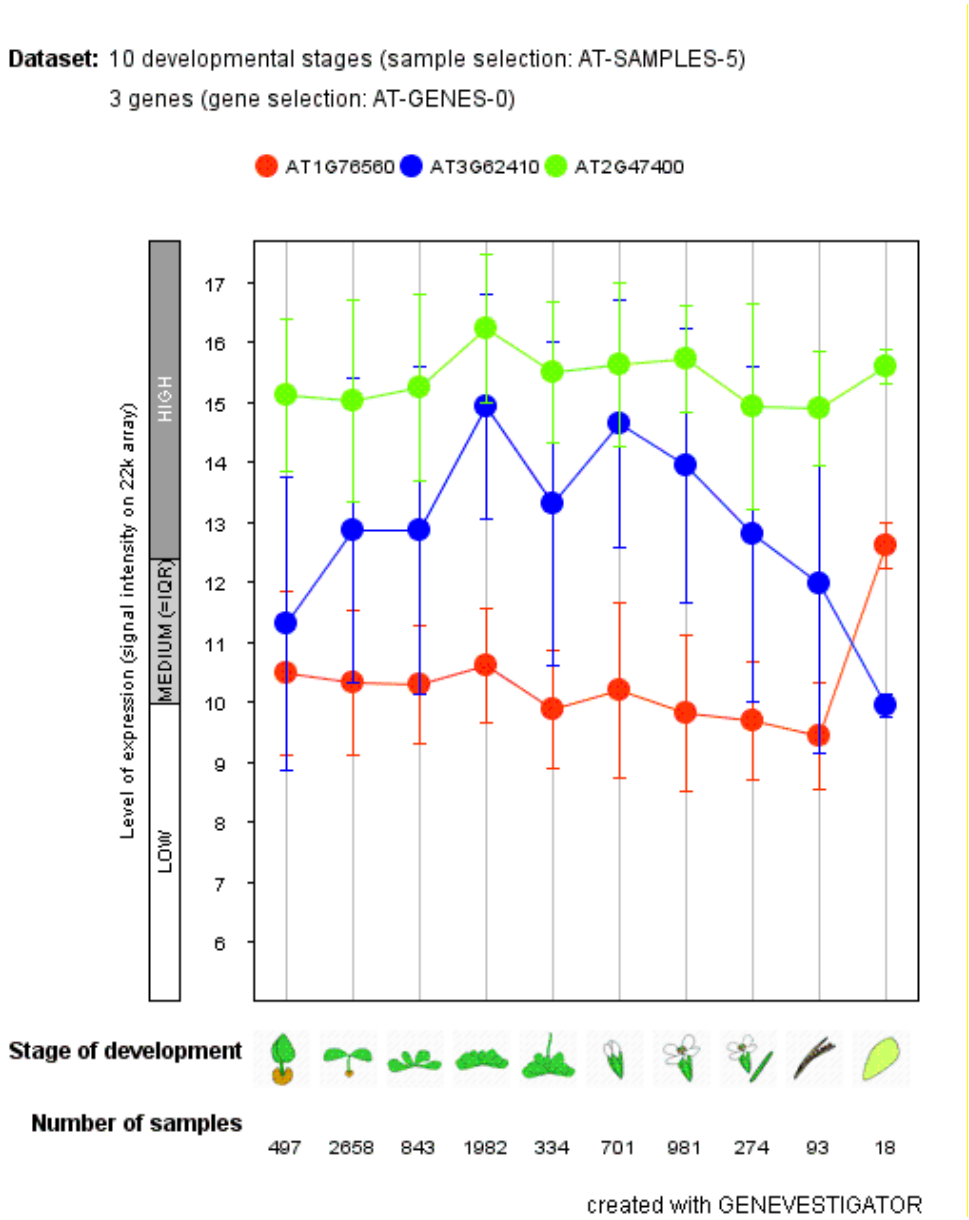

Figure 4.23 Expression level of CP12 genes in different developmental stages of *Arabidopsis thaliana*. Results from microarray analysis show the expression of CP12-1 (AT2G47400) green, CP12-2 (AT3G62410) blue and CP12-3 (AT1G76560) red in the following developmental stages; geminated seed, seedling, young rosette, developed rosette, bolting, young flower, developed flower, flowers and siliques, mature siliques and senescence. (Image created on GENEVESTIGATOR in March 2014. https://www.genvestigator.com/gv/).

Discussion

The study in this chapter describes several approaches used to explore the importance of the CP12 gene family to higher plants' growth and development.

First, the CP12 T-DNA insertion lines for each member of the CP12 gene family were identified in *Arabidopsis thaliana* and then used to determine the functional importance of each individual CP12 member. The analysis of the transcript level of these lines revealed a knockout for both CP12-1 and CP12-3, as well as a knockdown for the CP12-2 gene. The results of this study including the growth analysis and biomass did not reveal any significant change in the growth rate of the single insertion lines *cp12-2* and *cp12-3*. However, the multiple insertion lines that include the CP12-1 gene (*cp12-1/2*, *cp12-1/3* and *cp12-1/2/3*) seem to be significantly lower than the wild type. In addition, the comparison between the three single mutant lines revealed that *cp12-1* has a tendency to exhibit a slower growth rate when compared with the other two lines. These data might indicate the unequal relative importance of each gene in this family. Additionally, it is possible that the CP12-1 protein might have an additional effect, or play a more dominant role, than the other two proteins.

A further reduction of the transcript level of CP12-2 was needed in order to assess the individual importance of CP12-2 in the WT, as well as its importance together with one or more forms of CP12s. For this, RNAi-specific constructs targeting CP12-2 were introduced into the WT, double T-DNA insertion line *cp12-1/2* and triple T-DNA insertion line *cp12-1/2/3*. A growth analysis was performed for the T2 generation of the *WT.RNAi* lines and *TM.RNAi* lines. The results of this experiment revealed that reducing the level of CP12-2 in the WT plants did not affect the plants' growth and

development. However, this was not the case for the *cp12-1/2/3* plants, since for these plants, further reducing the level of CP12-2 using RNAi specific constructs resulted in a slower growth phenotype when compared to the *cp12-1/2/3* line.

The fact that a lack of more than one member of the CP12 gene family is necessary in order to be able to visualise the phenotype might be explained by functional redundancy among the CP12 family members.

The results of the present study are in agreement with Howard et al.'s (2011a) finding that CP12 antisense tobacco plants display a complex growth phenotype. In the same study, only a minor change in the photosynthetic carbon fixation in the antisense plants was found. In our study, photosynthesis via carbon assimilation was evaluated in mature plants of the line *cp12-1/2*, *cp12-1/3* and *cp12-1/2/3*. Although there is a tendency for lower carbon assimilation in these lines specifically *cp12-1/2* and *cp12-1/2/3*, no significant differences were found in these plants compared to the WT. Furthermore, at the early development stage, our study showed lower photosynthetic capacity through the PSII operating efficiency in the *cp12-1/2*, *cp12-1/2/3* and *TM.RNAi* lines. This could be a possible explanation for the growth phenotype that was previously observed.

Prior studies have noted the importance of chloroplast redox homeostasis, as well as how this can affect growth in both photosynthetic and non-photosynthetic tissues during the early stage of development. Additionally, the redox state of the chloroplast has been found to be essential for the formation of lateral roots in Arabidopsis (Ferrández et al., 2012, Kirchsteiger et al., 2012). Based on the fact that CP12 is a redox-sensitive regulatory protein, we investigated whether a lack of CP12 has an

impact on the growth of the roots. The results showed a mild slow growth rate phenotype and a slight reduction in the number of lateral roots. These data indicate that the CP12 protein might be important in root growth. Having this potential phenotype in the roots could give an explanation of the severe phenotype in the growth rate which was found in the T-DNA insertion lines and *RNAi* transgenic lines. Further studies are suggested to confirm and investigate this mild phenotype.

In addition, the results of the H_2O_2 measurement showed significant differences in lines *cp12-1/2/3* and *TM.R.53.1*, which might suggest that the CP12 protein is involved in the oxidative stress regulation of Arabidopsis.

As only one mutant allele of the CP12 gene was studied in this analysis, it is crucial to confirm whether the slower growth phenotype is due to the reduction in the CP12 level and not the result of any other insertion in the line. As mentioned previously, since the insertion of the CP12-1 gene seemed to have an additional effect on the double and triple mutants, a complementation study was conducted, using CP12-1 native promoter to express a CP12-1::FLAG fusion protein in the triple mutant background. The results of this experiment revealed that in two of the three lines (*1.1* and *2.1*) the phenotype seemed to be complemented by the expression of CP12-1::FLAG, as the transgenic plants displayed normal growth when compared with the WT. In addition, the statistics showed that these two lines significantly difference when compared to *cp12-1/2/3*. This finding further supports the idea that the redox-sensitive protein CP12 is required for normal growth and development.

The main aim of this project was to explore the role of the three copies of the CP12 protein in *Arabidopsis thaliana*. Crucially, the results detailed in this chapter are

consistent with those found in Howard et al.'s (2011a) study on tobacco, which showed that CP12 is essential for normal growth and development.

CHAPTER 5

Identification of *Arabidopsis thaliana* Cystathionine β-Synthase (CBSX) T-DNA mutant lines

Introduction

The CBS (cystathionine β-synthase) domain-containing proteins consist of a large family, including a conserved domain that is ubiquitous in the following three categories of life: archaea, bacteria and eukaryotes. CBS was first identified in the archaebacterium genome as a highly conserved domain of about 60 amino acids found in a variety of proteins (Bateman, 1997, Yoo et al., 2011). In humans, the functional analysis of a number of CBS-containing proteins have revealed the physiological importance of this domain through linking the mutation of the CBS domain enzymes and other proteins to a variety of hereditary diseases, including cystathionine synthesis in homocystinuria (Shan et al., 2001). However, in the plant world, the role of the CBS domain remains obscure (Yoo et al., 2011).

By conducting an analysis of the entire genome of *Arabidopsis thaliana* and rice (*Oryza sativa*), Kushwaha et al. (2009) revealed the presence of 34 CBS domain-containing proteins (CDCPs) in Arabidopsis and 59 CDCPs in rice. In this study, these proteins were classified into two major groups; the first containing only a single CBS pair and the second including all proteins with two CBS pairs. Further classification within these groups was performed in order to divide them into subgroups based on their additional structural domains (Figure 1.8).

In addition, a recent study to analyse the genome sequence data of cyanobacteria reported an unobserved diversity of CP12 proteins in this group (Stanley et al., 2013). These cyanobacterial CP12 proteins were classified into eight different types, according to the features of their primary structures. Interestingly, among these

proteins were CP12-CBS domain fusions. In addition, evidence from *in silico* modelling has revealed that this fusion, CBS-CP12, is unable to interact with glyceraldehyde 3-phosphate dehydrogenase (GAPDH), indicating that a different function of this protein should be considered (Stanley et al., 2013).

Despite the fact that a large family of CDCPs has been identified in higher plants, CBS-CP12 domain fusions have not been found. To date, only one study has focused on the CBS protein in Arabidopsis *in vivo*, which was conducted by Yoo et al. (2011). This study revealed that both types of chloroplast CBS (CBSX1 and CBSX2) participate in stabilising the cellular redox homeostasis. That was not all; it also showed that these proteins may be involved in plant development through the regulation of the thioredoxin system. The research into CBSX1 and CBSX2 produced the hypothesis that these proteins form a dimer under conditions of oxidative stress, and the level of the reduced TRX f and m is then increased. The reduced TRX then, in turn, maintains the level of reduced CP12 before affecting the regulation of the Calvin-Benson cycle. There is no evidence which directly support this explanation, however, it is worthy of consideration. These findings raise the question of whether CDCPs have any functional relationship with thioredoxin and CP12 within the Calvin-Benson cycle regulation in higher plants (Lopez-Calcagno et al., 2014).

The objectives of this study are; firstly, to identify single CBSX1 and CBSX2 insertional lines, secondly, to produce double homozygous line of both insertion.

This chapter describes the identification and characterisation of *Arabidopsis thaliana* CBSX T-DNA mutant lines and making use of them to produce double homozygous lines. As a future goal for this research, it is suggested that the double HM lines of CBSX should be crossed with a multiple mutant line of CP12, to allow for an

exploration of the importance of these two protein families and an investigation of whether CP12 can act with CBSX in higher plants.

Results

5.1 Identification and characterisation of *Arabidopsis thaliana* CBSX insertion lines

The Arabidopsis Information Resource (TAIR) database (htt://www.arabidopsis.org/) was used to search for possible chloroplast CBSX insertion mutants. This database boasts a wide collection of 56 CBSX polymorphisms, 24 of which are insertion mutants (14 lines for CBSX1 and 10 for CBSX2). According to the presence and position of the T-DNA insertion in the exon or promoter region, the following four lines were selected for both CBSX genes, which showed potential for disrupting the gene expression: two T-DNA insertion lines for the CBSX1 gene (At4g36910) and two lines targeting the CBSX2 gene (At4g34120).

Gene-specific primers and T-DNA insertion-specific primers (designed specifically for T-DNA insertion) were used to screen for homozygous insertion mutants. The gene-specific primers amplify a band when only a copy of the WT gene is present in the sample. However, the insertion-specific primers, would contain a sequence homology of both the T-DNA and the gene of interest, which will produce a PCR fragment if only T-DNA is present in the sample. Based on this, PCR analysis of a WT plant would produce a fragment when using gene-specific primers; homozygous plants would only yield a fragment with use of insertion-specific primers; and heterozygous primers would produce two bands, amplifying the one with the gene-specific and insertion-specific primers.

After the PCR analysis, only homozygous plants were selected from each line, the seeds of which were then bulked up.

5.1.1 Identification of CBSX1 insertion mutants

From the TAIR database, two putative CBSX1 insertion mutants were identified: CBSX1 SALK_038094 (*cbsx1.2*) and CBSX1 GK-050D12012185 (*cbsx1.3*). Based on the information provided by the database, these lines have their T-DNA insertion in the following locations: the first exon (134 bp downstream of the initiating ATG) for *cbsx1.2*, and the fourth intron (1047 bp downstream of the TCA) for *cbsx1.3.* PCR analysis was performed to assess whether the plants from these lines were homozygous or heterozygous, for the purposes of their insertion. Figures 5.1 and 5.2 represent the characterisation of these mutant lines, in which all homozygous lines were identified. To confirm the location of the insertion, as provided by TAIR, for each line, insertion-specific primers were used to amplify DNA fragments, which were then sequenced. In the case of the *cbsx1.2* mutant line, the results obtained from the sequence revealed the insertion site to be in the untranslated region 37 bp upstream of the ATG. For the *cbsx1.3* line, meanwhile, the results showed that the insertion was in the fourth intron, 1154 bp downstream of the ATG.

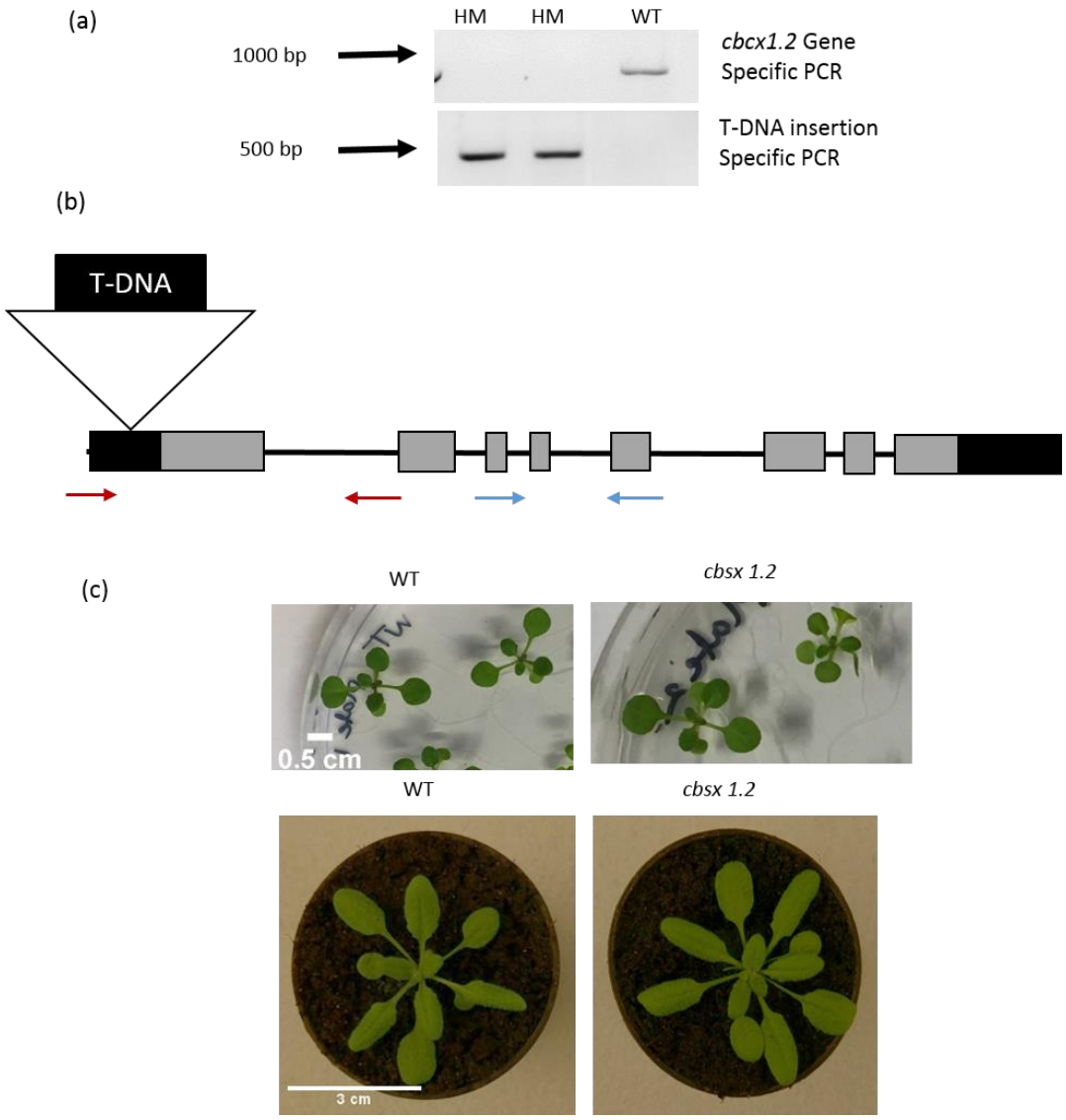

Figure 5.1 Analysis of CBSX1 AT4G36910 insertion mutant *cbsx1.2* (SALK_038094). (a) PCR analysis of the WT and the homozygous (HM) plants of the *cbsx1.2* mutant. Gene-specific primers were used to detect the WT allele (upper gel) and insertion-specific primers were used to detect the T-DNA insertion (lower gel). **(b)** CBSX1 gene map showing the insertion positions for *cbsx1.2*. CBSX1 contained seven introns and eight exons. The closed grey boxes indicate the exons, while the lines denote the introns. The black boxes signify the untranslated region (UTR). Red arrows point to the location of the gene-specific primers for the insertion and the blue arrows indicate to the qPCR primers. **(c)** WT plants (left) and *cbsx1.2* mutant plant (right). Top: 16-day-old seedlings on plates of half-MS media, and bottom: 25-day-old plant on soil. A 1 kb DNA ladder was used as a molecular marker.

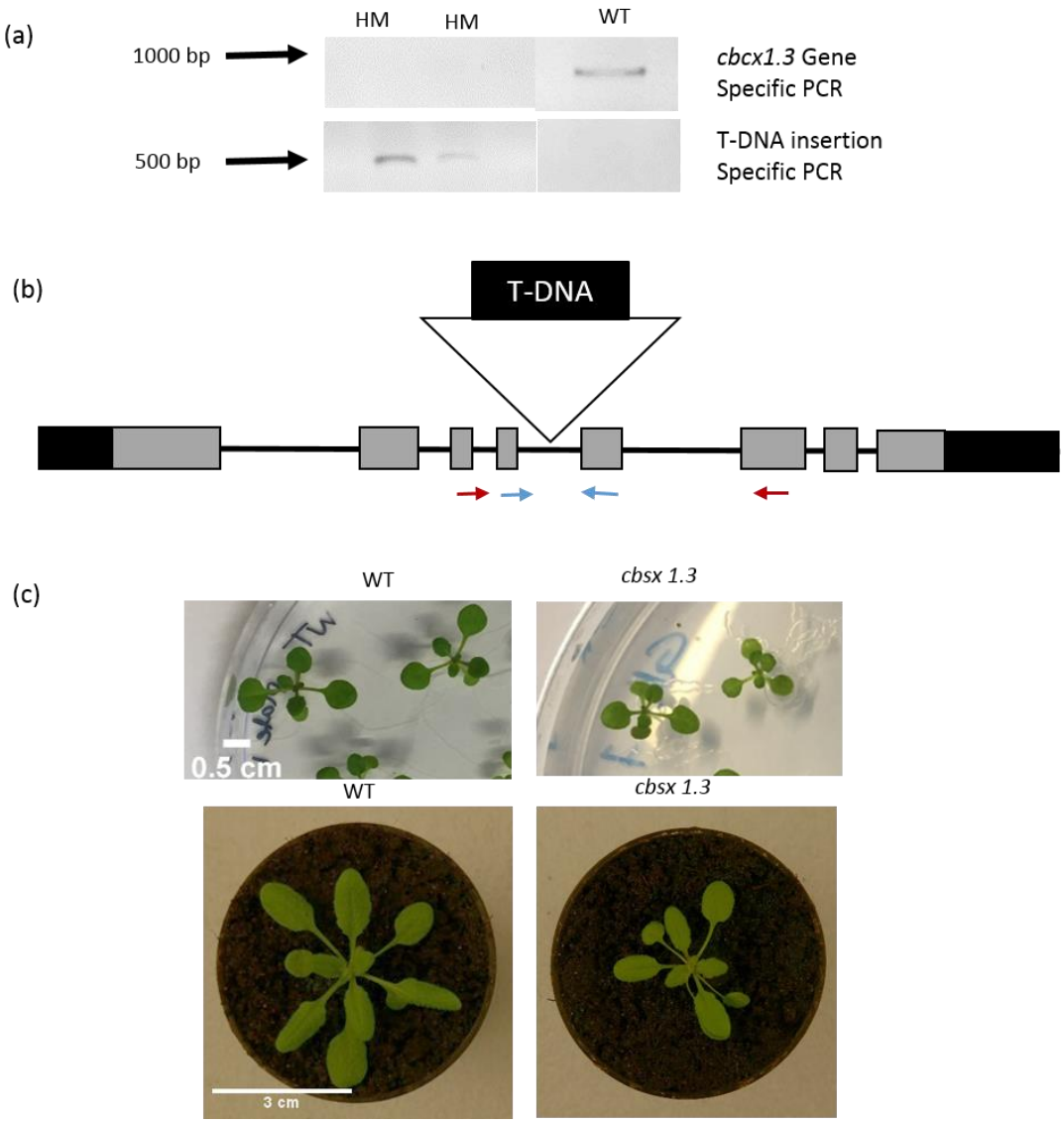

Figure 5.2 Analysis of CBSX1 AT4G36910 insertion mutant *cbsx1.3* (GK-050D12-012185). (a) PCR analysis of the WT and HM plants of the *cbsx1.3* mutant. Gene-specific primers were used to detect the WT allele (upper gel) and insertion-specific primers were used to detect the T-DNA insertion (lower gel). **(b)** CBSX1 gene map showing the insertion positions for *cbsx1.3*. CBSX1 contained seven introns and eight exons. The closed grey boxes indicate the exons, while the lines connote the introns. The black boxes embody the UTR, while the red arrows highlight the location of the gene-specific primers. Blue arrows indicate to the qPCR primers. **(c)** WT plants (left) and *cbsx1.3* mutant plant (right). Top: 16-day-old seedlings on plates of half-MS media; bottom: 25-day-old plant on soil. A 1 kb DNA ladder was used as a molecular marker.

5.1.2 Identification of CBSX2 insertion mutants

As described previously, and considering the essential criteria required for the selection of the T-DNA insertion mutants, two insertion mutant lines were identified for the CBXS2 gene from the TAIR database, as follows: CBSX2 SALK 02868 (*cbsx2.1*) and CBSX2 SALK 136943 (*cbsx2.2*). According to TAIR, these lines had their T-DNA insertion located in the first exon 72 bp downstream of the ATG for *cbsx2.1* and 15 bp downstream of the ATG for *cbsx2.2.* Using a combination of gene and insertion-specific primers, homozygous plants were identified though PCR analysis (Figure 5.3 a and 5.4 a). After that, the locations of the insertions were confirmed by sequencing the DNA fragments, which were yielded by the insertion-specific primers. The results of the sequencing revealed that the insertion of both lines that were present in the first exon agreed with the findings of the TAIR database. However, the specific site of the insertions for both lines were slightly different, in that both were found to be located 209 bp downstream of the ATG (Figure 5.3 b and 5.4 b). Additionally, to study the impact of the T-DNA and alteration the level of the expression of more than one CBSX gene, several attempts to generate double homozygous (HM) lines were conducted.

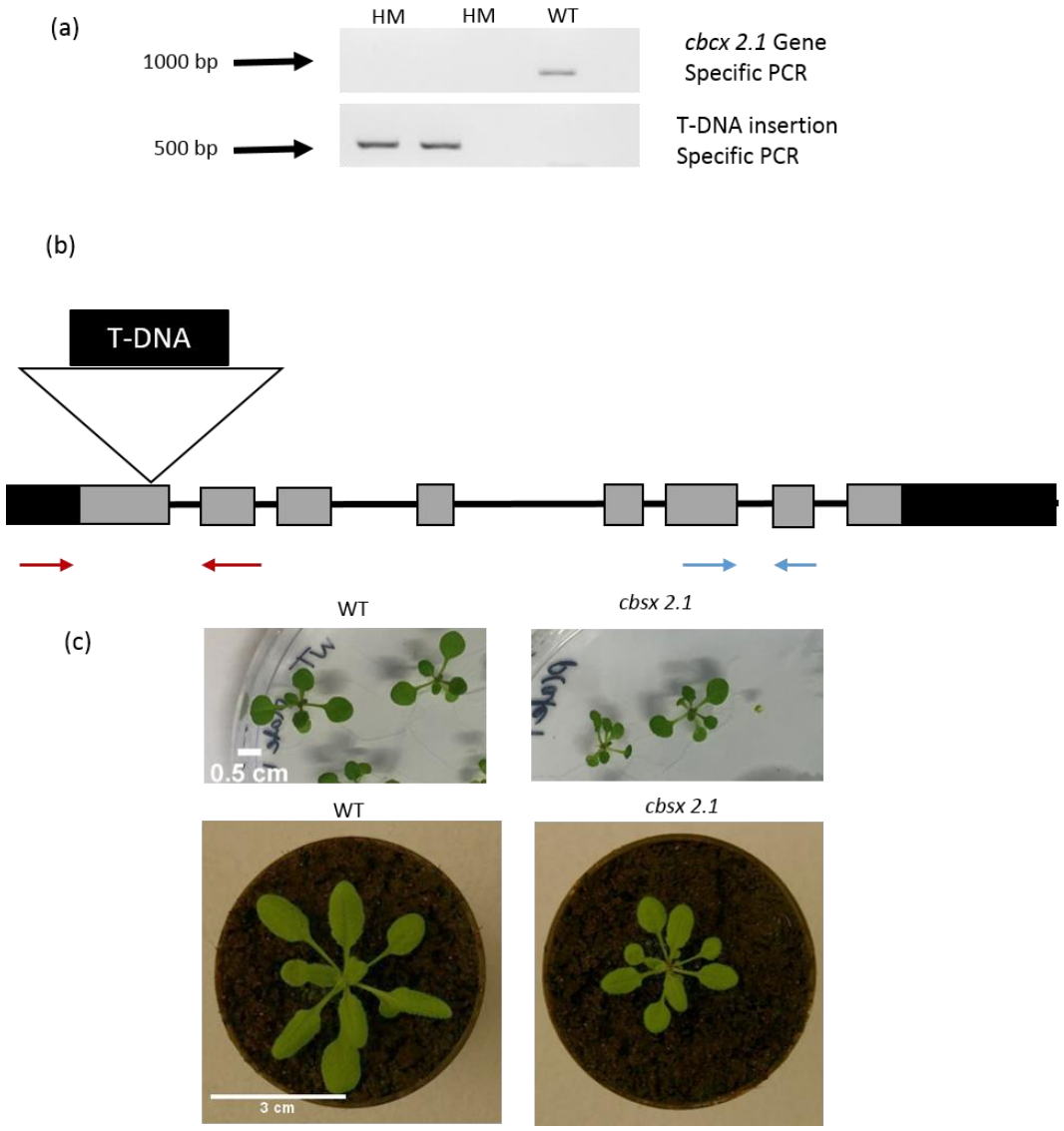

Figure 5.3 Analysis of CBSX2 AT4G34120 insertion mutant *cbsx2.1* (SALK_021868). (a) PCR analysis of the WT and HM plants of the *cbsx2.1* mutant. Gene-specific primers were used to detect the WT allele (upper gel) and insertion-specific primers were used to detect the T-DNA insertion (lower gel). **(b)** CBSX2 gene map showing the insertion positions for the *cbsx2.1*. Red arrows indicate the location of the gene-specific while blue arrows indicate to the qPCR primers. CBSX1 contained seven introns and eight exons. The closed grey boxes denote the exons, while the lines represent the introns. The black boxes pinpoint the UTR. **(c)** WT plants (left) and *cbsx2.1* mutant plant (right). Top: 16-day-old seedlings on plates of half-MS media and bottom: 25-day-old plant on soil. A 1 kb DNA ladder was used as a molecular marker.

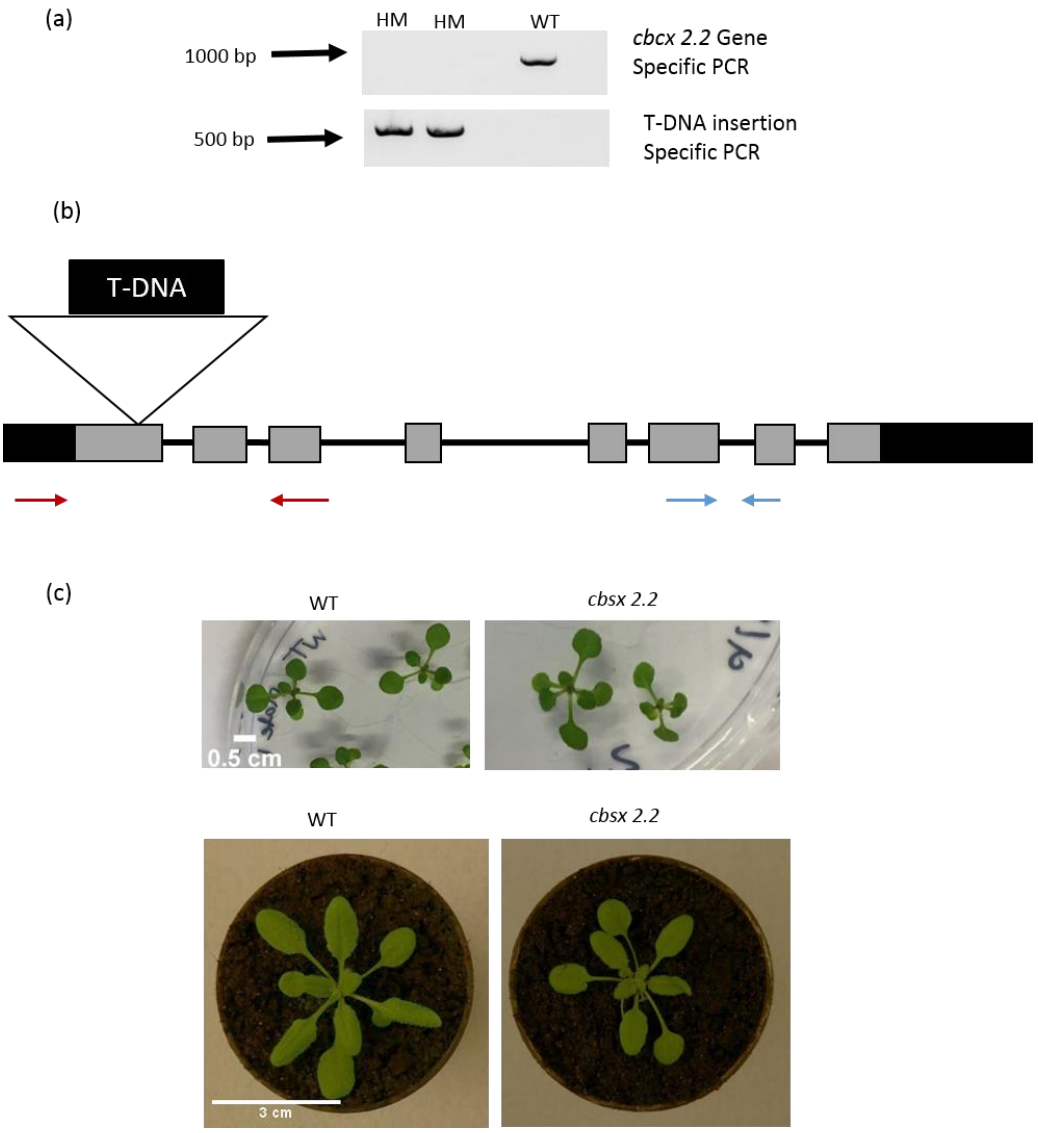

Figure 5.4 Analysis of CBSX2 AT4G34120 insertion mutants *cbsx2.2* (SALK_136934). (a) PCR analysis of the WT and HM plants of the *cbsx2.2* mutant. Gene-specific primers were used to detect the WT allele (upper gel) and insertion-specific primers were used to detect the T-DNA insertion (lower gel). **(b)** CBSX2 gene map showing the insertion positions for the *cbsx2.2*. CBSX1 contained seven introns and eight exons. The closed grey boxes evince the exons, while the lines reveal the introns. The black boxes point out the UTR, while the red arrows point to the location of the gene-specific primers. Blue arrows show the qPCR primers. **(c)** WT plants (left) and *cbsx2.2* mutant plant (right). Top: 16-day-old seedlings on plates of half-MS media; bottom: 25-day-old plant on soil. A 1 kb DNA ladder was used as a molecular marker.

5.2 Generation of CBSX double mutants

In order to identify whether a related functional role might occur between the CP12 protein family and the CBSX domain-containing proteins, all four previously identified HM lines were crossed with each other as follows: *cbsx1.2 /cbsx2.2, cbsx1.3/cbsx2.1, cbsx2.2/cbsx1.2* and *cbsx1.3/cbsx2.2.* From these four attempts, only two successful crosses were obtained, namely *cbsx1.3/cbsx2.1* and *cbsc2.2/cbsx1.2.* Seeds from each cross were collected and sown in soil and allowed to germinate and develop. The seeds grew relatively well, and the seedlings looked similar to the WT with some variation in both of the crosses.

The first generation from the crosses was expected to be heterozygous for both CBSX insertions. To confirm this, DNA was extracted from the leaf of each plant and screened by PCR using Dream Taq DNA polymerase.

The F1 heterozygous plants were allowed to self-fertilise to produce F2 segregation generation. F2 and F3 seeds were sown and genotyped. After that, DNA was extracted from 25 plants from the F3 segregation progeny, and PCR analysis was conducted in order to identify the homozygous plants containing the T-DNA insertions for both CBSX genes. The double homozygous will be referred to as *cbsx1.3/2.1* and *cbsx2.2/1.2*.

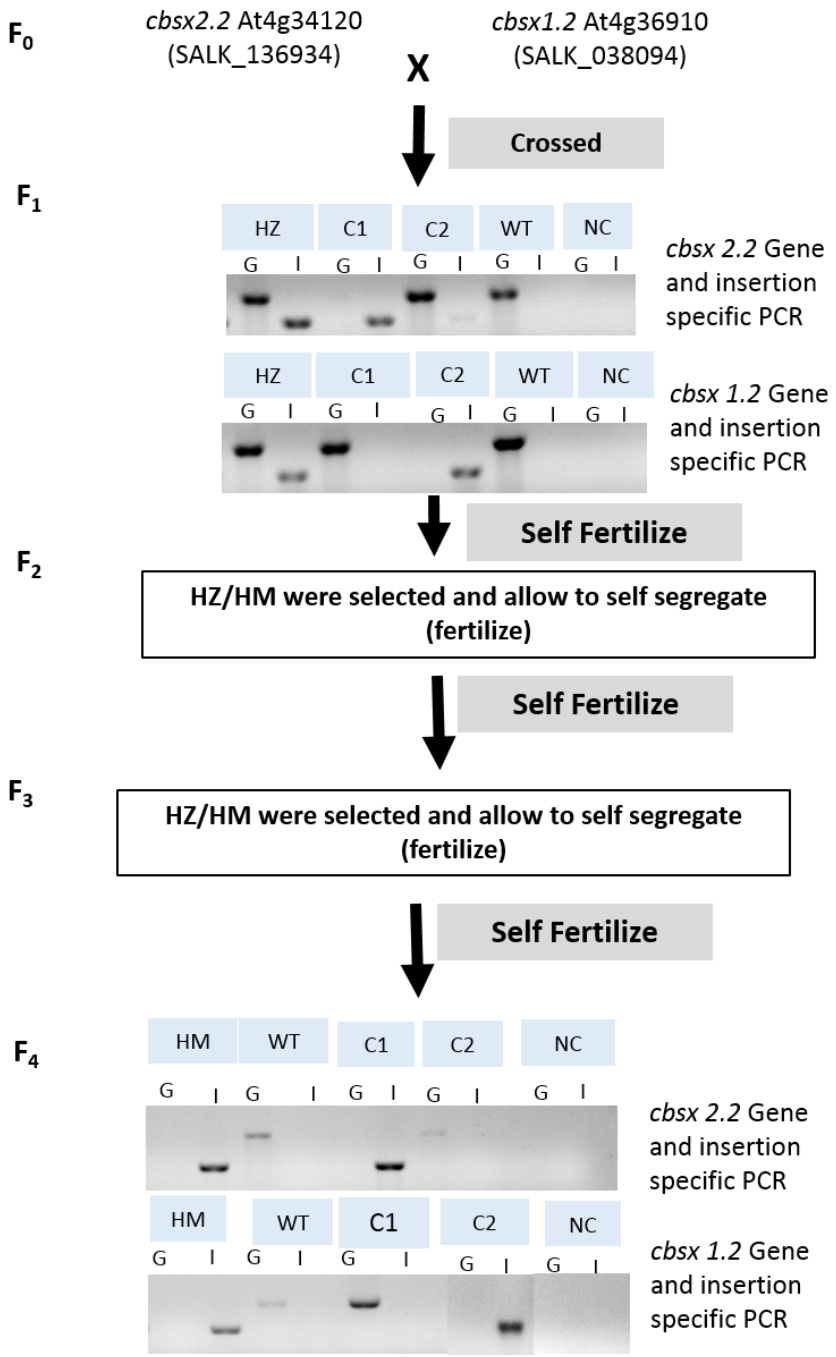

Figure 5.5 Isolation of *cbsx2.2/cbsx1.2* – double homozygous line. Crossing of single homozygous lines and screening of first generation. F0 shows the cross between homozygous *cbsx2.2* and the *cbsx1.2* insertion lines. F1 displays the PCR analysis of the heterozygous line (HZ). C1 indicates the *cbsx2.2* control (parent), C2 denotes the *cbsx1.2* control (parent) and NC represents the negative control (no template control). (G) is the gene-specific primers to detect the WT allele; (I) the insertion-specific primers to detect the T-DNA insert. F4 is the PCR analysis of WT and homozygous (HM) F4 segregation generation.

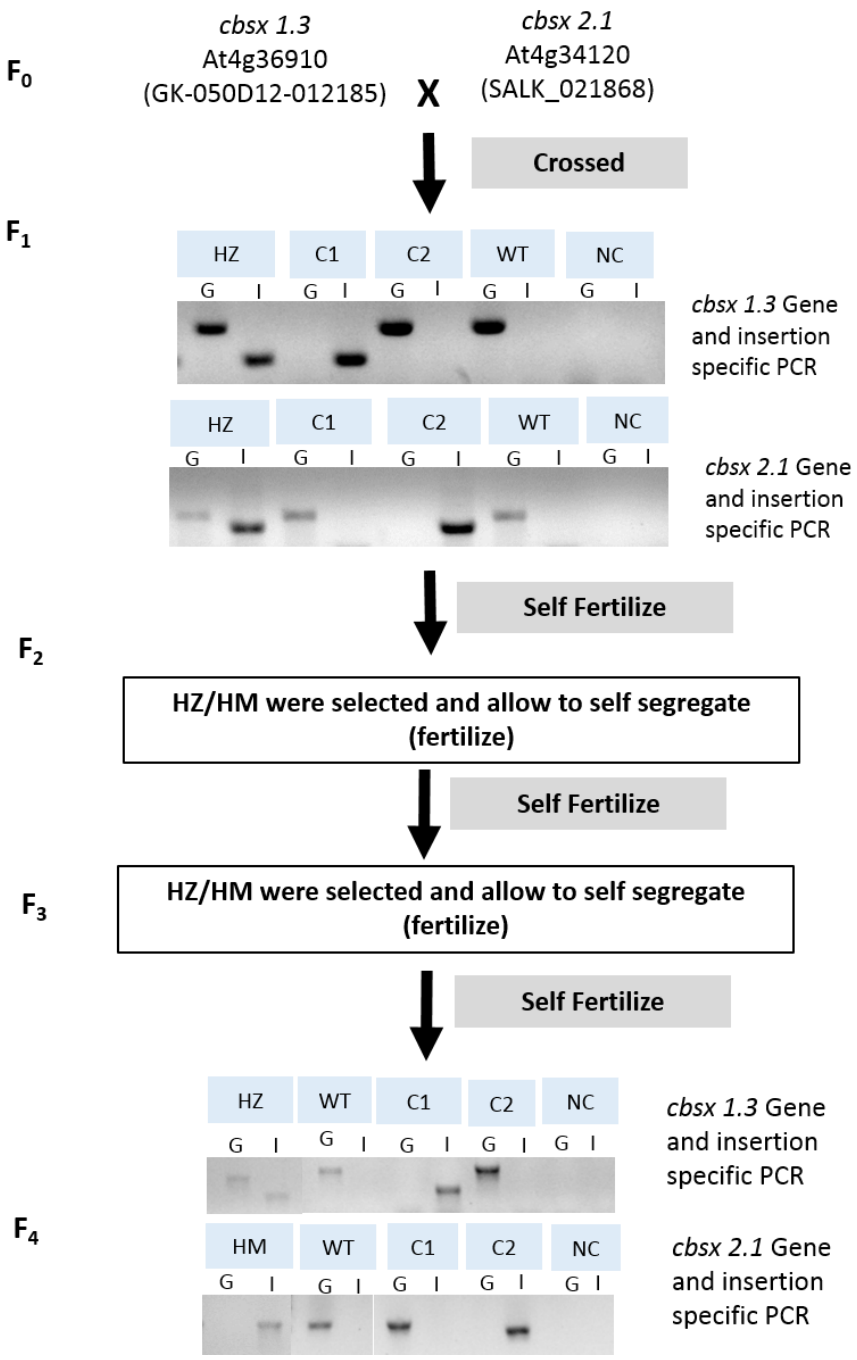

Figure 5.6 Isolation of *cbsx1.3/cbsx2.1* – double homozygous line. Crossing of single homozygous lines and screening of first generation. F0 indicates the cross between homozygous *cbsx1.3* and the *cbsx2.1* insertion lines. F1 shows the PCR analysis of the heterozygous line (HZ), C1 indicates to the *cbsx1.3* control (parent), C2 shows the *cbsx2.1* control (parent) and NC explains the negative control (no template control). (G) is the gene-specific primers reaction to detect the WT allele; (I) expresses the insertion-specific primers reaction to detect the T-DNA insert. F4 is the PCR analysis of WT and heterozygous (HZ) F4 segregation generation.

5.3 Quantification of the expression of CBSX genes

To investigate the impact of T-DNA insertion on the expression of the CBSX genes, the transcript levels of these plants were evaluated using qPCR analysis. The Col-0 background collection of mutants was germinated on half-MS media in plates for two weeks then transferred into soil and grown under short-day conditions. Leaf tissues were collected from adults' rosettes before bolting, and RNA extraction was conducted on three biological replicates from each genotype. In the next step, cDNA was produced for use in the quantification of the expression of the gene of interest's transcript. The results shown in Figure 5.7a clearly reveal that the insertion of the T-DNA in CBSX1 yielded over-expression (OX) for *cbsc1.2* allele and dramatic reduction of the expression of the *cbsx1.3* allele (potential KO). In addition, the insertion of CBSX2, as presented in Figure 5.7b, significantly knocked down the expression of this gene in the *cbsx2.1* allele. However, there is a variation in the expression of the *cbsx2.2* allele with some reduction compare with the WT.

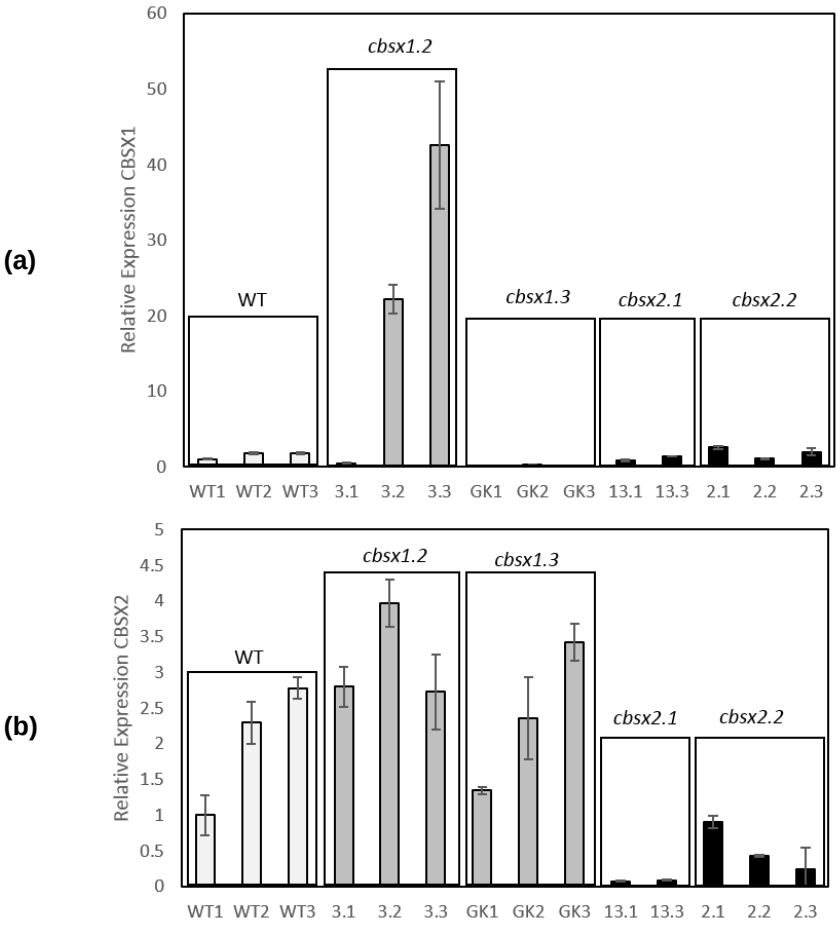

Figure 5.7 qPCR analysis of the expression of the CBSX family in the CBSX T-DNA mutant collection. Total RNA was extracted from the leaf tissue of adult rosettes and used for quantitative RT-PCR to estimate the relative levels of expression of the CBSX genes in the CBSX T-DNA mutant collection, with respect to the WT levels of expression. **(a)** Expression of CBSX1. **(b)** Expression of CBSX2. Error bars represent SE; all were calculated using the relative expression software tool (REST) group-wise comparison and statistical analysis of relative expression results in real-time PCR. Version 2009 (Pfaffl et al., 2002).

Discussion

The physiological importance of CBS domain-containing proteins has been the subject of considerable research in humans, whereby the mutation of these proteins has been linked to a number of hereditary diseases, such as cystathionine-β-synthase in homocystinuria (Shan et al., 2001) and inosine-5'-monophosphate dehydrogenase in retinitis pigmentosa (Kennan et al., 2002). However, in plants, the function of the CBS domain is still unknown (Yoo et al., 2011). In Arabidopsis, there is a large family of CDCPs, which is considered to be a domain with no defined function(s) (Kushwaha et al., 2009).

Based on the TAIR database and PSORT prediction, the members of the CBSX protein were located as follows: CBSX1 and CBSX2 in the chloroplast, CBSX3 in the mitochondria, CBSX4 in the cytosol, and CBSX5 and CBSX6 in the endoplasmic reticulum. CBSX1 and CBSX2 were reported to be able to interact with all four chloroplast TRX (f, m, x and y) also with the chloroplast ferredoxin-TRX system regulator, which affect them by increasing their activities (Yoo et al., 2011).

Plant thioredoxins are involved mainly in two redox system which are found in different components of the cell. Firstly, the NAD-TRX system (NTS) in the cytosol and mitochondria and secondly; the ferredoxin-TRX system (FTS) which is found in the chloroplast where the activities of various enzymes are regulated.

The only study to have focused on the function of CBS in Arabidopsis was conducted by Yoo et al. in 2011. In this study, it was reported that CBSXs are ubiquitous redox effectors that are involved in the redox regulation of protein function through the

regulation of TRX activities. In addition, it was suggested that CBSXs play a role in the redox system and that each member may have a specific function.

The newly available data from the genomic sequence of cyanobacteria revealed the unobserved diversity of CP12 proteins in cyanobacteria. According to the primary structure, the cyanobacterial CP12 proteins were classified into eight types; among these, a fusion of the CP12-CBS domain was found (Stanley et al., 2013).

In higher plants, this fusion of CP12-CBS was not identified; however, as mentioned above, the CBS domain is involved in the regulation of TRX activities, which in turn affect the CP12 and Calvin-Benson cycle. These findings raise the hypothesis of whether CDCPs can act with CP12 in the regulation of the Calvin-Benson cycle via TRX.

A set of tools that would allow the exploration of the possible novel function of CBS proteins, as well as the potential functional relationship between CBS and CP12 *in vivo*, is essential for research in this field.

An initial objective of this project was to identify homozygous (HM) insertion mutant lines for the chloroplast CBSX proteins. The results described in this chapter represent the identification of four lines of CBSX genes: two insertion lines for CBSX1, which are *cbsx1.2* and *cbsx1.3*, and two for CBSX2, namely *cbsx2.1* and *cbsx2.2*. At this stage, and during the growth of the plants, no obvious phenotype was visualised in the single mutant lines. The second goal of this project was to cross single homozygous lines, with the aim of producing a number of combinations of the double homozygous lines. Several crosses were preformed; two of them were successful

and have been taken forward based on the PCR analysis: *cbsx1.3* was crossed with *cbsx2.1* and *cbsx2.2* was crossed with *cbsx1.2*.

The latter cross was successful and we managed to create the double homozygous line; however, all attempts to effect the former combination were unsuccessful, possibly due to the lethality of this cross.

Future research is needed to cross the double homozygous with the triple mutant line of CP12. This will allow to investigate the effect of combined deficiencies of CP12 and CBSX proteins on the growth and development of Arabidopsis. Furthermore, this will enable to explore the possibilities of these genes interacting with each other or functionally related to each other.

CHAPTER 6

General Discussion

6.1 Overall aim and main findings

Prior studies have noted the importance of the CP12 protein in the formation of the multiprotein complex which involve PRK and GAPDH (Wedel et al., 1997, Wedel and Soll, 1998, Scheibe et al., 2002, Graciet et al., 2003a, Graciet et al., 2003b, Marri et al., 2008).

CP12 in higher plants is encoded by a multi gene family, CP12-1, CP12-2 and CP12-3. These three genes encode proteins which are highly similar in the amino acid sequences but have different expression patterns, indicating that the role of these proteins might not be restricted to the regulation of Calvin-Benson cycle. Although the role of CP12 in the regulation of Calvin-Benson Cycle has been well studied, it is still unclear whether these three proteins have additional, separate or overlapping functions in higher plants.

The main aim of this project is to explore the role of the three CP12 proteins in Arabidopsis using *in vivo*. In this study we have taken transgenic approach to explore the importance of CP12 for the growth and development. T-DNA insertion mutant lines were previously identified for each CP12 gene and multiple mutant lines of the double and the triple were produced previously by Patricia Lopez-Calcagno (Lopez-Calcagno, 2013). The study of these insertional mutants revealed no phenotype in the single mutants, however, the multiple mutant lines particularly the lines which included the CP12-1 insertion showed a slow growth phenotype in the lines *cp12-1/2*, *cp12-1/3* and *cp12-1/2/3*. This results are in line with those obtained by Howard et al., 2011 which suggest that CP12 is important for normal growth and development in higher plants.

Another important finding from our study was that the reduction of more than one member of the CP12 family was required in order to increase the severity of the phenotype, indicating that a functional redundancy occur among these protein family. Additionally, a slight phenotype was observed in the single *cp12-1* mutant line compared to *cp12-2* and *cp12-3*. Although this phenotype is not significant, it might give an indication that CP12-1 has a dominant role among the others.

The high similarity between CP12-1 and CP12-2 sequences and the overlapping expression patterns of these genes indicate that they may be functionally redundant. However, previous studies have shown the differences in the spatiotemporal expression which suggested that each gene might have individual/additional functions (Singh et al., 2008).

Unfortunately, the single *cp12-2* T-DNA insertion line was a knock down which prevented the evaluation of the importance of CP12-2 solely. To try to overcome this problem we have used an RNAi approach to reduce the level of CP12-2 in the WT and in the T-DNA insertion lines.

Further reduction of the CP12-2 level, using the RNAi, led to severe reductions in growth rate especially in the triple mutant *TM.RNAi*. This can provide evidence that CP12 proteins are essential for normal growth and development in *Arabidopsis thaliana.* Moreover, seed yield was significantly affected in the same lines which indicates the importance of CP12 protein to the seed yields. Further support to this hypothesis from Singh et al. (2008) which suggested that CP12-1 may play a role in the seeds and roots possibly at the early stage germination.

We investigated if there is any alteration in the carbon assimilation rate in the mature leaves; only a small decrease in the lines *cp12-1/2* and *cp12-1/2/3* was found. Although the decrease in the carbon assimilation was not significant, it could be one of the reasons behind the observed phenotype considering that a small alteration in the photosynthesis may have accumulative effect in the plant growth and development. This has been documented in the over expression of the sedoheptulose-1,7-bisphosphatase (SBPase) in tobacco plants, where a little increase of 6-12% in the carbon fixation can impact the leaf area and the biomass up to 30% (Lefebvre et al., 2005).

On the other hand, at the early stage of development, significant decreaces were found in the PSII operating effeciency in the lines *cp12-1/2*, *cp12-1/2/3* and *TM.RNAi*, which might be a good explanation for the slow growth phenotype. Based on these results, we suggest that a decrease in the level of CP12 in Arabidopsis can negatively affect the photosynthesis which in turn can impact the growth rate at the early development stages.

To further explore the observed phenotype, a root growth analysis was conducted to visualise if there is any changes in the root development which might cause the severe growth phenotype. The results from this experiment revealed that is a reduction in the number of the lateral roots for the *cp12-1/2/3* and *TM.RNAi* lines. Interestingly, previous studies have shown the existence of the NADPH-thioredoxin reductase C (NTCR) in the non-photosynthetic plastids and its role in the formation of the lateral roots. Also they have reported that the redox state of the chloroplast can affect the lateral root formation and development (Ferrández et al., 2012, Kirchsteiger et al., 2012). Based on these findings and since CP12 is considered as a redox

sensitive protein, we can infer from our results that CP12 may involve in the formation and development of the lateral roots through the known role of the redox regulation of Calvin-Benson Cycle in the chloroplast.

Finally, as shown previously in our results, *cp12-1/2/3* and the RNAi transgenic lines displayed slower growth rate and took longer to reach to the same developmental stage of the WT. Based on these results, it would be interesting to investigate the effects of reduced CP12 on the cell structure and development by preforming anatomical analysis. This will allow close inspection at the cellular level of the leaves and stalks anatomy and provide with more details of the changes in the developmental stages of the plants, lacking CP12 proteins.

6.2 A possible associated role between CP12 and CBS domain

A recent study which was conducted by Stanley et al. (2013) have revealed an unexpected diversity of CP12 proteins in Cyanobacteria which can be classified into 8 different types based on their primary structure features. This study shows a wide variety of CP12 proteins including CP12-like proteins fused to CBS (cystathionine-β-synthase) protein domains. Having this fusion of CP12-CBS in cyanobacteria, functionally connects these two proteins together. The presence of this fusion CP12-CBS and the variation of the distribution of CP12 protein indicates an unknown regulatory complexity of CP12 functions. In addition, *in silico* modelling studies provide evidence that the fusion of CP12-CBS proteins are unable to interact with GAPDH enzyme, suggesting an alternative function for these proteins (Stanley et al., 2013).

In Arabidopsis a total of 34 single and double CBS domain containing proteins are encoded for the genome, however, there is no evidence for the fusion of CP12-CBS among the eukaryotic CP12 homologs (Kushwaha et al., 2009).

Another study which focused on the chloroplast CBS proteins in Arabidopsis revealed that CBSX1 and CBSX2 are involved in the regulation of the thioredoxin within the thioredoxin-ferredoxin system. This study also showed that lack of CBSX1 can lead to growth retardation by the regulation of the Calvin-Benson cycle enzymes such as malate dehydrogenase through the homeostatic regulation of TRX (Yoo et al., 2011). In the same study they found that the insertion mutant of CBSX1 and CBSX2 form a dimer under the oxidation stress conditions and in these plants the level of the reduced TRX f and m was increased (Yoo et al., 2011). Based on this, a higher level of reduced CP12 will be maintained and as a result Calvin-Benson cycle activity is modulated (Lopez-Calcagno et al., 2014).

Considering the results from Stanley's study which showed the wide diversity of Cyanobacterial CP12 and the presence of the CP12-CBS fusion and the findings from Yoo et al., 2011, reporting that CBSX1 and CBSX2 express in the chloroplast and activate all type of TRX, and considering the fact that in higher plants the formation and disassociation of the complex GAPDH-PRK is mediated though the redox state of CP12 which in turn is mediated by TRX (Howard et al., 2008, Marri et al., 2009), all these data raise a question whether in higher plants these two proteins might be able to interact to each other or may play a redox rely-type role acting as a metabolic switches.

In order to explore the possibilities of CP12 and CBS having related functions in higher plants, a plant with lack or reduced level of these two proteins is needed. Here, we have identified a number of T-DNA insertion lines of chloroplast CBSX and we

made a crossing between two single homozygous lines to produce the double homozygous line.

Growth analysis of the plants from the double homozygous line is required to explore any phenotype. In addition, as a future work, a cross between the double homozygous line of CBSx and the triple homozygous line of CP12, to produce a plant with combined deficiencies of CP12 and CBS, is recommended. This would be a very useful tool to study the importance of these proteins and to investigate whether they can act together in higher plants.

6.3 CP12 as intrinsically unstructured protein and the possibility of having multiple partners

In silico studies have showed the similarity of the physicochemical properties of CP12 to those of “intrinsically unstructured proteins” (IUPs) which are involved in the regulation of macromolecular complex (Graciet et al., 2003a, Gardebien et al., 2006, Erales et al., 2009c, Mileo et al., 2013, Marri et al., 2010). *In vivo*, these proteins have a relatively little structure and they adopt more structured conformation upon binding their target ligand. They typically facilitate protein-protein interactions (Uversky, 2002, Tompa, 2005, Tompa et al., 2005, Uversky et al., 2005). CP12 is proposed to be a conditionally unstructured protein which is in the reduced state is believed to be disordered an inactive. However, under the oxidation state, the formation disulphide bridge and α-helice results in a more structured active protein.

The degree of disorder of CP12 protein has been found to increase in higher plants compared to other eukaryotic algae and cyanobacteria, suggesting that CP12 has evolved to become more flexible. This highly disorder may affect the function of CP12, considering the fact that high flexibility of other proteins is associated with a wider range of targets. Taken together, these data indicate that CP12 proteins may have additional role in higher plants (Groben et al., 2010, Marri et al., 2010).

Furthermore, previous study showed that other proteins such as malate dehydrogenase, elongation factor 1α2 and 38 kDa ribosome-associated proteins have the ability to interact with CP12, but to lesser extent than GAPDH, PRK and aldolase (Erales et al., 2008, Gontero and Maberly, 2012).

Bioinformatics analysis of the sequence of CP12 proteins has revealed some structural similarity with copper chaperone from Arabidopsis, which are found to be

important in copper homoeostasis (Himelblau et al., 1998, Mira Aparicio et al., 2001, Mira et al., 2001, Delobel et al., 2005).

Additionally in *C. reinhardtii,* CP12 was also found to be able to protect GAPDH against heat-induced inactivation and aggregation, which also act as a chaperon. Unlike other plant chaperons such as ERD10 and ERD14, which are involved in protection against abiotic stress with broad spectrum of substrates (Kovacs et al., 2008), CP12's protective function is specific to GAPDH (Erales et al., 2009b).

In addition, *in vitro* metal binding studies have revealed that *Chlamydomonas* CP12 has the ability to bind to nickel Ni^{2+} and copper Cu^{2+} ions with a low affinity (dissociation constants of 26 and 11 M respectively) (Multhaup et al., 2001, Cobine et al., 2002, Delobel et al., 2005, Erales et al., 2009a). Also, it has been found that copper ions were able to oxidize the reduced CP12 and aid the formation of the disulphide bonds, indicating that the role of CP12 might be linked to copper metabolisms (Delobel et al., 2005, Gontero and Maberly, 2012).

There are still many unanswered questions about the functions of CP12 and the possibilities of having different targets in higher plants. A number of approaches can be applied to shed light on these three proteins and its roles. By using approach such as co-immunoprecipitation might help to elucidate a novel CP12 protein-protein interactions which in turn could develop a full picture of the functions of CP12 and its mechanisms.

Conclusion

This project aimed to evaluate the importance of individual members of the CP12 protein in *Arabidopsis thaliana*, using an *in vivo* approach.

From this project, and according to our findings, we can conclude the following:

- Although a preliminary study conducted by Lopez-Calcagno (2013) revealed a role for CP12 in normal plant growth, using CP12 T-DNA insertion mutant lines, the results presented in this thesis are the first ones to fully address the importance of each member of the CP12 protein individually in plant growth. Our findings provide strong evidence that functional redundancy occurs in the CP12 gene family. The requirement for more than one gene transcript to be reduced in order to develop the phenotype, as well as, the observed compensation effect in the gene transcript of the T-DNA insertion mutant when another member of the family is reduced, strongly suggests that functional redundancy occurs between CP12 family members.
- To our knowledge, this is the first study to create the RNAi lines of CP12 *Arabidopsis thaliana* with the aim of reducing the level of CP12-2, allowing for the investigation of the importance of the absence of all CP12 genes on plant growth and development. The findings from the RNAi lines indicate that the increased reduction of CP12 increases the severity of the phenotype, which confirms the importance of CP12 for normal plant growth and development.
- Interestingly, our results show that, during the early stages of development, there is a clear reduction in the photosynthetic performance of the lines that have decreased levels of CP12. This reduction in the PSII operating efficiency could explain the slow growth phenotype that was observed in these lines of *Arabidopsis thaliana.*

- Additionally, this project was the first to study the complementation lines which were previously produced by Lopez-Calcagno (2013). The results from this experiment confirmed that the slow growth phenotype, which was observed in the growth analysis, was due to the absence of CP12 and not any other effects.
- Another interesting finding, which resulted from the root analysis experiment, showed a phenotype in the root length and the number of lateral roots for the *cp12-1/2/3* and *TM.R.45.1* lines. This observation suggests the possible involvement of the CP12 protein family in root development through thioredoxin. This is a preliminary result, and additional experiments to further investigate this phenotype are strongly recommended.

Despite the fact that the molecular mechanism underlying the importance of CP12 remains to be solved, our findings confirm the hypothesis that CP12 is necessary to higher plants' normal growth and development.

References

AGUADO-LLERA, D., OYENARTE, I., MARTÍNEZ-CRUZ, L. A. & NEIRA, J. L. 2010. The CBS domain protein MJ0729 of Methanocaldococcus jannaschii binds DNA. *FEBS letters,* 584**,** 4485-4489.

AITKEN, S. M. & KIRSCH, J. F. 2005. The enzymology of cystathionine biosynthesis: strategies for the control of substrate and reaction specificity. *Archives of biochemistry and biophysics,* 433**,** 166-175.

ARAD, M., BENSON, D. W., PEREZ-ATAYDE, A. R., MCKENNA, W. J., SPARKS, E. A., KANTER, R. J., MCGARRY, K., SEIDMAN, J. & SEIDMAN, C. E. 2002. Constitutively active AMP kinase mutations cause glycogen storage disease mimicking hypertrophic cardiomyopathy. *The Journal of clinical investigation,* 109**,** 357-362.

AVILAN, L., GONTERO, B., LEBRETON, S. & RICARD, J. 1997. Memory and imprinting effects in multienzyme complexes. *European Journal of Biochemistry,* 246**,** 78-84.

BAALMANN, E., BACKHAUSEN, J., KITZMANN, C. & SCHEIBE, R. 1994. Regulation of NADP-Dependent Glyceraldehyde 3-Phosphate Dehydrogenase Activity in Spinach Chloroplasts. *Botanica Acta,* 107**,** 313-320.

BAALMANN, E., SCHEIBE, R., CERFF, R. & MARTIN, W. 1996. Functional studies of chloroplast glyceraldehyde-3-phosphate dehydrogenase subunits A and B expressed in Escherichia coli: formation of highly active A4 and B4 homotetramers and evidence that aggregation of the B4 complex is mediated by the B subunit carboxy terminus. *Plant molecular biology,* 32**,** 505-513.

BARBAGALLO, R. P., OXBOROUGH, K., PALLETT, K. E. & BAKER, N. R. 2003. Rapid, noninvasive screening for perturbations of metabolism and plant growth using chlorophyll fluorescence imaging. *Plant Physiology,* 132**,** 485-493.

BASSHAM, J. A. 1971. Photosynthetic carbon metabolism. *Proceedings of the National Academy of Sciences,* 68**,** 2877-2882.

BASSHAM, J. A., BENSON, A. A. & CALVIN, M. 1950. The path of carbon in photosynthesis. *J Biol Chem,* 185**,** 781-7.

BATEMAN, A. 1997. The structure of a domain common to archaebacteria and the homocystinuria disease protein. *Trends in biochemical sciences,* 22**,** 12-13.

BENT, F. & CLOUGH, S. 1998. Floral dip: a simplified method for Agrobacterium-mediated transformation of Arabidopsis. *Plant J,* 16**,** 735-743.

BLAIR, E., REDWOOD, C., ASHRAFIAN, H., OLIVEIRA, M., BROXHOLME, J., KERR, B., SALMON, A., ÖSTMAN-SMITH, I. & WATKINS, H. 2001. Mutations in the γ2 subunit of AMP-activated protein kinase cause familial hypertrophic cardiomyopathy: evidence for the central role of energy compromise in disease pathogenesis. *Human molecular genetics,* 10**,** 1215-1220.

BLANKENSHIP, R. E. 2013. *Molecular mechanisms of photosynthesis*, John Wiley & Sons.

BOGGETTO, N., GONTERO, B. & MABERLY, S. C. 2007. Regulation of phosphoribulokinase and glyceraldehyde 3-phosphate dehydrogenase in a

freshwater diatom, Asterionella formosa1. *Journal of Phycology,* 43**,** 1227-1235.
BUCHANAN, B. B. 1980. Role of light in the regulation of chloroplast enzymes. *Annual Review of Plant Physiology,* 31**,** 341-374.
BUCHANAN, B. B. 1991. Regulation of CO 2 assimilation in oxygenic photosynthesis: the ferredoxin/thioredoxin system: perspective on its discovery, present status, and future development. *Archives of Biochemistry and Biophysics,* 288**,** 1-9.
BUCHANAN, B. B. & BALMER, Y. 2005. Redox regulation: a broadening horizon. *Annu. Rev. Plant Biol.,* 56**,** 187-220.
BUCHANAN, B. B., GRUISSEM, W. & JONES, R. L. 2015. *Biochemistry and molecular biology of plants*, John Wiley & Sons.
BUCHANAN, B. B., HOLMGREN, A., JACQUOT, J.-P. & SCHEIBE, R. 2012. Fifty years in the thioredoxin field and a bountiful harvest. *Biochimica et Biophysica Acta (BBA)-General Subjects,* 1820**,** 1822-1829.
BUCHANAN, B. B., SCHURMANN, P., WOLOSIUK, R. A. & JACQUOT, J. P. 2002. The ferredoxin/thioredoxin system: from discovery to molecular structures and beyond. *Photosynth Res,* 73**,** 215-22.
CLASPER, S., EASTERBY, J. S. & POWLS, R. 1991. Properties to two high-molecular-mass forms of glyceraldehyde-3-phosphate dehydrogenase from spinach leaf, one of which also possesses latent phosphoribulokinase activity. *European Journal of Biochemistry,* 202**,** 1239-1246.
COBINE, P. A., GEORGE, G. N., JONES, C. E., WICKRAMASINGHE, W. A., SOLIOZ, M. & DAMERON, C. T. 2002. Copper transfer from the Cu (I) chaperone, CopZ, to the repressor, Zn (II) CopY: metal coordination environments and protein interactions. *Biochemistry,* 41**,** 5822-5829.
COLLIN, V., ISSAKIDIS-BOURGUET, E., MARCHAND, C., HIRASAWA, M., LANCELIN, J.-M., KNAFF, D. B. & MIGINIAC-MASLOW, M. 2003. The Arabidopsis plastidial thioredoxins New functions and new insights into specificity. *Journal of Biological Chemistry,* 278**,** 23747-23752.
COLLIN, V., LAMKEMEYER, P., MIGINIAC-MASLOW, M., HIRASAWA, M., KNAFF, D. B., DIETZ, K.-J. & ISSAKIDIS-BOURGUET, E. 2004. Characterization of plastidial thioredoxins from Arabidopsis belonging to the new y-type. *Plant Physiology,* 136**,** 4088-4095.
DAI, S., FRIEMANN, R., GLAUSER, D. A., BOURQUIN, F., MANIERI, W., SCHÜRMANN, P. & EKLUND, H. 2007. Structural snapshots along the reaction pathway of ferredoxin–thioredoxin reductase. *Nature,* 448**,** 92-96.
DAY, P., SHARFF, A., PARRA, L., CLEASBY, A., WILLIAMS, M., HÖRER, S., NAR, H., REDEMANN, N., TICKLE, I. & YON, J. 2007. Structure of a CBS-domain pair from the regulatory γ1 subunit of human AMPK in complex with AMP and ZMP. *Acta Crystallographica Section D: Biological Crystallography,* 63**,** 587-596.
DE DIOS BARAJAS-LÓPEZ, J., SERRATO, A. J., OLMEDILLA, A., CHUECA, A. & SAHRAWY, M. 2007. Localization in roots and flowers of pea chloroplastic thioredoxin f and thioredoxin m proteins reveals new roles in nonphotosynthetic organs. *Plant Physiology,* 145**,** 946-960.
DELOBEL, A., GRACIET, E., ANDREESCU, S., GONTERO, B., HALGAND, F. & LAPRÉVOTE, O. 2005. Mass spectrometric analysis of the interactions between CP12, a chloroplast protein, and metal ions: a possible regulatory

role within a PRK/GAPDH/CP12 complex. *Rapid communications in mass spectrometry,* 19**,** 3379-3388.
DUNKER, A. K., LAWSON, J. D., BROWN, C. J., WILLIAMS, R. M., ROMERO, P., OH, J. S., OLDFIELD, C. J., CAMPEN, A. M., RATLIFF, C. M., HIPPS, K. W., AUSIO, J., NISSEN, M. S., REEVES, R., KANG, C., KISSINGER, C. R., BAILEY, R. W., GRISWOLD, M. D., CHIU, W., GARNER, E. C. & OBRADOVIC, Z. 2001. Intrinsically disordered protein. *J Mol Graph Model,* 19**,** 26-59.
DYSON, H. J. & WRIGHT, P. E. 2005. Intrinsically unstructured proteins and their functions. *Nature reviews Molecular cell biology,* 6**,** 197-208.
EDWARDS, K., JOHNSTONE, C. & THOMPSON, C. 1991. A simple and rapid method for the preparation of plant genomic DNA for PCR analysis. *Nucleic acids research,* 19**,** 1349.
ENGLER, C., GRUETZNER, R., KANDZIA, R. & MARILLONNET, S. 2009. Golden gate shuffling: a one-pot DNA shuffling method based on type IIs restriction enzymes. *PloS one,* 4**,** e5553.
ENGLER, C., KANDZIA, R. & MARILLONNET, S. 2008. A one pot, one step, precision cloning method with high throughput capability. *PloS one,* 3**,** e3647.
ERALES, J., AVILAN, L., LEBRETON, S. & GONTERO, B. 2008. Exploring CP12 binding proteins revealed aldolase as a new partner for the phosphoribulokinase/glyceraldehyde 3-phosphate dehydrogenase/CP12 complex–purification and kinetic characterization of this enzyme from Chlamydomonas reinhardtii. *FEBS Journal,* 275**,** 1248-1259.
ERALES, J., GONTERO, B., WHITELEGGE, J. & HALGAND, F. 2009a. Mapping of a copper-binding site on the small CP12 chloroplastic protein of Chlamydomonas reinhardtii using top-down mass spectrometry and site-directed mutagenesis. *Biochemical Journal,* 419**,** 75-86.
ERALES, J., LIGNON, S. & GONTERO, B. 2009b. CP12 from Chlamydomonas reinhardtii, a permanent specific “chaperone-like” protein of glyceraldehyde-3-phosphate dehydrogenase. *Journal of Biological Chemistry,* 284**,** 12735-12744.
ERALES, J., LORENZI, M., LEBRUN, R., FOURNEL, A., ETIENNE, E., COURCELLE, C., GUIGLIARELLI, B., GONTERO, B. & BELLE, V. 2009c. A New Function of GAPDH from Chlamydomonas reinhardtii: A Thiol− Disulfide Exchange Reaction with CP12. *Biochemistry,* 48**,** 6034-6040.
ERALES, J., MEKHALFI, M., WOUDSTRA, M. & GONTERO, B. 2011. Molecular mechanism of NADPH-glyceraldehyde-3-phosphate dehydrogenase regulation through the C-terminus of CP12 in Chlamydomonas reinhardtii. *Biochemistry,* 50**,** 2881-2888.
FENG, L., CAMPBELL, E. B., HSIUNG, Y. & MACKINNON, R. 2010. Structure of a eukaryotic CLC transporter defines an intermediate state in the transport cycle. *Science,* 330**,** 635-641.
FERMANI, S., SPARLA, F., FALINI, G., MARTELLI, P., CASADIO, R., PUPILLO, P., RIPAMONTI, A. & TROST, P. 2007. Molecular mechanism of thioredoxin regulation in photosynthetic A2B2-glyceraldehyde-3-phosphate dehydrogenase. *Proceedings of the National Academy of Sciences,* 104**,** 11109-11114.
FERMANI, S., TRIVELLI, X., SPARLA, F., THUMIGER, A., CALVARESI, M., MARRI, L., FALINI, G., ZERBETTO, F. & TROST, P. 2012. Conformational

selection and folding-upon-binding of intrinsically disordered protein CP12 regulate photosynthetic enzymes assembly. *Journal of Biological Chemistry,* 287**,** 21372-21383.
FERRÁNDEZ, J., GONZÁLEZ, M. & CEJUDO, F. J. 2012. Chloroplast redox homeostasis is essential for lateral root formation in Arabidopsis. *Plant signaling & behavior,* 7**,** 1177-1179.
FERRI, G., STOPPINI, M., MELONI, M. L., ZAPPONI, M. C. & IADAROLA, P. 1990. Chloroplast glyceraldehyde-3-phosphate dehydrogenase (NADP): amino acid sequence of the subunits from isoenzyme I and structural relationship with isoenzyme II. *Biochimica et Biophysica Acta (BBA)-Protein Structure and Molecular Enzymology,* 1041**,** 36-42.
FIRE, A., XU, S., MONTGOMERY, M. K., KOSTAS, S. A., DRIVER, S. E. & MELLO, C. C. 1998. Potent and specific genetic interference by double-stranded RNA in Caenorhabditis elegans. *nature,* 391**,** 806-811.
FLORENCIO, F. J., PÉREZ-PÉREZ, M. E., LÓPEZ-MAURY, L., MATA-CABANA, A. & LINDAHL, M. 2006. The diversity and complexity of the cyanobacterial thioredoxin systems. *Photosynthesis research,* 89**,** 157-171.
FUXREITER, M. & TOMPA, P. 2012. Fuzzy complexes: a more stochastic view of protein function. *Fuzziness.* Springer.
GARDEBIEN, F., THANGUDU, R. R., GONTERO, B. & OFFMANN, B. 2006. Construction of a 3D model of CP12, a protein linker. *Journal of Molecular Graphics and Modelling,* 25**,** 186-195.
GEIGER, D. R. & SERVAITES, J. C. 1994. Diurnal regulation of photosynthetic carbon metabolism in C3 plants. *Annual review of plant biology,* 45**,** 235-256.
GOLLOB, M. H., GREEN, M. S., TANG, A. S.-L., GOLLOB, T., KARIBE, A., HASSAN, A.-S., AHMAD, F., LOZADO, R., SHAH, G. & FANANAPAZIR, L. 2001. Identification of a gene responsible for familial Wolff–Parkinson–White syndrome. *New England Journal of Medicine,* 344**,** 1823-1831.
GONTERO, B. & AVILAN, L. 2011. Creating order out of disorder: structural imprint of GAPDH on CP12. *Structure,* 19**,** 1728-9.
GONTERO, B., CARDENAS, M. L. & RICARD, J. 1988. A functional five-enzyme complex of chloroplasts involved in the Calvin cycle. *European Journal of Biochemistry,* 173**,** 437-443.
GONTERO, B., LEBRETON, S. & GRACIET, E. 2001. Multienzyme complexes involved in the Benson–Calvin cycle and in fatty acid metabolism. *Protein-protein interactions in plant biology,* 7**,** 120-150.
GONTERO, B. & MABERLY, S. C. 2012. An intrinsically disordered protein, CP12: jack of all trades and master of the Calvin cycle. *Biochemical Society Transactions,* 40**,** 995-999.
GRACIET, E., GANS, P., WEDEL, N., LEBRETON, S., CAMADRO, J.-M. & GONTERO, B. 2003a. The small protein CP12: a protein linker for supramolecular complex assembly. *Biochemistry,* 42**,** 8163-8170.
GRACIET, E., LEBRETON, S., CAMADRO, J. M. & GONTERO, B. 2003b. Characterization of native and recombinant A4 glyceraldehyde 3-phosphate dehydrogenase. *European Journal of Biochemistry,* 270**,** 129-136.
GROBEN, R., KALOUDAS, D., RAINES, C. A., OFFMANN, B., MABERLY, S. C. & GONTERO, B. 2010. Comparative sequence analysis of CP12, a small protein involved in the formation of a Calvin cycle complex in photosynthetic organisms. *Photosynthesis research,* 103**,** 183-194.

GUILBAULT, G. G., KRAMER, D. N. & HACKLEY, E. B. 1967. New substrate for fluorometric determination of oxidative enzymes. *Analytical chemistry,* 39**,** 271-271.
HATTORI, M., TANAKA, Y., FUKAI, S., ISHITANI, R. & NUREKI, O. 2007. Crystal structure of the MgtE Mg2+ transporter. *Nature,* 448**,** 1072-1075.
HIMELBLAU, E., MIRA, H., LIN, S.-J., CULOTTA, V. C., PEÑARRUBIA, L. & AMASINO, R. M. 1998. Identification of a functional homolog of the yeast copper homeostasis gene ATX1 from Arabidopsis. *Plant Physiology,* 117**,** 1227-1234.
HIRAI, S. & KODAMA, H. 2008. RNAi vectors for manipulation of gene expression in higher plants. *The Open Plant Science Journal,* 2.
HOWARD, T. P., FRYER, M. J., SINGH, P., METODIEV, M., LYTOVCHENKO, A., OBATA, T., FERNIE, A. R., KRUGER, N. J., QUICK, W. P. & LLOYD, J. C. 2011a. Antisense suppression of the small chloroplast protein CP12 in tobacco alters carbon partitioning and severely restricts growth. *Plant physiology,* 157**,** 620-631.
HOWARD, T. P., LLOYD, J. C. & RAINES, C. A. 2011b. Inter-species variation in the oligomeric states of the higher plant Calvin cycle enzymes glyceraldehyde-3-phosphate dehydrogenase and phosphoribulokinase. *Journal of experimental botany,* 62**,** 3799-3805.
HOWARD, T. P., METODIEV, M., LLOYD, J. C. & RAINES, C. A. 2008. Thioredoxin-mediated reversible dissociation of a stromal multiprotein complex in response to changes in light availability. *Proc Natl Acad Sci U S A,* 105**,** 4056-61.
IGNOUL, S. & EGGERMONT, J. 2005. CBS domains: structure, function, and pathology in human proteins. *American Journal of Physiology-Cell Physiology,* 289**,** C1369-C1378.
JACQUOT, J.-P., VIDAL, J., GADAL, P. & SCHÜRMANN, P. 1978. Evidence for the existence of several enzyme-specific thioredoxins in plants. *Febs Letters,* 96**,** 243-246.
JONES, S. & THORNTON, J. M. 1996. Principles of protein-protein interactions. *Proceedings of the National Academy of Sciences,* 93**,** 13-20.
KENNAN, A., AHERNE, A., PALFI, A., HUMPHRIES, M., MCKEE, A., STITT, A., SIMPSON, D. A., DEMTRODER, K., ORNTOFT, T. & AYUSO, C. 2002. Identification of an IMPDH1 mutation in autosomal dominant retinitis pigmentosa (RP10) revealed following comparative microarray analysis of transcripts derived from retinas of wild-type and Rho–/–mice. *Human molecular genetics,* 11**,** 547-558.
KERY, V., PONELEIT, L. & KRAUS, J. P. 1998. Trypsin cleavage of human cystathionine β-synthase into an evolutionarily conserved active core: structural and functional consequences. *Archives of biochemistry and biophysics,* 355**,** 222-232.
KIRCHSTEIGER, K., FERRÁNDEZ, J., PASCUAL, M. B., GONZÁLEZ, M. & CEJUDO, F. J. 2012. NADPH thioredoxin reductase C is localized in plastids of photosynthetic and nonphotosynthetic tissues and is involved in lateral root formation in Arabidopsis. *The Plant Cell,* 24**,** 1534-1548.
KOVACS, D., KALMAR, E., TOROK, Z. & TOMPA, P. 2008. Chaperone activity of ERD10 and ERD14, two disordered stress-related plant proteins. *Plant physiology,* 147**,** 381-390.

KRUGER, N. J. & VON SCHAEWEN, A. 2003. The oxidative pentose phosphate pathway: structure and organisation. *Current opinion in plant biology,* 6**,** 236-246.
KRYSAN, P. J., YOUNG, J. C. & SUSSMAN, M. R. 1999. T-DNA as an insertional mutagen in Arabidopsis. *The Plant Cell,* 11**,** 2283-2290.
KUSHWAHA, H. R., SINGH, A. K., SOPORY, S. K., SINGLA-PAREEK, S. L. & PAREEK, A. 2009. Genome wide expression analysis of CBS domain containing proteins in Arabidopsis thaliana (L.) Heynh and Oryza sativa L. reveals their developmental and stress regulation. *BMC Genomics,* 10**,** 200.
LAEMMLI, U. K. 1970. Cleavage of structural proteins during the assembly of the head of bacteriophage T4. *nature,* 227**,** 680-685.
LEBRETON, S., ANDREESCU, S., GRACIET, E. & GONTERO, B. 2006. Mapping of the interaction site of CP12 with glyceraldehyde-3-phosphate dehydrogenase from Chlamydomonas reinhardtii. *FEBS Journal,* 273**,** 3358-3369.
LEBRETON, S. & GONTERO, B. 1999. Memory and Imprinting in Multienzyme Complexes EVIDENCE FOR INFORMATION TRANSFER FROM GLYCERALDEHYDE-3-PHOSPHATE DEHYDROGENASE TO PHOSPHORIBULOKINASE UNDER REDUCED STATE IN CHLAMYDOMONAS REINHARDTII. *Journal of Biological Chemistry,* 274**,** 20879-20884.
LEFEBVRE, S., LAWSON, T., FRYER, M., ZAKHLENIUK, O. V., LLOYD, J. C. & RAINES, C. A. 2005. Increased sedoheptulose-1, 7-bisphosphatase activity in transgenic tobacco plants stimulates photosynthesis and growth from an early stage in development. *Plant Physiology,* 138**,** 451-460.
LEMAIRE, S. D., COLLIN, V., KERYER, E., ISSAKIDIS-BOURGUET, E., LAVERGNE, D. & MIGINIAC-MASLOW, M. 2003. Chlamydomonas reinhardtii: a model organism for the study of the thioredoxin family. *Plant Physiology and Biochemistry,* 41**,** 513-521.
LEMAIRE, S. D., MICHELET, L., ZAFFAGNINI, M., MASSOT, V. & ISSAKIDIS-BOURGUET, E. 2007. Thioredoxins in chloroplasts. *Current genetics,* 51**,** 343-365.
LOPEZ-CALCAGNO, P. E. 2013. *Analysis of insertion mutants and construction of transgenic plants for the investigation of the CP12 protein family in Arabdopsis thaliana.* PhD, University of Essex.
LOPEZ-CALCAGNO, P. E., HOWARD, T. P. & RAINES, C. A. 2014. The CP12 protein family: a thioredoxin-mediated metabolic switch? *Front Plant Sci,* 5**,** 9.
LORENZI, M., PUPPO, C., LEBRUN, R., LIGNON, S., ROUBAUD, V., MARTINHO, M., MILEO, E., TORDO, P., MARQUE, S. R. & GONTERO, B. 2011. Tyrosine-Targeted Spin Labeling and EPR Spectroscopy: An Alternative Strategy for Studying Structural Transitions in Proteins. *Angewandte Chemie International Edition,* 50**,** 9108-9111.
MARRI, L., PESARESI, A., VALERIO, C., LAMBA, D., PUPILLO, P., TROST, P. & SPARLA, F. 2010. In vitro characterization of Arabidopsis CP12 isoforms reveals common biochemical and molecular properties. *Journal of plant physiology,* 167**,** 939-950.
MARRI, L., SPARLA, F., PUPILLO, P. & TROST, P. 2005a. Co-ordinated gene expression of photosynthetic glyceraldehyde-3-phosphate dehydrogenase,

phosphoribulokinase, and CP12 in Arabidopsis thaliana. *Journal of experimental botany,* 56**,** 73-80.
MARRI, L., TROST, P., PUPILLO, P. & SPARLA, F. 2005b. Reconstitution and properties of the recombinant glyceraldehyde-3-phosphate dehydrogenase/CP12/phosphoribulokinase supramolecular complex of Arabidopsis. *Plant Physiol,* 139**,** 1433-43.
MARRI, L., TROST, P., TRIVELLI, X., GONNELLI, L., PUPILLO, P. & SPARLA, F. 2008. Spontaneous assembly of photosynthetic supramolecular complexes as mediated by the intrinsically unstructured protein CP12. *Journal of biological chemistry,* 283**,** 1831-1838.
MARRI, L., ZAFFAGNINI, M., COLLIN, V., ISSAKIDIS-BOURGUET, E., LEMAIRE, S. D., PUPILLO, P., SPARLA, F., MIGINIAC-MASLOW, M. & TROST, P. 2009. Prompt and easy activation by specific thioredoxins of calvin cycle enzymes of Arabidopsis thaliana associated in the GAPDH/CP12/PRK supramolecular complex. *Mol Plant,* 2**,** 259-69.
MATSUMURA, H., KAI, A., MAEDA, T., TAMOI, M., SATOH, A., TAMURA, H., HIROSE, M., OGAWA, T., KIZU, N. & WADANO, A. 2011. Structure basis for the regulation of glyceraldehyde-3-phosphate dehydrogenase activity via the intrinsically disordered protein CP12. *Structure,* 19**,** 1846-1854.
MCLEAN, J. E., HAMAGUCHI, N., BELENKY, P., MORTIMER, S. E., STANTON, M. & HEDSTROM, L. 2004. Inosine 5′-monophosphate dehydrogenase binds nucleic acids in vitro and in vivo. *Biochemical Journal,* 379**,** 243-251.
MEYER, Y., BUCHANAN, B. B., VIGNOLS, F. & REICHHELD, J.-P. 2009. Thioredoxins and glutaredoxins: unifying elements in redox biology. *Annual review of genetics,* 43**,** 335-367.
MEYER, Y., REICHHELD, J. P. & VIGNOLS, F. 2005. Thioredoxins inArabidopsis and other plants. *Photosynthesis Research,* 86**,** 419-433.
MEYER, Y., RIONDET, C., CONSTANS, L., ABDELGAWWAD, M. R., REICHHELD, J. P. & VIGNOLS, F. 2006. Evolution of redoxin genes in the green lineage. *Photosynthesis Research,* 89**,** 179-192.
MICHELET, L., ZAFFAGNINI, M., MORISSE, S., SPARLA, F., PÉREZ-PÉREZ, M. E., FRANCIA, F., DANON, A., MARCHAND, C. H., FERMANI, S. & TROST, P. 2013. Redox regulation of the Calvin–Benson cycle: something old, something new. *Frontiers in plant science,* 4.
MICHELET, L., ZAFFAGNINI, M., MORISSE, S., SPARLA, F., PÉREZ-PÉREZ, M. E., FRANCIA, F., DANON, A., MARCHAND, C. H., FERMANI, S. & TROST, P. 2014. Redox regulation of the Calvin–Benson cycle: something old, something new. *Thiol-based redox homeostasis and signalling***,** 8.
MILEO, E., LORENZI, M., ERALES, J., LIGNON, S., PUPPO, C., LE BRETON, N., ETIENNE, E., MARQUE, S. R., GUIGLIARELLI, B. & GONTERO, B. 2013. Dynamics of the intrinsically disordered protein CP12 in its association with GAPDH in the green alga Chlamydomonas reinhardtii: a fuzzy complex. *Molecular BioSystems,* 9**,** 2869-2876.
MINDELL, J. A., MADUKE, M., MILLER, C. & GRIGORIEFF, N. 2001. Projection structure of a ClC-type chloride channel at 6.5 Å resolution. *Nature,* 409**,** 219-223.
MIRA APARICIO, H., VILAR CERVERO, M., PEREZ PAYA, E. & PEÑARRUBIA BLASCO, D. 2001. Functional and conformational properties of the exclusive C-domain from the Arabidopsis copper chaperone (CCH).

MIRA, H., MARTÍNEZ-GARCÍA, F. & PEÑARRUBIA, L. 2001. Evidence for the plant-specific intercellular transport of the Arabidopsis copper chaperone CCH. *The Plant Journal,* 25**,** 521-528.
MIZIORKO, H. M. 2000. Phosphoribulokinase: current perspectives on the structure/function basis for regulation and catalysis. *Advances in Enzymology and Related Areas of Molecular Biology, Volume 74***,** 95-127.
MOUCHE, F., GONTERO, B., CALLEBAUT, I., MORNON, J.-P. & BOISSET, N. 2002. Striking conformational change suspected within the phosphoribulokinase dimer induced by interaction with GAPDH. *Journal of Biological Chemistry,* 277**,** 6743-6749.
MÜLLER, B. 1972. A labile CO2-fixing enzyme complex in spinach chloroplasts. *Zeitschrift für Naturforschung B,* 27**,** 925-932.
MULTHAUP, G., STRAUSAK, D., BISSIG, K.-D. & SOLIOZ, M. 2001. Interaction of the CopZ copper chaperone with the CopA copper ATPase of Enterococcus hirae assessed by surface plasmon resonance. *Biochemical and biophysical research communications,* 288**,** 172-177.
NARUSAKA, M., SHIRAISHI, T., IWABUCHI, M. & NARUSAKA, Y. 2010. The floral inoculating protocol: a simplified Arabidopsis thaliana transformation method modified from floral dipping. *Plant Biotechnology,* 27**,** 349-351.
NÉE, G., ZAFFAGNINI, M., TROST, P. & ISSAKIDIS-BOURGUET, E. 2009. Redox regulation of chloroplastic glucose-6-phosphate dehydrogenase: A new role for f-type thioredoxin. *FEBS letters,* 583**,** 2827-2832.
OESTERHELT, C., KLOCKE, S., HOLTGREFE, S., LINKE, V., WEBER, A. P. & SCHEIBE, R. 2007. Redox regulation of chloroplast enzymes in Galdieria sulphuraria in view of eukaryotic evolution. *Plant and Cell Physiology,* 48**,** 1359-1373.
PEDERSEN, T., KIRK, M. & BASSHAM, J. 1966. Light-Dark Transients in Levels of Intermediate Compounds during Photosynthesis in Air-Adapted Chlorella. *Physiologia plantarum,* 19**,** 219-231.
PETERSEN, J., BRINKMANN, H. & CERFF, R. 2003. Origin, evolution, and metabolic role of a novel glycolytic GAPDH enzyme recruited by land plant plastids. *Journal of molecular evolution,* 57**,** 16-26.
PETERSEN, J., TEICH, R., BECKER, B., CERFF, R. & BRINKMANN, H. 2006. The GapA/B gene duplication marks the origin of Streptophyta (charophytes and land plants). *Molecular biology and evolution,* 23**,** 1109-1118.
PFAFFL, M. W., HORGAN, G. W. & DEMPFLE, L. 2002. Relative expression software tool (REST©) for group-wise comparison and statistical analysis of relative expression results in real-time PCR. *Nucleic acids research,* 30**,** e36-e36.
PFANNSCHMIDT, T. & YANG, C. 2012. The hidden function of photosynthesis: a sensing system for environmental conditions that regulates plant acclimation responses. *Protoplasma,* 249**,** 125-136.
POHLMEYER, K., PAAP, B. K., SOLL, J. & WEDEL, N. 1996. CP12: a small nuclear-encoded chloroplast protein provides novel insights into higher-plant GAPDH evolution. *Plant molecular biology,* 32**,** 969-978.
PORTIS JR, A. R. 1992. Regulation of ribulose 1, 5-bisphosphate carboxylase/oxygenase activity. *Annual review of plant biology,* 43**,** 415-437.
PUSCH, M. 2002. Myotonia caused by mutations in the muscle chloride channel gene CLCN1. *Human mutation,* 19**,** 423-434.

RAINES, C. & PAUL, M. 2006. Products of leaf primary carbon metabolism modulate the developmental programme determining plant morphology. *Journal of Experimental Botany,* 57**,** 1857-1862.
RAINES, C. A. 2011. Increasing photosynthetic carbon assimilation in C3 plants to improve crop yield: current and future strategies. *Plant Physiol,* 155**,** 36-42.
RIUS, S. P., CASATI, P., IGLESIAS, A. A. & GOMEZ-CASATI, D. F. 2008. Characterization of Arabidopsis lines deficient in GAPC-1, a cytosolic NAD-dependent glyceraldehyde-3-phosphate dehydrogenase. *Plant physiology,* 148**,** 1655-1667.
ROBBENS, S., PETERSEN, J., BRINKMANN, H., ROUZÉ, P. & VAN DE PEER, Y. 2007. Unique regulation of the Calvin cycle in the ultrasmall green alga Ostreococcus. *Journal of molecular evolution,* 64**,** 601-604.
SAINIS, J. K. & HARRIS, G. C. 1986. The association of ribulose-1, 5-bisphosphate carboxylase with phosphoriboisomerase and phosphoribulokinase. *Biochemical and biophysical research communications,* 139**,** 947-954.
SAMBROOK, J. & RUSSELL, D. W. 2001. Molecular cloning: a laboratory manual 3rd edition. *Coldspring-Harbour Laboratory Press, UK*.
SCAGLIARINI, S., TROST, P., PUPILLO, P. & VALENTI, V. 1993. Light activation and molecular-mass changes of NAD (P)-glyceraldehyde 3-phosphate dehydrogenase of spinach and maize leaves. *Planta,* 190**,** 313-319.
SCHEIBE, R. 1991. Redox-modulation of chloroplast enzymes A common principle for individual control. *Plant Physiology,* 96**,** 1-3.
SCHEIBE, R., WEDEL, N., VETTER, S., EMMERLICH, V. & SAUERMANN, S. M. 2002. Co-existence of two regulatory NADP-glyceraldehyde 3-P dehydrogenase complexes in higher plant chloroplasts. *European Journal of Biochemistry,* 269**,** 5617-5624.
SCHÜRMANN, P. & BUCHANAN, B. B. 2008. The ferredoxin/thioredoxin system of oxygenic photosynthesis. *Antioxidants & redox signaling,* 10**,** 1235-1274.
SCHÜRMANN, P. & JACQUOT, J.-P. 2000. Plant thioredoxin systems revisited. *Annual review of plant biology,* 51**,** 371-400.
SCOTT, J. W., HAWLEY, S. A., GREEN, K. A., ANIS, M., STEWART, G., SCULLION, G. A., NORMAN, D. G. & HARDIE, D. G. 2004. CBS domains form energy-sensing modules whose binding of adenosine ligands is disrupted by disease mutations. *The Journal of clinical investigation,* 113**,** 274-284.
SHAN, X., DUNBRACK JR, R. L., CHRISTOPHER, S. A. & KRUGER, W. D. 2001. Mutations in the regulatory domain of cystathionine β–synthase can functionally suppress patient-derived mutations in cis. *Human molecular genetics,* 10**,** 635-643.
SHARPE, M. L., GAO, C., KENDALL, S. L., BAKER, E. N. & LOTT, J. S. 2008. The structure and unusual protein chemistry of hypoxic response protein 1, a latency antigen and highly expressed member of the DosR regulon in Mycobacterium tuberculosis. *Journal of molecular biology,* 383**,** 822-836.
SINGH, P. 2007. *Molecular analysis of the Arabidopsis CP12 gene family.* University of Essex.
SINGH, P., KALOUDAS, D. & RAINES, C. A. 2008. Expression analysis of the Arabidopsis CP12 gene family suggests novel roles for these proteins in roots and floral tissues. *Journal of experimental botany,* 59**,** 3975-3985.

SMITH, A. M. & STITT, M. 2007. Coordination of carbon supply and plant growth. *Plant, cell & environment,* 30**,** 1126-1149.
SPARLA, F., PUPILLO, P. & TROST, P. 2002. The C-terminal extension of glyceraldehyde-3-phosphate dehydrogenase subunit B acts as an autoinhibitory domain regulated by thioredoxins and nicotinamide adenine dinucleotide. *Journal of Biological Chemistry,* 277**,** 44946-44952.
STANLEY, D. N., RAINES, C. A. & KERFELD, C. A. 2013. Comparative analysis of 126 cyanobacterial genomes reveals evidence of functional diversity among homologs of the redox-regulated CP12 protein. *Plant physiology,* 161**,** 824-835.
STITT, M., LUNN, J. & USADEL, B. 2010. Arabidopsis and primary photosynthetic metabolism–more than the icing on the cake. *The Plant Journal,* 61**,** 1067-1091.
SUSS, K.-H., ARKONA, C., MANTEUFFEL, R. & ADLER, K. 1993. Calvin cycle multienzyme complexes are bound to chloroplast thylakoid membranes of higher plants in situ. *Proceedings of the National Academy of Sciences,* 90**,** 5514-5518.
TAMOI, M., MIYAZAKI, T., FUKAMIZO, T. & SHIGEOKA, S. 2005. The Calvin cycle in cyanobacteria is regulated by CP12 via the NAD (H)/NADP (H) ratio under light/dark conditions. *The Plant Journal,* 42**,** 504-513.
THOMPSON, L. R., ZENG, Q., KELLY, L., HUANG, K. H., SINGER, A. U., STUBBE, J. & CHISHOLM, S. W. 2011. Phage auxiliary metabolic genes and the redirection of cyanobacterial host carbon metabolism. *Proceedings of the National Academy of Sciences,* 108**,** E757-E764.
TOMPA, P. 2002. Intrinsically unstructured proteins. *Trends in biochemical sciences,* 27**,** 527-533.
TOMPA, P. 2005. The interplay between structure and function in intrinsically unstructured proteins. *FEBS letters,* 579**,** 3346-3354.
TOMPA, P., SZASZ, C. & BUDAY, L. 2005. Structural disorder throws new light on moonlighting. *Trends in biochemical sciences,* 30**,** 484-489.
TRAVERSO, J. A., VIGNOLS, F., CAZALIS, R., SERRATO, A. J., PULIDO, P., SAHRAWY, M., MEYER, Y., CEJUDO, F. J. & CHUECA, A. 2008. Immunocytochemical localization of Pisum sativum TRXs f and m in non-photosynthetic tissues. *Journal of Experimental Botany,* 59**,** 1267-1277.
TROST, P., FERMANI, S., MARRI, L., ZAFFAGNINI, M., FALINI, G., SCAGLIARINI, S., PUPILLO, P. & SPARLA, F. 2006. Thioredoxin-dependent regulation of photosynthetic glyceraldehyde-3-phosphate dehydrogenase: autonomous vs. CP12-dependent mechanisms. *Photosynthesis Research,* 89**,** 263-275.
UVERSKY, V. N. 2002. Natively unfolded proteins: a point where biology waits for physics. *Protein science,* 11**,** 739-756.
UVERSKY, V. N., OLDFIELD, C. J. & DUNKER, A. K. 2005. Showing your ID: intrinsic disorder as an ID for recognition, regulation and cell signaling. *Journal of Molecular Recognition,* 18**,** 343-384.
VON CAEMMERER, S. V. & FARQUHAR, G. 1981. Some relationships between the biochemistry of photosynthesis and the gas exchange of leaves. *Planta,* 153**,** 376-387.
WARA-ASWAPATI, O., KEMBLE, R. J. & BRADBEER, J. W. 1980. Activation of glyceraldehyde-phosphate dehydrogenase (NADP) and phosphoribulokinase

in Phaseolus vulgaris leaf extracts involves the dissociation of oligomers. *Plant physiology,* 66**,** 34-39.
WEDEL, N. & SOLL, J. 1998. Evolutionary conserved light regulation of Calvin cycle activity by NADPH-mediated reversible phosphoribulokinase/CP12/ glyceraldehyde-3-phosphate dehydrogenase complex dissociation. *Proceedings of the National Academy of Sciences,* 95**,** 9699-9704.
WEDEL, N., SOLL, J. & PAAP, B. K. 1997. CP12 provides a new mode of light regulation of Calvin cycle activity in higher plants. *Proceedings of the National Academy of Sciences,* 94**,** 10479-10484.
WENDEROTH, I., SCHEIBE, R. & VON SCHAEWEN, A. 1997. Identification of the cysteine residues involved in redox modification of plant plastidic glucose-6-phosphate dehydrogenase. *Journal of Biological Chemistry,* 272**,** 26985-26990.
WINKEL, B. S. 2004. Metabolic channeling in plants. *Annu. Rev. Plant Biol.,* 55**,** 85-107.
WOLOSIUK, R. A. & BUCHANAN, B. B. 1977. Thioredoxin and glutathione regulate photosynthesis in chloroplasts.
WOLOSIUK, R. A., CRAWFORD, N. A., YEE, B. C. & BUCHANAN, B. B. 1979. Isolation of three thioredoxins from spinach leaves. *Journal of Biological Chemistry,* 254**,** 1627-1632.
WOODROW, I. E. & BERRY, J. 1988. Enzymatic regulation of photosynthetic CO2, fixation in C3 plants. *Annual Review of Plant Physiology and Plant Molecular Biology,* 39**,** 533-594.
YOO, K. S., OK, S. H., JEONG, B.-C., JUNG, K. W., CUI, M. H., HYOUNG, S., LEE, M.-R., SONG, H. K. & SHIN, J. S. 2011. Single cystathionine β-synthase domain–containing proteins modulate development by regulating the thioredoxin system in Arabidopsis. *The Plant Cell,* 23**,** 3577-3594.
ZAPPONI, M. C., IADAROLA, P., STOPPINI, M. & FERRI, G. 1993. Limited proteolysis of chloroplast glyceraldehyde-3-phosphate dehydrogenase (NADP) from Spinacia oleracea. *Biological Chemistry Hoppe-Seyler,* 374**,** 395-402.
ZHANG, R.-G., EVANS, G., ROTELLA, F. J., WESTBROOK, E. M., BENO, D., HUBERMAN, E., JOACHIMIAK, A. & COLLART, F. R. 1999. Characteristics and Crystal Structure of Bacterial Inosine-5 '-monophosphate Dehydrogenase†. *Biochemistry,* 38**,** 4691-4700.
ZIEGLER, H. & ZIEGLER, I. 1965. Der Einfluß der Belichtung auf die NADP+-abhängige Glycerinaldehyd-3-phosphat-Dehydrogenase. *Planta***,** 369-380.
ZIMMERMANN, P., HIRSCH-HOFFMANN, M., HENNIG, L. & GRUISSEM, W. 2004. GENEVESTIGATOR. Arabidopsis microarray database and analysis toolbox. *Plant Physiol,* 136**,** 2621-32.

APPENDICES

Appendix 1. List of primers used for the T-DNA inerstion line. Primers in the table represent the gene specific primers to detect the WT allele.

Name	Sequence	Annealing Temperature	Expected fragment size
CP12-1 CP12-1-AF-P (forward)	CAAGCTTTATGAAAGCGCATC	55 ˚C	1053 bp
CP12-1 CP12-1-A-RP (reverse)	CGACATCATCAGTCTCAGG		
CP12-2 BX28711_CP12-LP(forward)	TCAGCTTTAGGAATCGTGAGC	56 ˚C	986 bp
CP12-2 BX28711_CP12-RP(reverse)	TACGTCCGATATCCCTCCTTC		
CP12-3 CP12-BFP(forward)	TTCATCAGTCAGTATCGATGGG	45 ˚C	985 bp
CP12-3 CP12-B-RP(reverse)	AACACGATGAACAACGGTTTC		
Cbsx1.2(forward)	TCTTCTCTCCTAGGGCGAGTC	60 ˚C	1213 bp
Cbsx1.2(reverse)	CTAGGCTAAGATCGAATCCCG		
Cbsx1.3(forward)	CCATTGGTTTTGCTGAGTAGC	60 ˚C	971 bp
Cbsx1.3(reverse)	TTGACGAAGACTGGAAATTGG		
Cbsx2.1(forward)	TTTCCAGTACATTGCGTCATG	60 ˚C	1142 bp
Cbsx2.1(reverse)	CAGAAGTTCCAACGCTGAAAG		
Cbsx2.2(forward)	AAAGTCTTCATCTACGCCAAGG	60 ˚C	1049 bp
Cbsx2.2(reverse)	TGTCTCGGAGTCATGAAATCC		

Appendix 2. List of primers used for the T-DNA inerstion line. Primers in the table represent the insertion specific primers to detect the T-DNA insert

Name	Sequence	Annealing Temperature	Expected fragment size
CP12-1 CP12-1-A-RP (reverse)	CGACATCATCAGTCTCAGG	55 ˚C	472 bp
LBb1	GCGTGGACCGCTTGCTGCAACT		
CP12-2 BX28711_CP12-RP (reverse)	TACGTCCGATATCCCTCCTTC3	56 ˚C	580 bp
GK-BP	ATATTGACCATCATACTCATTGC		
CP12-3 CP12-B-RP(reverse)	AACACGATGAACAACGGTTTC	45 ˚C	361 bp
LB1 Sail	GCCTTTTCAGAAATGGTAAATAGCCTTGCTTC		
cbsx1.2(reverse)	CTAGGCTAAGATCGAATCCCG	60 ˚C	579-879 bp
SALK LBb1.3	GCGTGGACCGCTTGCTGCCAACT		
cbsx1.3(reverse)	TTGACGAAGACTGGAAATTGG	60 ˚C	440-740 bp
GK	GTGGATTGATGTGATATCTCC		
cbsx2.1(reverse)	CAGAAGTTCCAACGCTGAAAG	60 ˚C	594-894 bp
SALK LBb1.3	GCGTGGACCGCTTGCTGCCAACT		
cbsx2.2(reverse)	TGTCTCGGAGTCATGAAATCC	60 ˚C	532-832 bp
SALK LBb1.3	GCGTGGACCGCTTGCTGCCAACT		

.

Appendix 3. List of primers used for the T-DNA inerstion line. Primers in the table represent the qPCR primers.

Name	Sequence	Annealing Temperature	Expected fragment size
CP12-1 CP12-1-qPCR-LP	GAAGCGGATGGTTGTGGTT	65 ˚C	63 bp
CP12-1 CP12-1-qPCR-RP	CTCTTCTCCACCTTCTCCGATA		
CP12-2 CP12-1-qPCR-LP	TTCACAGGCTGCCGTGTACC	65˚C	85 bp
CP12-2 CP12-1-qPCR-LP	GACGAAGACACGCTGGGTTG		
CP12-3 QPCR_CP12-3sail_FP	AGCCTGATGATGGTGACGAAGG	65 ˚C	113 bp
CP12-3 QPCR_CP12-3sail_FP	TCGCAAACCTCTGTCGCTTCC		
Cbsx1.2 & cbsx1.3(forward)	CGAGGTTTCTCTCCGTTCAG	65 ˚C	1213 bp
Cbsx1.2 7cbsx1.3 (reverse)	CAACCTGCAGCAACAAAGAA		
Cbsx2.1 & cbsx2.2(forward)	TGGAGACTTGATGACACCGT	65 ˚C	206 bp
Cbsx2.1 & cbsx2.2 (reverse)	ATCAGCATCAACAACGGGTA		
Cyclophilyn (forward)	TCTTCCTTCGGAGCCATA	65 ˚C	250 bp
Cycolphilyn (reverse)	AAGCTGGGAATGATTCGCTTCC		
Actin (forward)	ACCTTGCTGGACGGACCTTACTGAT	65 ˚C	57 bp
Actin (reverse)	GTTGTCTCGTGGATTCCAGCAGCTT		

Appendix 4. Gene map of the CP12 family. (a) CP12-1 **(b)** CP12-2 **(c)** CP12-3**.**

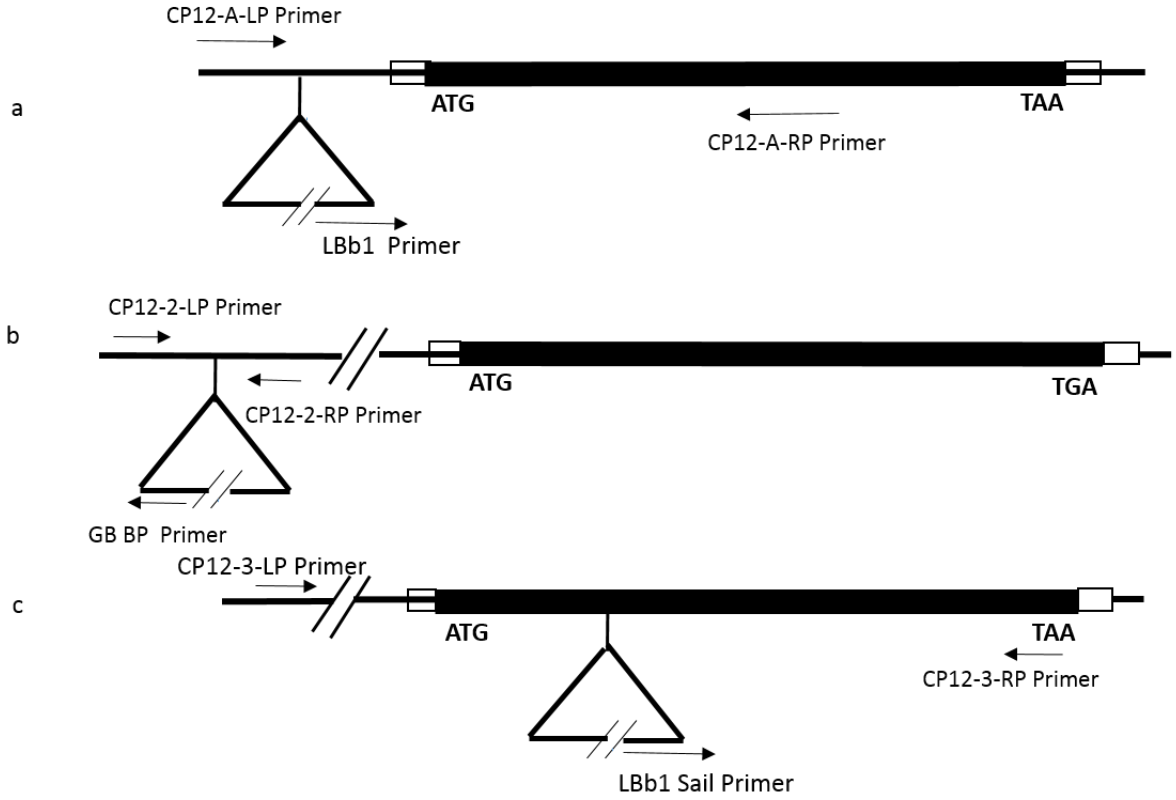

Appendix 5. RNAi constructs. (a) Generic RNAi construct 52. **(b)** Specific RNAi construct 53**. (c)** Specific RNAi 54**.**

a

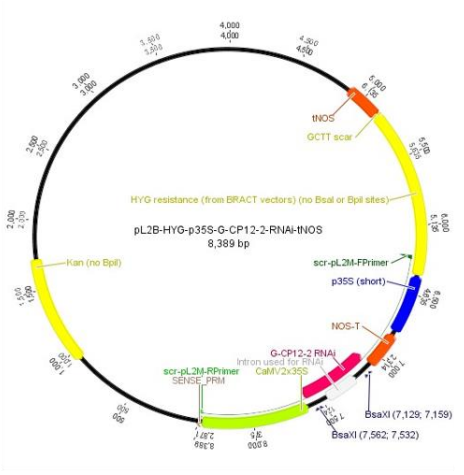

b

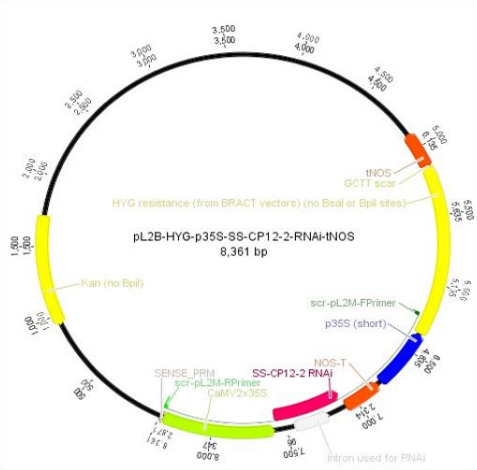

c